UC Berkeley
UC Berkeley Electronic Theses and Dissertations

Title
Methylmercury Production in Tidal Salt Marsh Sediments and Potential Control Using Iron Amendments

Permalink
https://escholarship.org/uc/item/5f4064q4

Author
Ulrich, Patrick Dennis

Publication Date
2011

Peer reviewed|Thesis/dissertation

eScholarship.org Powered by the California Digital Library
University of California

Methylmercury Production in Tidal Salt Marsh Sediments and Potential Control Using Iron Amendments

by

Patrick Dennis Ulrich

A dissertation submitted in partial satisfaction of the

requirements of the degree of

Doctor of Philosophy

in

Engineering – Civil and Environmental Engineering

in the

Graduate Division

of the

University of California, Berkeley

Committee in charge:

Professor David Sedlak, Chair

Professor Kara Nelson

Professor Todd Dawson

Fall 2011

Methylmercury Production in Tidal Salt Marsh Sediments and Potential Control Using Iron Amendments

© 2011

By Patrick Dennis Ulrich

Abstract

Methylmercury Production in Tidal Salt Marsh Sediments and Potential Control Using Iron Amendments

by

Patrick Dennis Ulrich

Doctor of Philosophy in Civil and Environmental Engineering

University of California, Berkeley

Professor David Sedlak, Chair

Tidal wetlands can be important sources of methylmercury (MeHg) in aquatic ecosystems, such as the San Francisco Bay-Delta estuary. As a result of the tendency of bacteria in wetland sediments to methylate mercury, the restoration of wetland habitat may cause an increase of MeHg concentrations. To balance the need for tidal wetland habitat with concerns over increased MeHg exposure, landscape-scale techniques for minimizing the production and export of MeHg from wetland sediments are needed. One potential approach is to use an iron sediment amendment to reduce net MeHg production. The addition of Fe[II] decreases MeHg production by lowering the concentration of the inorganic Hg[II] species that are methylated by bacteria. In this research, the potential for reducing MeHg production and export via an iron amendment was evaluated in laboratory microcosm experiments and a field study in a tidal salt marsh in the San Francisco Bay estuary. Additionally, sediment incubation experiments were conducted in anaerobic containers and in *in situ* cores to evaluate the effect of iron and sulfur redox cycling on MeHg production.

Two laboratory microcosm experiments (Chapter 2) were conducted to test the iron amendment hypothesis under simulated tidal wetland conditions: one with devegetated sediments and one with live wetland vegetation. The microcosms consisted of intact sediment cores collected from Gambinini Marsh, a tidal salt marsh in the San Francisco Bay estuary dominated by pickleweed (*Sarcocornia pacifica*). The microcosms were maintained under simulated tidal conditions and amended at four iron doses (0, 180, 360, and 720 g-Fe/m^2). Following iron addition to the devegetated sediments, porewater S[-II] concentrations decreased for each dose relative to the control. The average weekly export of MeHg in the surface water decreased by 82% and 89% for the two highest iron doses, respectively. Despite substantial variability within

treatment groups, similar trends were observed in the vegetated microcosms. The results suggest that iron addition has the potential to provide a landscape-scale control on MeHg export from restored tidal wetlands under certain conditions.

The cycling of iron, sulfur, and mercury in tidal wetlands is a complex process, with the combination of daily tides, changes in the growth state of wetland plants, and a highly productive microbial community resulting in temporal and spatial variations in MeHg production and export. Sediment incubation experiments (Chapter 3) were used to evaluate the effect of these processes on MeHg concentrations in the sediments of Gambinini Marsh. Sediments were incubated for 7-days in sealed jars under the following conditions: untreated sediments, addition of sodium molybdate to suppress sulfate reduction, and the addition of formaldehyde as an abiotic control. Similar rates of Fe[II] production were observed in both the untreated and Mo-amended incubations, suggesting that both iron-reducing and sulfate-reducing bacteria co-existed in the same sediment layers. Additionally, MeHg production was not observed when sulfate reduction was suppressed, suggesting that mercury methylation was mediated by sulfate-reducing bacteria. The *in situ* incubations, which were conducted with open and closed cores, demonstrated that during the summer months when plants were active, separation of sediments from live plant roots and gas exchange with the atmosphere resulted in more reduced sediment conditions. Additionally, sediments at the surficial layers (0-1 cm and 3-4 cm depths) exhibited more reducing conditions during the winter than in the summer, suggesting that the oxidation of reduced iron species occurs more rapidly during the summer.

To better understand the effect of iron amendments on *in situ* tidal marsh biogeochemistry, a 17-month field study was conducted in the Gambinini Marsh (Chapter 4). Before and after amending the sediments with 77 g-Fe/m^2, porewater from pickleweed-dominated sediments in the high marsh plain were analyzed for iron, sulfur, organic carbon, and methylmercury. Sulfide was not detected in the sediment porewater, and the iron amendment had no observable effect on net MeHg production. However, porewater iron concentrations were elevated for at least 6 weeks following the amendment. Porewater concentrations of MeHg and dissolved organic carbon were lower throughout 2010 than during the summer of 2009 when the experiment was initiated. However, these concentrations increased during the period of pickleweed flowering in 2010, further demonstrating the strong effect that wetland vegetation can have on sediment biogeochemical processes.

This research demonstrated that an iron sediment amendment has the potential to be an effective control of MeHg production and export in tidal wetland sediments under certain conditions. While the *in situ* amendment showed no effect in the high marsh plain of Gambinini Marsh, the microcosm experiments demonstrated that a strong effect may be possible in sulfide-rich sediments. Additional research is necessary to evaluate the efficacy of the iron amendment in sulfide-rich field sediments, such as those found in low marsh environments.

This dissertation is dedicated to my father, Dennis, whose life was cut too short to see the completion of his own Ph.D., but whose advice and legacy will always be a part of me.

Table of Contents

Acknowledgements

My time as a Ph.D. student was altogether challenging, rewarding, and remarkably fun throughout. Of course, it would not have been so without the support of my mentors, peers, friends, and family along the way, and I would like to begin my dissertation with a "Thank you" to everyone who has helped me with this achievement. While I won't be able to fully describe what each of you has meant to me in this short section, please do know that all of you have my utmost gratitude.

First and foremost, I would like to thank my advisor and mentor, David Sedlak, for all of his advice, suggestions, and support. David gave me the freedom to select the type of project I wanted to work on, as well as to define the goals and objectives of my research. I really appreciated that he gave me the flexibility to chart my own path, and that he always offered helpful guidance whenever I needed it. I really valued his constant optimism, and I was always amazed at how every time I left his office I felt so much better about my research than I did when our meeting started. I learned so much from his mentorship throughout my time as a graduate student, and I know that my accomplishments at Berkeley were in no small part because of the hard work and effort he invested in me.

I would like to acknowledge and thank Kara Nelson and Todd Dawson for reviewing my dissertation and for serving on my Qualifying Exam committee. I really appreciated their thoughtful comments on my dissertation, as well as the really enjoyable courses that I took from each of them during my time here. Additionally, I would like to thank the exceptional faculty of the Environmental Engineering Program for their outstanding courses and dedication to teaching, and especially Jim Hunt and Mark Stacey for also serving on my Qualifying Exam committee.

I was fortunate to work with one graduate student and three undergraduates who assisted me with this research: Caroline Mahe, Carolina Mendez, Tasha Kamegai-Karadi, and Yan Nusinovich. I would like to express my gratitude to each of them. Not only did they help to make my life easier in the lab, but they were all fantastic people that were fun to be around, and I know that each one has a very bright future ahead!

I am much in debt to the kindness of the support staff in both the Civil & Environmental Engineering Department and the Engineering Research Support Office. I would especially like to thank Shelley Okimoto and Mary Cuison, who helped me out on so many occasions and were always willing to answer my questions.

I was very fortunate to have had the financial support of two research fellowships and a grant from the University of California Water Resources Center. My fellowship from the National Science Foundation's Graduate Research Fellowship Program primarily supported the microcosm studies described in Chapter 2, and a predoctoral fellowship from the CALFED/Bay Delta Science Program supported the incubation and field studies presented in Chapters 3 and 4.

My research revolved around samples collected from the Gambinini Marsh in Sonoma County, and I cannot thank Stewart Brand and Ryan Phelan enough for their kindness and for granting me access to their gorgeous property. Some of my fondest memories from my time as a graduate student are from the days spent in that beautiful marsh, and it is a place I won't ever forget.

I would like to thank all of the current and former members of the Sedlak Lab, including, Anh Pham, Scott Mansell, Eva Agus, Erika Houtz, Justin Jasper, Amanda Ackerman, Ekrem Karpuzcu, Haizhou Liu, Christy Keenan, Changha Lee, Joonseon Jeong, and Jorge Loyo-Rosales. Your encouragement and support were vital to my success, and I always enjoyed our conversations during group happy hours. I would also like to thank all of my fellow denizens of

O’Brien Hall, since you’ve made our building a great place to work. I would like to extend a special thanks to Paul Koster van Groos. The long hours spent manning the CVAFS were made much easier by having a friend to chat with, and our conversations about research, careers, and life were always enjoyable and helpful. Outside of the lab, I want to thank Anh, Paul, Scott and his wonderful family, Janet Casperson, and Nick and April Mostek for our many fun dinners and weekend excursions throughout northern California.

I would like to acknowledge my gratitude and great appreciation for the public lands of California, and especially Point Reyes National Seashore. My early morning hikes and wildlife encounters kept me grounded, helped to clear my thoughts, and gave me constant reminders of why this planet’s amazing biodiversity is worth fighting to save!

I would not have made it this far without the support of my family, and I thank each and every one of you for your encouragement and love, and for instilling such a strong sense of morals and purpose in me. I know it was difficult to be on opposite coasts, but you always encouraged me to work hard and do my best, and when we were able to spend time together, it was so easy to forget that we lived so far apart.

Lastly, I must thank the most important inspiration in my life, my beautiful wife, Theresa. She is my rock, my confidant, and my biggest fan. She has supported me in all aspects of my life, always encouraged me to follow my heart, and made me laugh and smile on so many occasions every single day. I love you so much, Theresa, and I cannot imagine a more amazing partner to have shared this journey with.

Chapter 1. Introduction

1.1 The Connection between Wetlands and Mercury

1.1.1 Global Importance of Wetland Systems

Wetland ecosystems provide many benefits to both society and the environment, as they provide habitat for wildlife including endangered and commercially valuable species, offer flood mitigation and aquifer recharge, improve water quality, and have aesthetic and heritage value (Mitsch & Gosselink 2007). In terms of primary productivity, tidal wetlands are among the world's most productive ecosystems, and they are now being considered for their carbon sequestration capacities in climate change mitigation strategies (Miller & Fujii 2010). Wetlands have significant economic value as well, and attempts to estimate the value of the ecosystem services provided by major ecosystem types have shown that wetlands have a higher economic value per area than most terrestrial systems, including being an estimated 7 times more valuable than tropical forests, and 150 times more valuable than cropland (Costanza et al. 1997).

1.1.2 Historical Wetland Losses and Restoration

Wetlands were historically viewed as wastelands and were often drained or filled in to create agricultural fields or housing. This historical trend resulted in the loss of an estimated 53% of the wetland area in the continental U.S. between the 1780's and 1980's. California lost an estimated 91% of its wetlands during this period, which was the highest percentage of any state (Dahl 1990). However, near the end of the 20th century both government agencies and private landowners started to realize the many benefits that wetlands offer and began restoring and creating wetland habitat, which is evident in the increase of wetland acreage by 17,700 hectares in the United States between 1986 and 1997 (Dahl 2000).

The San Francisco Bay-Delta estuary (hereafter called the Bay-Delta) lost an estimated 85-95% of its historical tidal marshes to urban development, agriculture, and commercial salt production since the middle of the 19th century (Dingler 1996). There are many current initiatives underway to re-establish important ecosystem functions and critical wildlife habitat in wetlands throughout the estuary. One of the largest tidal wetland restoration projects in North America is the planned conversion of over 10,000 hectares of commercial salt production ponds back to tidal salt marsh habitat in the southern end of San Francisco Bay (Takekawa et al. 2006). There are many other smaller restoration projects planned throughout the Bay-Delta and these restored wetland areas will provide much needed habitat for a large number of migratory bird species that winter in the region or stop-over on the their migration along the Pacific Flyway. The restoration projects will also provide viable habitat to resident federally listed endangered species like the salt marsh harvest mouse (*Reithrodontomys raviventris*) and the California clapper rail (*Rallus longirostris obsoletus*). Additionally, the restoration can offer flood protection for the surrounding urban areas and increased local wildlife-oriented recreation opportunities.

1.1.3 Tidal Wetland Biogeochemistry

The exact definition of a wetland varies, as evidenced by the many legal definitions employed, but the common link between definitions is that wetlands are areas of land distinguished by "the presence of standing water for some period during the growing season, unique soil conditions, and organisms, especially vegetation, adapted to or tolerant of saturated soils" (Mitsch & Gosselink 2007). In essence, wetlands serve as the transition zone between the aquatic and terrestrial environments. Tidal wetlands cover the range of wetland environments influenced by the tidal cycles of the ocean. They stretch from salt marshes receiving seawater in coastal environments, to brackish marshes of varying salinity in estuaries, and include freshwater marshes that experience tidal flow patterns in the upstream reaches of the estuarine environment.

While the historical coverage of tidal marshes on the eastern coast of the U.S. was extensive, with large marshes dominated by cordgrass (*Spartina spp.)*, the western coast of the U.S. consisted of smaller pockets of tidal marshes, mostly in embayments protected from the wave action of the Pacific Ocean. The Bay-Delta, which is the largest estuary on the western coast of the United States, supports the largest area of tidal wetlands in California (Watson & Byrne 2009).

Tidal inundation patterns create areas of different geochemical conditions within the marsh sediments, and discrete zones exist based on height relative to the tides and inundation frequency. These areas are often visually observed by distinct changes between bands of vegetation types. In the salt marshes of the Bay-Delta, the low-marsh, which extends from the mean tidal level to the mean high water level (MHW), is dominated by nearly monoculture stands of cordgrass, including both the native Pacific cordgrass (*Spartina foliosa*) and invasive smooth cordgrass (*Spartina alterniflora)*. In the high marsh zone, at an elevation between MHW and the highest extent of the tides, Spartina species give way to dominant growth of pickleweed (*Sarcocornia pacifica*), which is a halophyte that can withstand the elevated salinities of the high marsh caused by evapotranspiration. At the highest extent of the marsh, near the transition to upland areas, pickleweed can be found in association with peripheral halophytes like salt grass (*Distichlis spicata*) and fathen (*Atriplex triangularis*) (Best et al. 2008).

Salt marshes are highly productive ecosystems, and exhibit high rates of microbial respiration in the sediments. This results in the depletion of oxygen within a few millimeters below the surface of the saturated sediments due to the limited rates of diffusion of oxygen into the sediment porewater (Brendel & Luther 1995, Choe et al. 2004). Thus, most of the carbon mineralization in wetland sediments occurs under conditions where microbes use terminal electron acceptors other than oxygen. According to equilibrium thermodynamics, redox conditions in wetland sediments should be vertically stratified as organic matter is oxidized by bacteria that sequentially deplete the most favorable terminal electron acceptor with increasing depth. Under typical conditions, microbial respiration will use the following sequence of electron acceptors: oxygen, nitrate, manganese, iron, sulfate, carbon dioxide, and water (Mitsch & Gosselink 2007). Through these processes, reduced forms of the terminal electron acceptors will be produced (i.e., H_2O, N_2, Mn[II], Fe[II], S[-II], CH_4, and H_2) within the sediments.

Tidal salt marshes typically exhibit high concentrations of sulfate (due to the influence of seawater) and Fe[III]-(hydr)oxides (which are present in the sediments). Because Fe[III]-(hydr)oxides are not continuously replenished by input sources, sulfate is the dominant electron acceptor for organic matter mineralization in salt marsh sediments (Howarth & Giblin 1983, King et al. 1985). Once all of the Fe[III] has been reduced, if conditions stay anoxic, there can be

very low iron availability compared to the continued high sulfate inputs. Additionally, the end product of sulfate reduction (sulfide) can reduce most Fe[III]-containing minerals (Canfield 1989, Canfield et al. 1992), thereby decreasing the availability of Fe[III] for respiration. However, research over the past decade has started to change this view of sulfate-dominated microbial respiration in tidal salt marsh sediments. Measured rates of microbial iron reduction in the salt marshes on the eastern coast of the U.S. have demonstrated that sulfate reduction and iron reduction may occur simultaneously in the same sediment depth layer (Lowe et al. 2000), and that iron reduction can account for a majority of total carbon oxidation (Gribsholt et al. 2003, Hyun et al. 2007, Koretsky et al. 2003).

Salt marsh vegetation can also play a critical role in microbial respiration in the sediments. In order to survive the anaerobic conditions encountered in salt marsh sediments, many plants have the ability to transport oxygen to their root systems. Some of this oxygen leaks into the rhizosphere (Howes et al. 1981), which is the area of sediment immediately surrounding the roots and rhizomes. The release of oxygen enables the plants to avoid sulfide toxicity because sulfide is readily oxidized by O_2 (Lee 1999, 2003). This presence of oxygen can also result in the formation of Fe[III]-(hydr)oxide plaques immediately adjacent to the roots (Weiss et al. 2004), which can result in iron-reduction accounting for the vast majority of total carbon metabolized in the rhizosphere (Gribsholt et al. 2003). Additionally, salt marsh vegetation can exude organic acids into the rhizosphere (Mucha et al. 2005), which can stimulate microbial respiration by providing an additional labile carbon source in the zone where oxygen is released (Hyun et al. 2009, Windham-Myers et al. 2009).

1.1.4 Methylmercury Production in Wetlands

A potential drawback to wetland restoration and construction is the formation of monomethylmercury (MeHg), a potent neurotoxin that affects both humans and wildlife. Wetlands contain large areas of anoxic sediments, which have the ideal conditions necessary for MeHg production. Although wetlands typically serve as sinks for inorganic mercury, as well as many other metals, they are often sources of MeHg (St Louis et al. 1994). The percentage of freshwater wetland area in a watershed can often be the best predictor of the concentration of MeHg in both the water column and the biota (Babiarz et al. 1998, Guentzel 2009, Hurley et al. 1995). Recent research has shown tidal salt marshes to be hotspots of methylmercury production in coastal ecosystems as well (Canario et al. 2007, Hall et al. 2008, Langer et al. 2001, Marvin-DiPasquale et al. 2003, Mitchell & Gilmour 2008).

1.1.5 Mercury Exposure to Humans and Wildlife

While MeHg is typically present at sub-nanomolar levels in natural waters (Conaway et al. 2003), it poses a significant health risk to high trophic level consumers because concentrations increase with increasing trophic level in the food web (Jaeger et al. 2009, Kehrig et al. 2010). This process, known as biomagnification, can result in MeHg concentrations that are up to six or seven orders of magnitude higher in fish than in the surrounding water column (Mason et al. 2006, Sveinsdottir & Mason 2005).

The biomagnification of MeHg begins at the lowest level of the food web, where phytoplankton readily bioaccumulate MeHg to concentrations that are up to 10^4-10^5 times greater than the surrounding water (Pickhardt & Fisher 2007). This initial step in the biological uptake process occurs because once MeHg diffuses into cells it preferentially binds to thiol groups in proteins and other cellular components in the cytoplasm. When zooplankton graze on phytoplankton, they readily incorporate the dissolved cytoplasmic components into their own bodies (Mason et al. 1995). This transfer of MeHg continues with increasing trophic level, and explains why typically greater than 85-95% of the mercury in fish is MeHg, while typically less than 10-30% of the total mercury in the aqueous phase is MeHg (Ullrich et al. 2001). The primary pathway for human exposure to mercury is through the consumption of fish, which is especially problematic in communities that rely on local fisheries as the primary source of protein in their diet. The dangers of mercury contamination are recognized as a public health hazard throughout the United States, where 76% of all fish consumption advisories issued by the EPA are due, at least in part, to elevated levels of MeHg (EPA 2009). Mercury primarily affects the central nervous system, and because MeHg readily crosses the placenta, the neurological development of fetuses and young children is especially susceptible to MeHg exposure. Chronic exposure to MeHg in adults is also dangerous, and has been shown to cause impairment of the peripheral vision, speech, hearing, motility, and even coma and death (CDC 2009).

MeHg also poses significant threats for the reproductive success and survival of piscivorous birds and mammals (Wolfe et al. 1998), as well as benthic omnivores in tidal wetlands, such as the endangered California clapper rail. Previous research has shown that elevated mercury levels in failed California clapper rail eggs were linked to deformities, embryo hemorrhaging, and embryo malpositions (Schwarzbach et al. 2006). Furthermore, chronic low-level dietary exposure to MeHg has been shown to alter the behavior of great egret (*Ardea albus*) juveniles (Bouton et al. 1999). High trophic level fish species can also experience detrimental effects due to dietary exposure of MeHg. For example, the maternal transfer of MeHg to eggs of Atlantic croaker (*Micropogonias undulates*) impairs the survival skills related to foraging and predator evasion in planktonic larval-stage offspring (Alvarez et al. 2006).

1.2 The Biogeochemistry of Mercury in Wetlands

1.2.1 Mercury Speciation

Approximately two-thirds of the mercury found in the global atmosphere can be traced back to anthropogenic emissions of mercury into the environment, from sources including coal-fired power plants, metal mining and production facilities, and the chlor-alkali industry. The remaining third is attributed to natural sources, including volcanic eruptions, forest fires, and degassing from mercury-rich geologic formations (Morel et al. 1998). Anthropogenic emissions have tripled the mercury concentrations in the atmosphere and ocean surface over the past 150 years (Mason et al. 1994). As a result, mercury concentrations are even elevated in aquatic ecosystems far from anthropogenic sources (Gobeil et al. 1999, Wiener et al. 2006). The residence time of Hg^0 in the atmosphere is on the order of a year (Fitzgerald & Mason 1997), which provides sufficient time for global distribution via atmospheric currents (Durnford et al.

2010). Mercury is returned to the Earth's surface through deposition of both elemental and oxidized mercury species (i.e., Hg[II]) (Zhang et al. 2009).

In the aquatic environment, mercury occurs in both the dissolved elemental form ($Hg^0_{(aq)}$), which is volatile and relatively unreactive, and as Hg[II], which can be present in a variety of forms. Under conditions encountered in the aquatic environment, Hg^{2+} ions are thermodynamically unstable and react with various ligands to form aqueous complexes. In oxic surface waters, dissolved Hg[II] is primarily present in a hydrolyzed form (e.g., $Hg(OH)_2$) or as a complex with chloride (e.g., $HgCl^+$, $HgCl_2$) depending on the pH and chloride concentrations. Natural organic matter (NOM) can be an important ligand for dissolved Hg[II] as well, because Hg[II] strongly binds to reduced sulfur functional groups, which can lead to sulfur-rich NOM dominating mercury speciation in oxic surface waters (Hsu-Kim & Sedlak 2005, Ravichandran 2004). Under the typical conditions of oxic estuarine surface waters, mercury is predominantly present as $HgCl_3^-$ or $HgCl_2$ in the absence of dissolved organic matter (DOM), with $HgCl_2$ predominating at chloride concentrations between approximately 10^{-2} M and $10^{-1.1}$ M at pH 8, and between approximately $10^{-2.9}$ M and $10^{-1.1}$ M at pH 7 (Morel et al. 1998). However, even at low levels of DOM (0.1 to 1 mg-C/L of dissolved organic carbon), the formation of Hg-DOM complexes is favored over the chloro-species (Fitzgerald et al. 2007).

In sulfide-containing anoxic waters and sediments, mercury speciation is nearly completely dominated by sulfide and bisulfide complexes (e.g., HgS^0, $HgHS^+$), even at nanomolar total S[-II] levels (Morel et al. 1998). Sulfur-rich NOM and polysulfides (i.e., molecules containing multiple sulfur atoms that form from the reaction of sulfide with elemental sulfur and take the form of S_n^{2-}) also are potentially important to mercury speciation under anoxic conditions (Jay et al. 2000, Skyllberg 2008). However, equilibrium calculations predict that sulfide dominates the speciation of Hg[II] in the presence of polysulfide in estuarine and marine waters (Fitzgerald et al. 2007).

Mineral mercuric sulfide ($HgS_{(s)}$), which occurs in both the black metacinnabar and red cinnabar forms, is thought to be the dominant mercury mineral phase under anoxic conditions. The solubility of $HgS_{(s)}$ is very low ($\log K_S = -52.7$, (Morel et al. 1998)), however, the apparent solubility of $HgS_{(s)}$ increases with increasing concentrations of S[-II], due to the formation of mercury-sulfide complexes (see Table 1-1). The presence of other competitive ligands, such as polysulfides formed from coupled sulfide oxidation and Fe[III] reduction, can also contribute to the total dissolved mercury concentration in anoxic porewaters (Slowey & Brown 2007). In organic-rich sediments, dissolved organic matter may enhance Hg[II] dissolution and prevent the precipitation of $HgS_{(s)}$ (Ravichandran et al. 1999). Hg[II] also may be present on inorganic surfaces, like $FeS_{(s)}$ (Jeong et al. 2007, Merritt & Amirbahman 2007) and can coprecipitate during authigenic pyrite ($FeS_{2(s)}$) formation (Huerta-Diaz & Morse 1992).

Mercury speciation in the environment is important for both large-scale processes, such as the transport of particle-associated mercury over large distances, as well as local processes, such as determining the partitioning to sediments in porewater and uptake by aquatic biota. Additionally, in the sediment porewater where methylmercury is produced, the speciation of inorganic-Hg is one of the most important factors controlling the rates of MeHg production.

Table 1-1. Equilibrium constants for mercury speciation.

Reaction	Log K	Reference
$Hg^{2+} + HS^- \leftrightarrow HgS_{(s)} + H^+$	52.7	(Morel et al. 1998)
$Hg^{2+} + HS^- \leftrightarrow HgHS^+$	30.5	(Benoit et al. 1999b)
$Hg^{2+} + HS^- \leftrightarrow HgS^0 + H^+$	26.5	(Benoit et al. 1999b)
$Hg^{2+} + 2HS^- \leftrightarrow Hg(HS)_2^0$	37.5	(Benoit et al. 1999b)
$Hg^{2+} + 2HS^- \leftrightarrow HgS_2H^- + H^+$	32.0	(Benoit et al. 1999b)
$Hg^{2+} + 2HS^- \leftrightarrow HgS_2^{2-} + 2H^+$	23.5	(Benoit et al. 1999b)
Binding to Organic Matter (L is reactive functional group on DOM)		
$Hg^{2+} + L \leftrightarrow HgL$	21.8 - 23.7	(Dong et al. 2011)
$Hg^{2+} + 2L \leftrightarrow HgL_2$	30.0 - 31.8	(Dong et al. 2011)
$Hg^{2+} + L \leftrightarrow HgL$	29.9 - 33.5	(Black et al. 2007)
$Hg^{2+} + L \leftrightarrow HgL$	21 - 24	(Lamborg et al. 2003)

1.2.2 Mercury Methylation

Mercury methylation, the conversion of inorganic Hg[II] to MeHg, typically occurs under anoxic conditions. While it is possible for methylation to occur abiotically from the donation of methyl-groups from organic molecules to Hg[II] complexes (Celo et al. 2006), under the conditions typically found in the aquatic environment, methylation is primarily a biological process. In aquatic sediments, the process is primarily attributed to the activity of sulfate-reducing bacteria (Compeau & Bartha 1985, Gilmour et al. 1992), and it is believed to be an accidental consequence of a metabolic process (Choi et al. 1994a, b). Recent research also has shown that iron-reducing bacteria are capable of mercury methylation (Fleming et al. 2006, Kerin et al. 2006), although the impact of iron-reducers on the production of MeHg in the environment has yet to be determined.

Demethylation, the conversion of MeHg to inorganic mercury, also occurs in the aquatic environment. In the water column, demethylation can occur via photolysis (Hammerschmidt & Fitzgerald 2006, Sellers et al. 1996). Within sediments, demethylation is attributable to bacteria responding to MeHg toxicity in heavily contaminated areas (Marvin-DiPasquale et al. 2000) or as a co-metabolic oxidative process at low sediment MeHg concentrations (Marvin-DiPasquale et al. 2000, Oremland et al. 1991). The balance between the rates of methylation and demethylation determines the net MeHg production rate and the concentration of MeHg present in an aquatic system.

Because mercury methylation is biologically mediated, the rate of MeHg production depends on both microbial growth rates and on the bioavailability of mercury. Methylation is believed to occur in the cytoplasm, and under conditions encountered in wetland sediments, the uptake of inorganic mercury is believed to be a passive, diffusion-driven process in which only small, uncharged compounds (e.g., HgS^0 and $HgCl_2^0$) are capable of passing through the lipid bilayer (Benoit et al. 1999b). As described in the previous section, dissolved mercury speciation in the porewater of anoxic sediments is often controlled by the presence of S[-II]. Under these conditions, only small, uncharged mercury-sulfide complexes (e.g., HgS^0 and $Hg(HS)_2^0$) are believed to be bioavailable for methylation (Benoit et al. 1999a, Drott et al. 2007). Thus, the bioavailability of inorganic mercury for methylation is affected by the chemistry of the porewater.

Organic matter has been shown to both increase and decrease the net rate of mercury methylation. Because organic matter can alter the speciation of Hg[II] in the sediment porewater, it can lower mercury methylation rates by lowering the concentrations of bioavailable Hg[II] complexes, since Hg-NOM complexes are typically charged and too large to pass through bacterial membranes. However, organic matter can also stimulate microbial activity by providing a labile carbon source, which in turn enhances respiration rates and increases rates of MeHg production (Kim et al. 2011, Lambertsson & Nilsson 2006).

Much effort has been dedicated to predicting net MeHg production from measureable environmental variables, including temperature, pH, salinity, concentrations of sulfate, sulfide, total mercury, DOC, acid volatile-sulfides (AVS), and Fe[II]. While correlations can be found for certain data sets, it has been difficult to make generalizations that are valid across environmental gradients, habitats, and regions. For example, managers in the Bay-Delta would like to know if lowering total mercury concentrations in point sources such as sewage effluent would decrease MeHg concentrations in biota. Several studies have indicated a positive correlation between total mercury and MeHg in waters and sediments (Benoit et al. 1998,

Hammerschmidt & Fitzgerald 2004, Heim et al. 2007), while others have found no correlation (Choe et al. 2004, Lambertsson & Nilsson 2006). It is becoming increasingly clear that the balance of site-specific biogeochemical parameters dictate the concentration of MeHg present in biota. From a mercury management perspective, it is important to understand the local processes that control MeHg production and export within a specific watershed. Such information might also be used to design control measures that would be most effective for each unique situation.

1.2.3 Methylmercury in Tidal Wetland Environments

In estuarine sediments, methylmercury production rates are often highest a few centimeters below the sediment surface (Marvin-DiPasquale & Agee 2003), and MeHg measurements made in sediment cores have shown maximum MeHg concentrations at depths between 0 and 6 cm (Choe et al. 2004, Hammerschmidt et al. 2008, Mitchell & Gilmour 2008). As a result, surficial sediment samples are often collected to evaluate MeHg concentrations in an ecosystem. In addition to varying with depth, MeHg concentrations can vary from near shore submerged sediments, to mudflats, and into vegetated tidal marsh habitats (Canario et al. 2007, Hall et al. 2008). Within a tidal marsh, MeHg concentrations can also vary between low and high marsh elevations and between edge and interior sites with different species of dominant vegetation, where high-elevation and interior sites often exhibit the highest MeHg concentrations (Choe et al. 2004, Heim et al. 2007, Windham-Myers et al. 2009).

Wetland vegetation also may play an important role in net MeHg production in salt marshes (Marvin-DiPasquale et al. 2003, Valega et al. 2008, Windham-Myers et al. 2009), as plants significantly alter the biogeochemistry of the rhizosphere and may cause shifts in sulfur and iron cycling (Hyun et al. 2009, Hyun et al. 2007). In addition to directly altering the redox conditions of the rhizosphere through radial oxygen loss from roots, wetland plant species may affect net mercury methylation via the secretion of readily degradable organic acids. These small organic compounds provide a carbon source for microbial metabolism, and have the potential to increase metabolic rates of microbial communities. In this way, plants can increase the production of MeHg, which may account for the elevated concentrations of MeHg associated with vegetated wetland sediments (Windham-Myers et al. 2009). Additionally, wetland vegetation may play an important role in the transfer of mercury to the food web in tidal marsh environments, because plant species translocate mercury from the sediments into the aboveground biomass, which can then be transferred to the food web by direct grazing of live plants or through the consumption of detritus (Best et al. 2008).

Bioturbation by burrowing macrofauna also can influence methylmercury production rates and MeHg concentrations in sediments (Benoit et al. 2006, Hammerschmidt et al. 2004). As the density of infaunal burrows increases, there is a greater surface area at the boundary between oxygenated water and sulfate-reducing sediments located just below the sediment-water interface. Additionally, the presence of burrows can increase fluxes of MeHg from sediments to the surface water (Hammerschmidt & Fitzgerald 2008), because biological irrigation can increase the exchange of solutes by as much as five times relative to diffusion (Schluter et al. 2000).

1.2.4 Mercury in the San Francisco Bay-Delta Estuary

While mercury pollution is a global problem, it is of special concern in the San Francisco Bay-Delta estuary, where there are substantial additional regional and local sources of inorganic mercury. Historic mining activities, including the use of mercury in hydraulic gold mining in the Sierra Nevada mountains and mercury mining in the California Coast Range mountains have increased inorganic mercury loading through transport from tributaries and rivers (Conaway et al. 2007, Conaway et al. 2004). The continual transport of mercury from upstream sources, in addition to atmospheric deposition has resulted in elevated mercury concentrations in the water, sediments, and biota of the Bay-Delta (Macleod et al. 2005, Yee et al. 2011).

The Bay-Delta estuary is an important migration and wintering site for over 1.5 million waterbirds on the west coast of North America (Takekawa et al. 2002), and its wetlands have been identified as critically important for shorebirds on the Pacific Flyway migration route (Page et al. 1999). As a result, elevated mercury levels in the estuary can impact both resident breeding populations as well as migratory birds that utilize the area for a portion of the year. Mercury concentrations in the blood of migrant birds tend to increase with time spent in the estuary. For example, MeHg concentrations in surf scoters (*Melanitta perspicillata*) tripled during their six-month overwintering, and Forster's terns (*Sterna forsteri*) showed up to a 5-fold increase in blood mercury concentrations between their arrival time and the start of breeding (Eagles-Smith et al. 2009). The importance of salt marshes to the transfer of mercury to shorebird populations also has been demonstrated, where species that frequent salt marsh and salt pond habitats had higher concentrations than similar species that utilized tidal mudflat or open bay habitats (Eagles-Smith et al. 2009). In addition, mercury concentrations are higher in forage fish that utilize mudflat and wetland habitats compared to those that use offshore environments in the Bay-Delta (Greenfield & Jahn 2010).

To address concerns related to mercury in the estuary, a variety of studies have been carried out to assess MeHg sources and concentrations in different components of the Bay-Delta ecosystem. These studies suggest that wetland environments have elevated MeHg concentrations compared to other habitat types in the Bay-Delta (Choe et al. 2004, Heim et al. 2007, Marvin-DiPasquale et al. 2003). However, these sources of MeHg vary among wetland types. For example, caged fish were placed at the outlet of geographically co-located permanently flooded wetlands and seasonally flooded wetlands used for rice production. Fish associated with the agricultural wetlands showed up to a 12-fold increase in mercury concentrations, while the fish associated with the permanent wetland only showed a 3-fold increase (Ackerman & Eagles-Smith 2010).

The legacy contamination of mercury within the Bay-Delta ecosystem has led regulators to question whether or not increased wetland area would detrimentally affect the wildlife and people using the restored habitat (Wood et al. 2006). In response to these concerns, the Basin Plan Amendment to the San Francisco Bay Basin Water Quality Control Plan (CSWRCB 2006) stated that the San Francisco Bay mercury Total Maximum Daily Load (TMDL) will "include provisions that the restored wetland region be designed and operated to minimize methylmercury production and biological uptake, and result in no net increase in mercury or methylmercury loads to the Bay." How to achieve these objectives in a cost-effective manner is a serious challenge for researchers, regulators, and land managers.

1.3 Motivation and Objectives

1.3.1 Motivation

To balance the need for wetland restoration and conservation with concerns over increased MeHg concentrations from restored wetlands, it is desirable to minimize the potential for mercury methylation while maximizing the benefits provided by wetland ecosystems. While the scientific community has made great strides towards understanding the complex fate and transport of mercury within the aquatic environment, there has been very little research into actual landscape-scale controls that could be implemented during wetland restoration and construction to help decrease the production and export of MeHg.

This dissertation describes research carried out to assess the efficacy of one such control method, the amendment of sediments with iron to reduce net MeHg production and export in tidal wetland sediments from San Francisco Bay. In addition, the long-term monitoring of the complex and interconnected cycling of sulfur, iron, and mercury provided new insights into temporal variations affecting MeHg exports from tidal salt marsh sediments.

1.3.2 Control of MeHg Production Via Iron Amendment

The concentrations of MeHg in water, sediment, and biota are affected by complex processes that regulate the net production and transport of MeHg. When considering potential controls that could be implemented to reduce MeHg concentrations, each step of the aquatic mercury cycle should be considered. Potential approaches for controlling MeHg in wetlands include limiting diffusion of MeHg from the sediments by installation of a layer of uncontaminated sediments or by connecting the outlet of a seasonal wetland to a permanent pond (Heim et al. 2010). While minimizing contact between contaminated sediments and bacteria or installation of ponds to augment MeHg loss might be useful, it could prove more practical to control the *in-situ* production of MeHg. If it is possible to decrease the bioavailability of inorganic mercury for methylation in the sediments, the net production of MeHg will decrease, ultimately resulting in decreased concentrations of MeHg in wetland sediments, water, and biota. The research described in this dissertation addresses the potential for using an iron sediment amendment for this purpose.

As described in Section 1.2.1, sulfide controls mercury solubility and speciation under anoxic conditions. Addition of iron has the potential to alter the activity of sulfide, which in turn, alters mercury bioavailability. The presence of reduced iron (i.e., Fe[II]) in sediment porewater can decrease the concentration of dissolved sulfide through the formation of $FeS_{(s)}$ and other minerals. Because sulfide is the strongest ligand for Hg[II] under anoxic conditions, the decrease in sulfide activity should result in a decrease in the concentration of soluble inorganic mercury. The reduction in the concentration of dissolved Hg[II] should also decrease the concentration of uncharged, bioavailable mercury-sulfide complexes. Research in freshwater (Smolders et al. 1995, Van der Welle et al. 2007) and marine (Ruiz-Halpern et al. 2008) environments conducted to develop ways to minimize sulfide toxicity to plants (Marba et al. 2008) has shown that the addition of ferrous iron to anoxic sediments can result in substantial reductions in the concentration of sulfide in sediment porewater. However, the use of iron addition to control

mercury bioavailability and methylation has been limited to laboratory experiments conducted under simple, well-controlled conditions.

Previous research demonstrated that the addition of ferrous iron to pure cultures of the sulfate reducing bacteria *Desulfobulbus propionicus* (1pr3) in a closed anoxic system decreased net mercury methylation by approximately 75% relative to controls without changing microbial metabolic rates during a three day incubation (Mehrotra et al. 2003). A follow-up study, with anoxic incubations of sediment slurries collected from five estuarine wetlands around the San Francisco Bay, also indicated a similar reduction in net MeHg production relative to controls, suggesting that the presence of diverse bacterial communities and natural minerals did not affect the process (Mehrotra & Sedlak 2005). Since these studies were published, this approach has been reproduced with sediments from other locations (Han et al. 2008, Liu et al. 2009).

Although the results of these laboratory studies were promising, they were limited to a period of seven days or less. Furthermore, the sediments used in these studies were amended with mercury at levels greater than those typically encountered in wetland environments, and the experimental design (e.g., use of closed containers, absence of plants) excluded many of the environmental factors that drive biogeochemical processes within actual wetland systems.

In addition to decreasing sulfide concentrations to control dissolved mercury concentrations, the formation of iron-sulfur minerals from the amended iron could also impact mercury bioavailability by serving as a sink for mercury. For example, synthetic forms of $FeS_{(s)}$ are efficient scavengers of inorganic Hg via surface sorption processes when molar ratios of Hg to $FeS_{(s)}$ are below 0.05 (Jeong et al. 2007). Additionally, the formation of pyrite ($FeS_{2(s)}$) in the sediments has the potential to further influence mercury bioavailability because inorganic Hg can coprecipitate with authigenic pyrite in marine sediments (Huerta-Diaz & Morse 1992) and Hg[II] can be effectively adsorbed to pyrite surfaces under anoxic conditions (Bower et al. 2008). Methylmercury does not form a solid MeHg-sulfide mineral, however, its ability to form surface complexes with iron-sulfur minerals has not been well studied and could potentially be an important process controlling the export of MeHg from sediments.

1.3.3 Objective 1 – Evaluate iron addition in sediment microcosms

While the previous sediment incubation studies provided evidence in support of the iron addition strategy, it was still unclear if an iron amendment would be effective under field conditions. To bridge the gap between simplified short-term anoxic incubations and long-term field studies, experiments were conducted in sediment microcosms operated under controlled laboratory conditions. Exposure of intact sediment cores to a simulated tidal cycle made it possible to extend the duration of the studies to several months, while preserving the vertical stratification of solutes and redox conditions within the sediments, simulating the replenishment of electron acceptors by tidal cycles, and allowing the exchange of H_2S and O_2 with the atmosphere. Additionally, because a large volume of sediment (approximately 22 kg) was used, it was possible to conduct the experiments at ambient mercury concentrations, eliminating the potential for artifacts related to amending samples with mercury.

1.3.4 Objective 2 – Evaluate iron, sulfur, and mercury cycling under field conditions

As described in the previous sections, the cycling of iron, sulfur, and mercury in tidal wetlands is a complex process, with the combination of daily tides, plants, and a highly productive microbial community resulting in temporal and spatial variability in MeHg production and export. To apply findings from laboratory microcosm experiments to field conditions, the concentration of iron, sulfur, and mercury in surficial sediments and porewater at a field site in the Gambinini Marsh were studied for a 17-month period. In addition, data were collected from four other wetlands in the estuary, to determine if results from experiments conducted at the field site might be applicable to other tidal salt marshes in San Francisco Bay. Sediment incubation experiments, conducted using both laboratory and field conditions, were used to evaluate iron, sulfur, and mercury cycling in the presence and absence of sulfate-reduction, and to compare *in-situ* biogeochemical cycling between seasons.

1.3.5 Objective 3 – Test iron addition under field conditions

While laboratory experiments utilizing sediment incubations and microcosms can help to elucidate the mechanisms through which iron addition reduces net MeHg production, an assessment of the true efficacy of the approach requires experiments conducted under field conditions. Studies at the test-plot scale are important because it is extremely difficult to simulate all of the environmental variations encountered within an actual tidal wetland. For example, tidal wetlands experience seasonal variations in sunlight, temperature, vegetation, and salinity as well as varied sediment composition and inorganic mercury loading levels. By conducting an iron addition experiment in the field and monitoring the effect on net MeHg production over the 17-month observation period, it was possible to gain insight into the efficacy of an iron amendment within an existing tidal wetland and to indentify factors affecting the performance of the approach.

Chapter 2. Impact of Iron Amendment on Net Methylmercury Export from Tidal Wetland Microcosms

Reprinted with permission from Ulrich, P. D.; Sedlak, D. L. Impact of Iron Amendment on Net Methylmercury Export from Tidal Wetland Microcosms. *Environmental Science & Technology* **2010**, *44* (19), 7659-7665.

Copyright 2010 American Chemical Society.

2.1 Introduction

During the past 200 years, wetlands have been drained or filled to increase agricultural productivity or to make land more suitable for habitation (Dahl 1990). In recognition of the ecosystem services that wetlands provide, this trend has recently been reversed in many locations worldwide. A potential drawback to wetland restoration, however, is the formation and subsequent bioaccumulation of monomethylmercury (MeHg). MeHg can lower the reproductive success and survival of piscivorous birds and mammals (Wolfe et al. 1998), as well as benthic omnivores endemic to tidal wetlands (Schwarzbach et al. 2006). The primary exposure pathway of MeHg for humans is through the consumption of fish, and most fish advisories are due, at least in part, to elevated levels of MeHg (EPA 2009).

Under the anoxic conditions typical of wetland sediments, mercury methylation is primarily mediated by sulfate-reducing bacteria (Compeau & Bartha 1985; Gilmour et al. 1992), although iron-reducing bacteria are also capable of methylation (Fleming et al. 2006; Kerin et al. 2006). Because mercury methylation is predominantly a biotic process, the production rate of MeHg depends on both bacterial activity and the bioavailability of Hg[II]. In the presence of S[-II] produced by sulfate-reducing bacteria, Hg[II] solubility and speciation is controlled by cinnabar ($HgS_{(s)}$). Under these conditions, the uptake and subsequent methylation of Hg[II] depends upon the concentration of uncharged mercury complexes (e.g., HgS^0 and $Hg(HS)_2^0$) that are capable of passively-diffusing into bacterial cells (Benoit et al. 1999; Drott et al. 2007b). Dissolved organic matter in sediment porewater affects the bioavailability of mercury by enhancing Hg[II] dissolution and preventing the precipitation of cinnabar (Ravichandran et al. 1999). Organic matter in sediments can also alter Hg[II] speciation and bioavailability, and stimulate microbial activity, which in turn enhances MeHg production (Lambertsson & Nilsson 2006).

Due to their high productivity and anoxic sediments, tidal wetlands typically contain elevated concentrations of MeHg (Canario et al. 2007; Hall et al. 2008; Mitchell & Gilmour 2008). Thus, tidal wetland restoration has the potential to exacerbate existing mercury contamination problems by increasing concentrations of MeHg. In recognition of this potential problem, the merits of wetland restoration without simultaneous control of MeHg have been questioned (CSWRCB 2006). To facilitate the restoration of coastal wetlands without increasing MeHg, landscape-scale controls are needed.

Previous incubation studies in both pure cultures and tidal wetland sediment slurries have demonstrated the use of a ferrous iron (Fe[II]) amendment to lower dissolved sulfide concentrations via the formation of $FeS_{(s)}$, which subsequently decreased the pool of bioavailable neutral mercury-sulfide species (Mehrotra et al. 2003; Mehrotra & Sedlak 2005). This approach has since been reproduced in experiments using sediments from other locations (Han et al. 2008; Liu et al. 2009), but the efficacy of the process has not been demonstrated under the complex conditions encountered in tidal marshes.

In this Chapter, the potential for reducing MeHg production and export was evaluated in microcosms that approximated the conditions encountered in a tidal marsh, using sediments and plants from a tidal wetland that contained elevated concentrations of mercury from historical mining activities (Conaway et al. 2007). This is the first study to demonstrate the efficacy of this approach under simulated field conditions and at ambient mercury concentrations. By exposing intact sediment cores to a simulated tidal cycle we were able to extend the studies to several months, preserve vertical stratification of solutes and redox conditions within the sediments,

simulate cycling of electron acceptors by tidal cycles, and allow the exchange of H_2S and O_2 with the atmosphere.

2.2 Methods

2.2.1 Microcosm Collection and Operation

Intact sediment cores (50 x 25 x 15 cm) were collected from the Gambinini Marsh, a tidal salt marsh near Petaluma, CA (38.207°N,122.584°W), that has tidal exchange with the Petaluma River, which drains into San Pablo Bay in the San Francisco Bay estuary. The marsh is dominated by a large area of monoculture growth of pickleweed (*Sarcocornia pacifica)*, and the sediment was highly organic near the surface (typically around 20-30% loss on ignition) with a dense layer of roots throughout the top few centimeters. Twelve sediment cores were collected from the same area of the marsh plain that had a similar density of pickleweed for the devegetated experiment in October 2007 and for the vegetated experiment in September 2008.

The microcosms consisted of an intact sediment core placed into a 50 x 25 x 30 cm acrylic aquarium (GlassCages.com, Dickson, TN). The sediment had a clay-like consistency below the root layer and held together easily, which facilitated the collection of intact cores. Hand shovels were used to cut out a block of sediment that was measured to be the approximate surface area of a microcosm, and that was deeper than the desired 15 cm depth. These blocks of sediment were carefully pulled up out of the ground using the shovels, and the bottom of the core was leveled off to a depth of 15 cm. This created an in-tact block of sediment that was approximately 50 x 25 x 15 cm in size. This sediment core was then picked up by multiple people to ensure that it stayed intact while it was placed into a microcosm container. Additional sediment was added to the core edges as necessary to prevent pooling of surface waters and minimize short circuiting.

Microcosms were transported back to the laboratory immediately after collection and connected to a simulated light and tidal system (Figure 2-1). Two 1000-W metal halide grow lamps were operated on a daily automated schedule of 15 hours of light, 9 hours of darkness. The microcosms were separated into two sets of six, and each group was placed under one grow lamp to provide uniform light coverage over the entire microcosm area. Each microcosm was connected to an individual reservoir (14-L HDPE plastic bucket) that contained 5 L of simulated estuarine water at a salinity of around 12 parts per thousand. The simulated estuarine water was made by mixing deionized water with Instant Ocean aquarium salts to the desired salinity, followed by the addition of half-strength Hoagland's Nutrient Solution reagents to support microbial and plant growth. The microcosms were operated on a weekly basis, where the water was sampled and then replaced by fresh simulated estuarine water on the first day of the week and was kept in the reservoir for 7 days. Since evaporation of the reservoir water occurred during exposure to the grow lamps, additional deionized water was added to bring each reservoir back to approximately 5 L in total volume during the middle of the week.

A simulated tidal regime was provided via a system of automated multichannel peristaltic pumps. Inlet and outlet ports were drilled in the acrylic microcosm before sample collection and were fitted with PTFE connectors for the FEP tubing (0.125-in o.d.) used to provide the surface water supply. To minimize potential clogging of the effluent line due to sediment settling, water

was brought in at the sediment surface via the lower port, and sent out using a short length of FEP tubing oriented vertically from the top port such that its opening was just above the sediment surface. The simulated tidal regime included two uniform high-tide events during each 24-hour period; one during the morning daylight hours and one during the dark overnight period. For these events, the inlet pump was turned on for 1 hour of incoming tide which gave between 1 and 2 cm of surface water over the microcosm sediments. The surface water then was retained in the microcosm for 1 hour before the effluent pump was turned on for 1 hour to drain the surface water. This resulted in the sediments being covered in surface water for a maximum of 6 hours per day with the remaining 18 hours open to exchange with the atmosphere. The microcosm system was checked daily for clogs in tidal system lines, which occasionally occurred due to uptake of solid material into the effluent tubes. When this occurred, the clog was removed or that section of tubing was replaced and the outgoing pump was turned on for a sufficient time to drain the remaining surface water. To reduce the growth of algae, aluminum foil was placed around the sediment filled portion of the microcosms, as well as over the inlet and outlet lines, and around the plastic reservoir buckets.

Twelve microcosms were used in this setup for both the devegetated and vegetated experiments. To provide continuity between experiments, a devegetated control was included in the vegetated experiment at the expense of being able to include a vegetated group at all three iron doses. Since the response of the medium and high dose groups was similar in the devegetated experiment, only the medium dose group was used in the vegetated experiment. The selection of the medium group was advantageous since future studies at the field scale would be most informed by knowing what the lowest effective dose is, since managers would want to minimize iron addition to keep costs lower and help reduce the potential for negative effects.

Figure 2-1. Laboratory microcosm setup used for the two experiments. The vegetated microcosms are shown, and this image was taken during the initial setup before the aluminum foil was added to the sides of the tanks up to the height of the sediment surface.

2.2.2 Iron Sediment Amendment

For the devegetated experiment, microcosms were equilibrated under laboratory conditions for 4 months before the aboveground vegetation was removed. 100 g of dried pickleweed collected from the microcosms was added to the sediment surface. The microcosms were randomly assigned to one of four iron treatment groups (n=3 per group): a control dose (0 g-Fe/m^2), a low dose (180 g-Fe/m^2), a medium dose (360 g-Fe/m^2), and a high dose (720 g-Fe/m^2). These dosing levels were selected such that the dose applied to the medium group would approximately double the reduced iron initially present in the sediments, assuming that all of the measured acid-volatile sulfides (AVS) consisted of $FeS_{(s)}$. These application rates were similar to the ranges used for the suppression of methane production in rice paddies (Jackel et al. 2005) and phosphorus removal in treatment wetlands (Ann et al. 2000), and were around an order of magnitude higher than those used to reduce sulfide toxicity in seagrass beds (Ruiz-Halpern et al. 2008).

The iron amendment solution consisted of 0.28-1.1 M $FeCl_2$ in a de-aerated 1.0-2.0 M Na_2CO_3/$NaHCO_3$ buffer adjusted to pH 7. The amendment occurred over 3 days, with 0.5 L of solution being amended in around 20 minutes per day, for a total injection volume of 1.5 L per microcosm. Plastic syringes (20 mL) with stainless steel needles were used to inject the solution at a depth of 2.5 cm using a grid pattern of 32 injections per day (a row of 4 injections across the width, and 8 rows down the length) to ensure coverage over the entire area of the sediments. For the control group, a suspension of 1.0 M $CaCO_{3(s)}$ was injected under the same conditions.

For the vegetated experiment, microcosms were allowed to equilibrate to the laboratory conditions for a period of 3 weeks before the iron amendment. The 12 tanks were randomly assigned into 4 treatment groups (n=3 per group): a control with no iron added and the above-ground vegetation removed (devegetated control), and a control, low, and medium iron dose with the vegetation present at doses of 0, 180, and 360 g-Fe/m^2, respectively. The iron was amended in the same manner as in the devegetated experiment, and the control group also received a suspension of 1.0 M $CaCO_{3(s)}$.

2.2.3 Sample Collection

During the course of the experiment, surface water and porewater samples were collected from each microcosm for the measurement of a variety of parameters at weekly or biweekly intervals. For the devegetated experiment, samples were collected weekly for Weeks 1-4, biweekly for Weeks 6-14, and for the final collection in Week 17. For the vegetated experiment, samples were collected weekly for Weeks 1-4, then biweekly for Weeks 6-8. Surface water was collected from the reservoir following the morning high tide before the reservoir water was replaced for the week by submerging the sample vessel under the water surface in the reservoir and filling to no headspace. The total volume of surface water remaining in the reservoir was also measured to correct for differences in evaporation between microcosms (typically less than 25% for the devegetated microcosms and less than 15% for the vegetated microcosms), and surface water data are reported as normalized to the initial 5 L reservoir volume concentration. After sample collection, the reservoir was refilled with 5 L of simulated estuarine water

Samples for mercury analysis were collected into acid-cleaned glass jars with Teflon-lined lids, and were preserved with H_2SO_4 for MeHg samples and HCl for total mercury samples.

New polypropylene test tubes were used to collect samples for sulfate, dissolved iron, and total organic carbon. Samples for iron analysis were preserved with HNO_3, and samples for sulfate and organic carbon analysis were kept at 4 °C or frozen until analysis.

Prior to the experiment, a permanent in-situ porewater sampler (10-cm Rhizon Soil Moisture Sampler; Rhizosphere Research Products, Netherlands) was installed in each microcosm at a depth of 3.5-cm, with an average pore size of 0.1 μm. On sample collection days, around 7-mL of porewater was collected in a 10-mL plastic syringe from each sampler for the measurement of dissolved sulfide, sulfate, total dissolved iron, pH, and dissolved organic carbon. Dissolved sulfide and pH were measured immediately following collection, and samples for sulfate and organic carbon analysis were acidified with HCl and purged with N_2 to remove sulfide before being stored at 4 °C or frozen until analysis, and porewater iron samples were preserved with HNO_3.

Following the end of the water sample collection period for the experiments, sediment cores were collected from each microcosm using acrylic tubes (6-cm i.d.), and were sectioned at 1-cm resolution to a depth of 10-cm. For the devegetated sediment experiment, sediment cores were taken between 6-8 weeks after the last surface water measurements, during which time the microcosms were continued under the standard tidal conditions. Triplicate cores were collected from each microcosm from random positions at least a 2-3 cm away from the walls of the aquarium, and the cores were immediately sectioned using plastic tools. It is important to limit the reoxidation of reduced species present in the sediments during sampling (Drott et al. 2007a), and care was taken to minimize the exposure time of the sediment samples to the air during the dissection process. The depth layers from each of the triplicate cores were sectioned at the same time, and a subsample of each layer was combined into a single composite sample to account for spatial variability. To minimize exposure to the air, a section from the interior of each core slice was quickly homogenized and a subsample was immediately analyzed via sequential extraction to determine acid-volatile sulfides (AVS) and chromium reducible sulfur (CRS, the pyritic experimental fraction) concentrations.

For the vegetated experiment, triplicate cores were collected for all microcosms during the week following the final water sampling date, and the in-tact cores were capped with rubber stoppers on both ends, wrapped in Parafilm, and frozen until analysis between 4 and 8 weeks later. On the day of analysis, the cores were kept sealed and allowed to partially thaw at room temperature in the dark for just enough time to allow them to be extruded from the acrylic coring tubes. The still frozen cores were sectioned at 1-cm intervals using a hand saw with replaceable stainless steel blades that were rinsed with diluted HCl and replaced between each layer. As in the devegetated sediment experiment, care was taken to minimize exposure time to the air, and composite samples were made from each depth interval by mixing sediments from each of the three individual cores into one sample for analysis. The sections for compositing were allowed to thaw enough to be able to remove a piece from the interior of each, which was then roughly homogenized and immediately subjected to the AVS-CRS extraction.

2.2.4 Analytical Methods

Water and sediment samples were analyzed using established methods. Method detection limits were defined as three times the standard deviation of the blanks, unless otherwise noted.

For samples with concentrations below the detection limit, one-half of the detection limit was used for calculations.

Total iron was measured in water samples by graphite furnace atomic absorption spectroscopy (Perkin-Elmer 3300, average daily detection limit 0.23 μM) and organic carbon was measured via combustion and infrared detection (Shimadzu TOC-5000A, detection limit 0.9 mg/L). Sulfate was measured by ion chromatography (Dionex DX-120, average daily detection limit 21 μM), and porewater sulfide was measured with the methylene blue colorimetric method (detection limit 0.43 μM). Reduced sulfur speciation in sediments was measured using a modified diffusion method for the sequential extraction of AVS and CRS (Hsieh & Shieh 1997), with quantification of trapped sulfide by methylene blue (recovery of a spiked Na_2S standard was 106 ± 17% for AVS and 107 ± 18% for CRS) .

Total mercury in the surface water was measured by BrCl oxidation, reduction with $SnCl_2$, trapping on gold traps, thermal desorption, and cold vapor atomic fluorescence (CVAFS) detection (Bloom & Fitzgerald 1988). The detection limit was computed for each analytical run and had an average of 0.6 pM for a 100 mL bubbler volume. Relative percent difference between duplicate sample bottles averaged 16 ± 17% (n=16), and recovery of Hg spikes into duplicate samples averaged 97 ± 20% (n=10). MeHg in surface water was measured by acidic chloride distillation (Horvat et al. 1993; Olson et al. 1997), aqueous phase ethylation, collection on Tenax traps, thermal desorption, GC separation, and detection by CVAFS (Bloom 1989). Percent recovery of MeHg spiked into a distillation blank averaged 103 ± 11% (n=13), recovery of MeHg spikes into duplicate samples averaged 95 ± 28% (n=17) with relative percent difference of duplicate samples of 23 ± 21% (n=16), and recovery of distilled NIST mussel tissue standard (NIST SRM 2976) was 93 ± 17% (n=11). The detection limit was defined as 0.9 pM, which was the typical lowest point on the daily calibration curve in a 55 mL sample.

2.3 Results

2.3.1 Dissolved Sulfur and Iron in Devegetated Microcosms

Samples were collected over a 17-week period following the iron amendment. A pump failure occurred during Week 6, which resulted in flooded conditions for approximately 72 hours. During the 2-week period when the pump system was being repaired (Weeks 7-8), the microcosms received a single daily high tide.

Surface water sulfate concentrations (Figure 2-2) exhibited a decrease of approximately 7 mM during the weeklong exposure period. Dissolved porewater sulfide concentrations were decreased by the addition of Fe[II] (Figure 2-3(a)). The low dose group typically showed decreases in weekly porewater sulfide concentrations of greater than 70% relative to the control group, and the medium and high dose groups showed decreases of up to 80 to 90% for most weeks. Porewater sulfate concentrations (Figure 2-4) were similar between the groups each week, with the medium dose group typically having the highest average concentration. The highest iron dose groups had the lowest porewater pH (Figure 2-5), which was expected due to the hydrolysis of the dissolved iron. However, the buffering capacity of the amendment solutions kept all of the dose groups in a circumneutral range, with typical average pH values between 6.4-

7.4, and the lowest values for all groups coming during the week 6 flood event. After the pump system was repaired, the average pH for all groups stayed fairly constant between 6.7-7.3.

The concentration of iron measured in the surface water was similar among the treatment groups, with weekly averages ranging between 0.5 and 27 μM (data not shown). Relatively large differences in the porewater dissolved iron concentrations were observed among the treatment groups (Figure 2-3(b)), with the high-dose groups exhibiting iron concentrations that were up to three orders of magnitude higher than the control. The concentration of porewater iron for both the medium and high treatment groups decreased over the first 12 weeks.

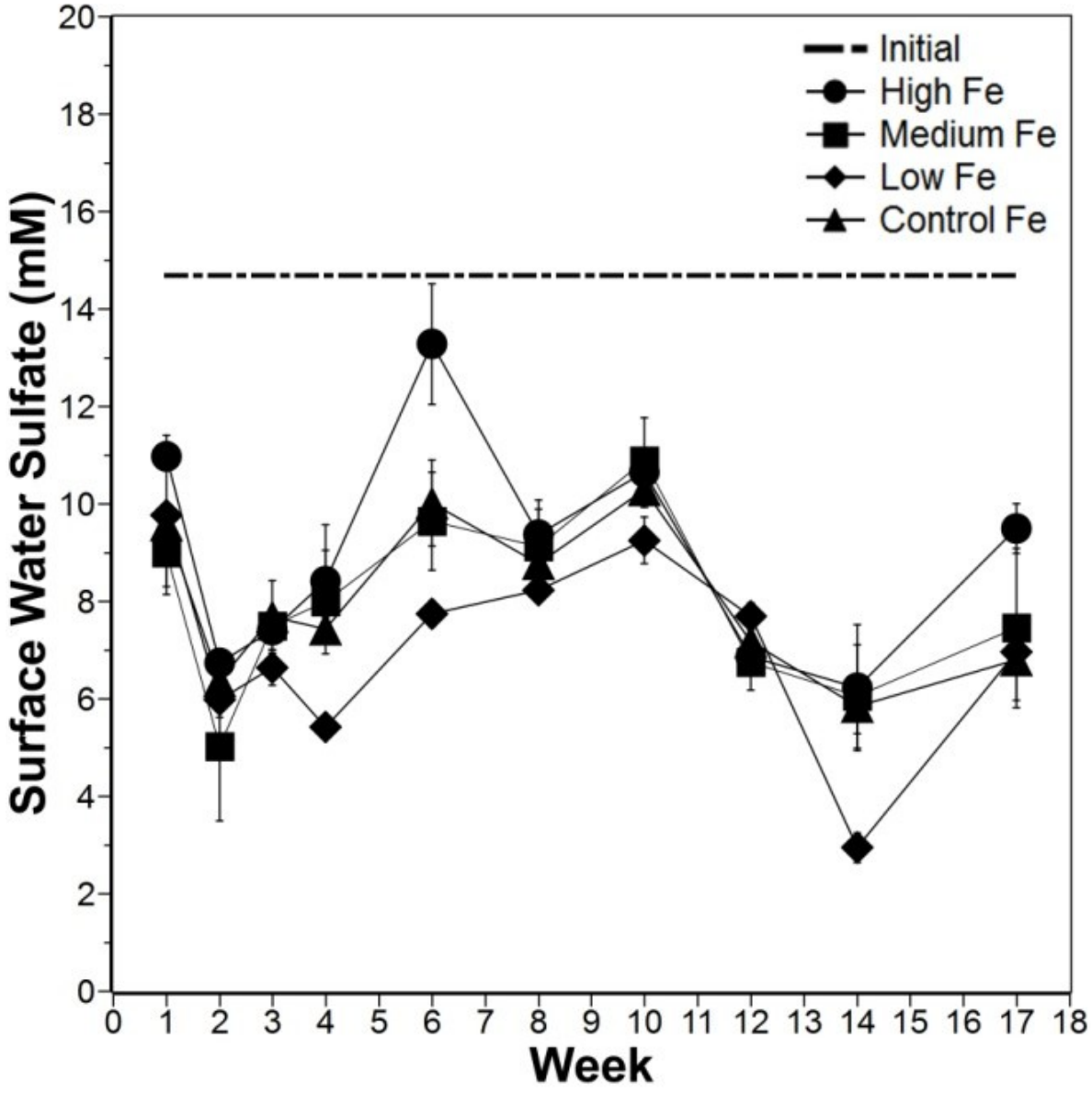

Figure 2-2. Concentration of sulfate remaining in devegetated microcosm reservoirs, normalized to the 5 L volume, after one week of tidal exposure. The dashed line represents the average initial sulfate concentration in the simulated estuarine water each week. Values are average ± standard error for the triplicate microcosms in each group.

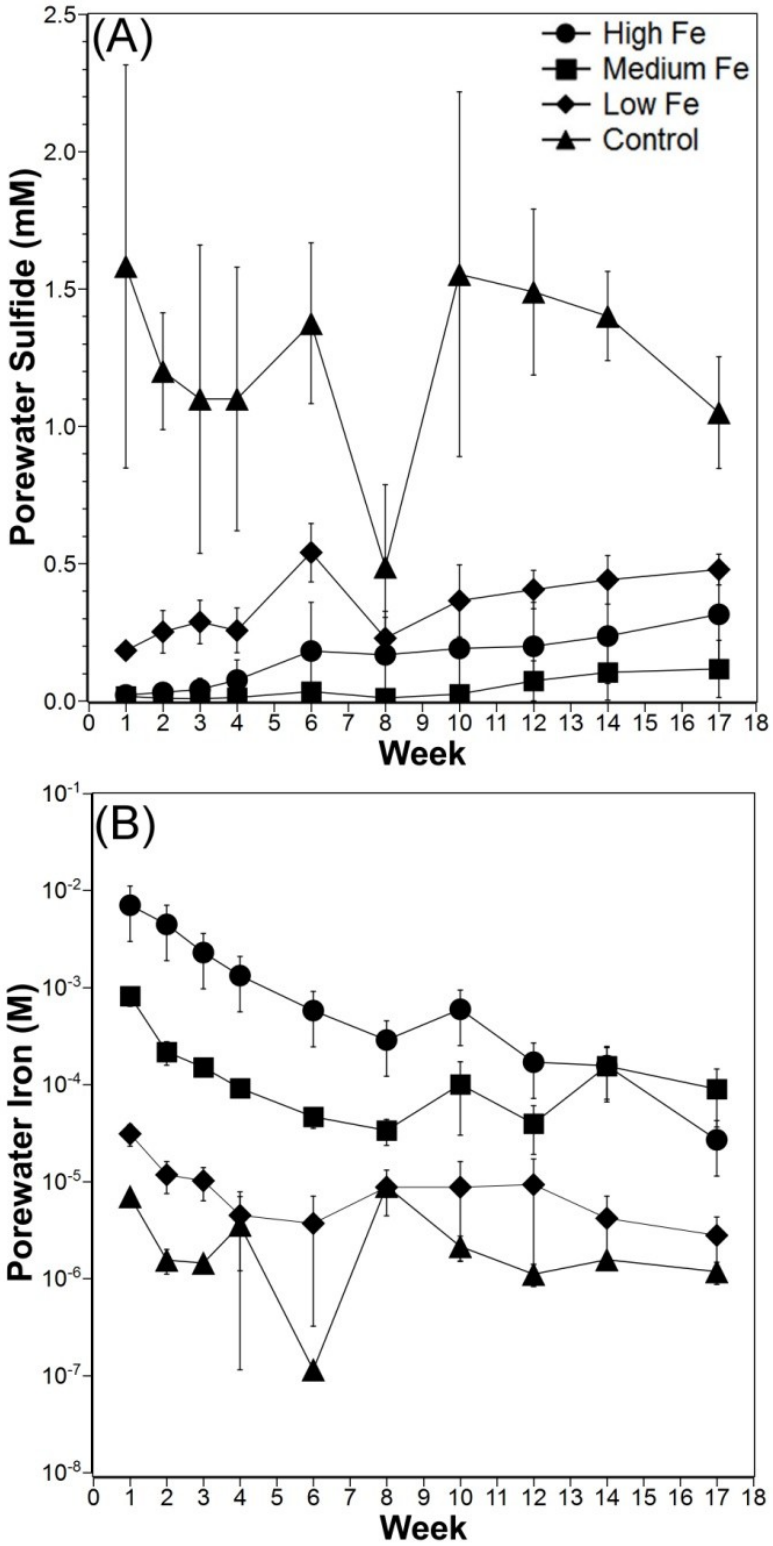

Figure 2-3. Average porewater concentrations in the devegetated microcosms for dissolved sulfide (A) and dissolved iron (B). Values shown are the average concentration of the three replicate microcosms ± standard error for each iron treatment group.

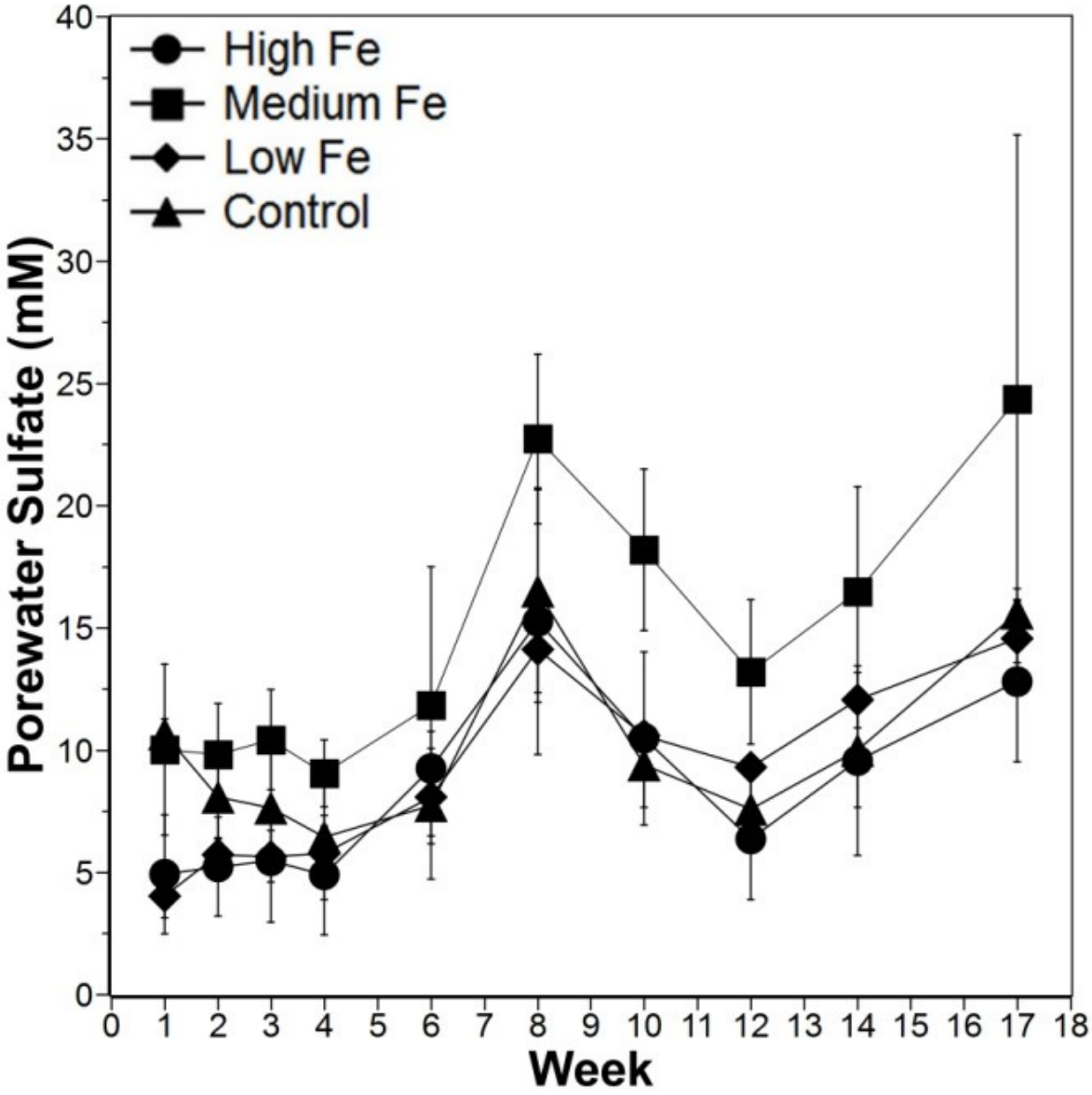

Figure 2-4. Porewater sulfate concentrations for the devegetated microcosms. Values are shown as average of the triplicate microcosms ± standard error.

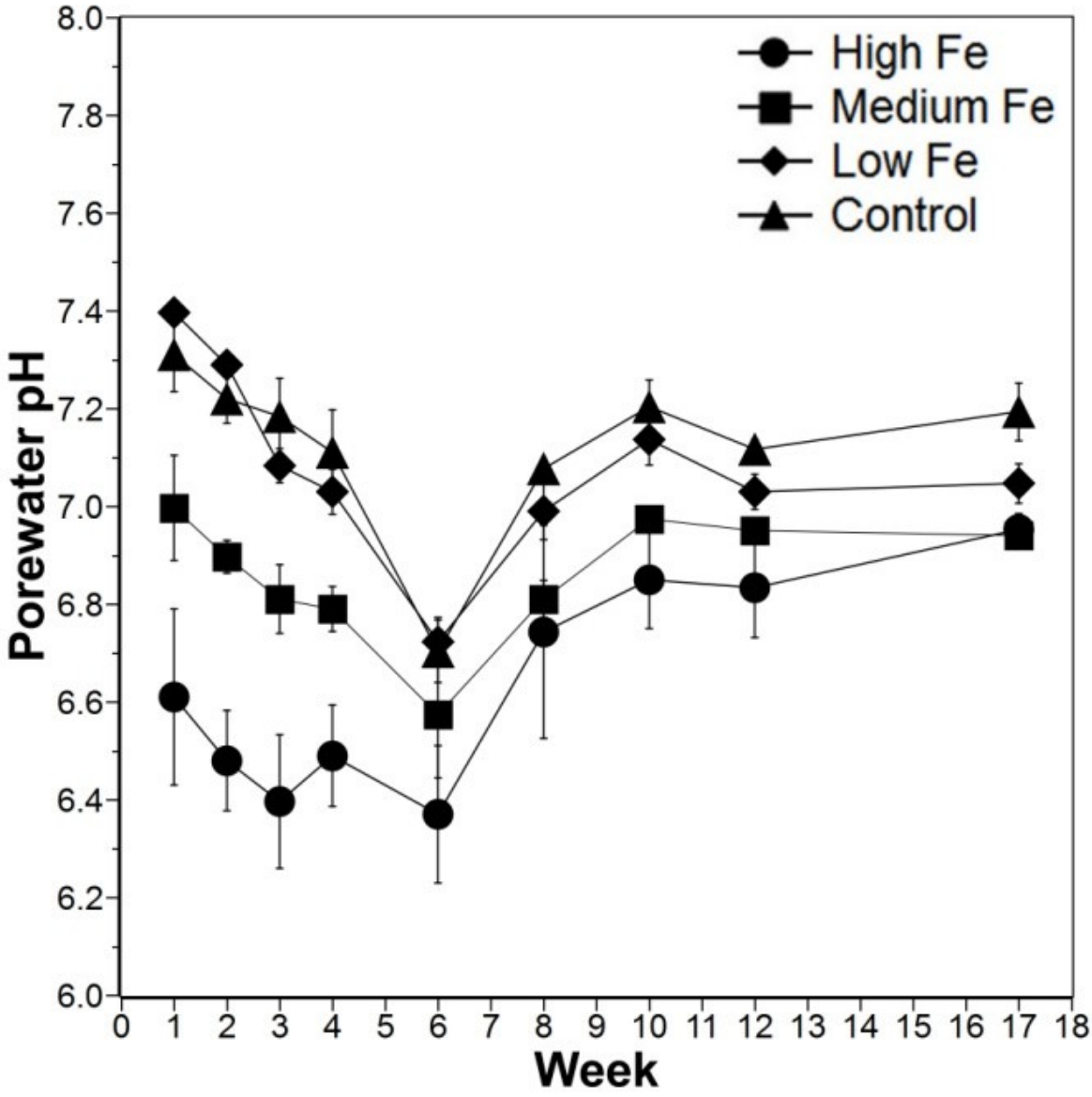

Figure 2-5. Porewater pH values for the devegetated microcosms. pH was not measured in the porewater samples for Week 14. Values are shown as average of the triplicate microcosms ± standard error.

2.3.2 Mercury in Devegetated Microcosms

Total concentration of inorganic mercury in the surface water (defined as the difference between 5 L reservoir normalized concentrations of total mercury and MeHg), was similar among all treatment groups with average concentrations ranging from around 20 to 50 pM, except for Week 6, when the pump failed and average concentrations increased to as much as 90 pM (Figure 2-6). On the basis of equilibrium predictions (Fitzgerald et al. 2007), it is likely that inorganic mercury was associated with chloride or organic matter in the surface water. Dissolved organic carbon (DOC) in the surface water exhibited decreased concentrations for the high dose, and porewater concentrations were fairly constant among treatments (Figure 2-7).

In contrast, methylmercury concentrations in the surface water reservoirs showed clear differences among treatments (Figure 2-8(a)) with the medium and high groups exhibiting average concentrations less than 5 pM and the low dose and control groups exhibiting average concentrations between 10 and 60 pM (see Table 2-1for individual microcosm concentrations). Concentrations of MeHg for the low and control groups were highest during and immediately following the flooded period when the pumps failed. After 12 weeks, the concentrations of MeHg for the low and control groups decreased to levels similar to the medium and high groups.

The average mass of MeHg exported from the sediment porewater to the surface water each week (Figure 2-8(b)) was significantly higher for the low and control treatments compared to the medium and high treatment groups. A one-way ANOVA ($\alpha = 0.05$, $p < 0.001$) followed by a Tukey's HSD test showed that both the medium and high dose groups were significantly different than the control group. The medium dose exhibited an 82% decrease in weekly MeHg export and the high dose showed an 89% decrease. While the low dose group was 57% greater than the control group, the averages were not significantly different.

Throughout the experiment, the low iron dose group typically had an average concentration of surface water MeHg that was greater than the control group. While this increase was not statistically significant, it was consistent with the results of previous studies (Mehrotra et al. 2003; Mehrotra & Sedlak 2005). This phenomenon warrants further attention if an iron amendment is used at the field scale because it would be problematic if elevated MeHg production occurs in areas that receive lower-than-planned iron doses. Previous research indicates that mercury methylation rates in sediment slurries decrease at high sulfide concentrations due to sulfide toxicity (Han et al. 2008). When porewater sulfide concentrations were reduced to below 1 mM by the low iron dose in the microcosms, the rate of sulfate reduction may have increased slightly between Weeks 4 and 10. Elevated sulfide concentrations also can inhibit mercury methylation due to the formation of non-bioavailable mercury-sulfide complexes in sediment porewater (Benoit et al. 1999). If this was the case in the microcosms, it is possible that when the sulfide concentrations were reduced in the low dose group, there was a shift in predominance of dissolved mercury speciation from a charged form to bioavailable HgS^0.

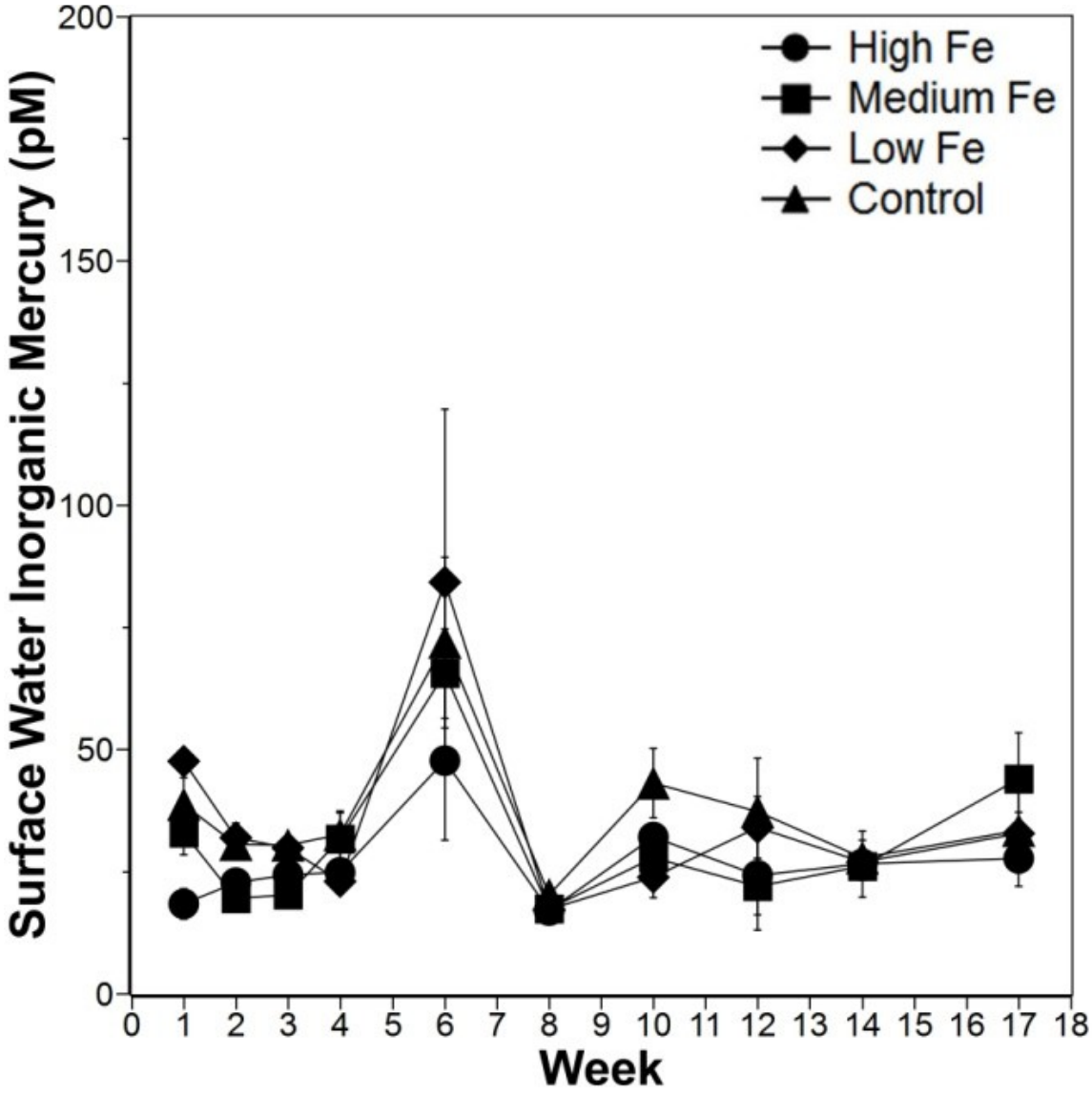

Figure 2-6. Inorganic mercury concentrations (normalized to 5 L reservoir volume) in the surface water for the devegetated microcosms. Values are shown as average of the triplicate microcosms ± standard error.

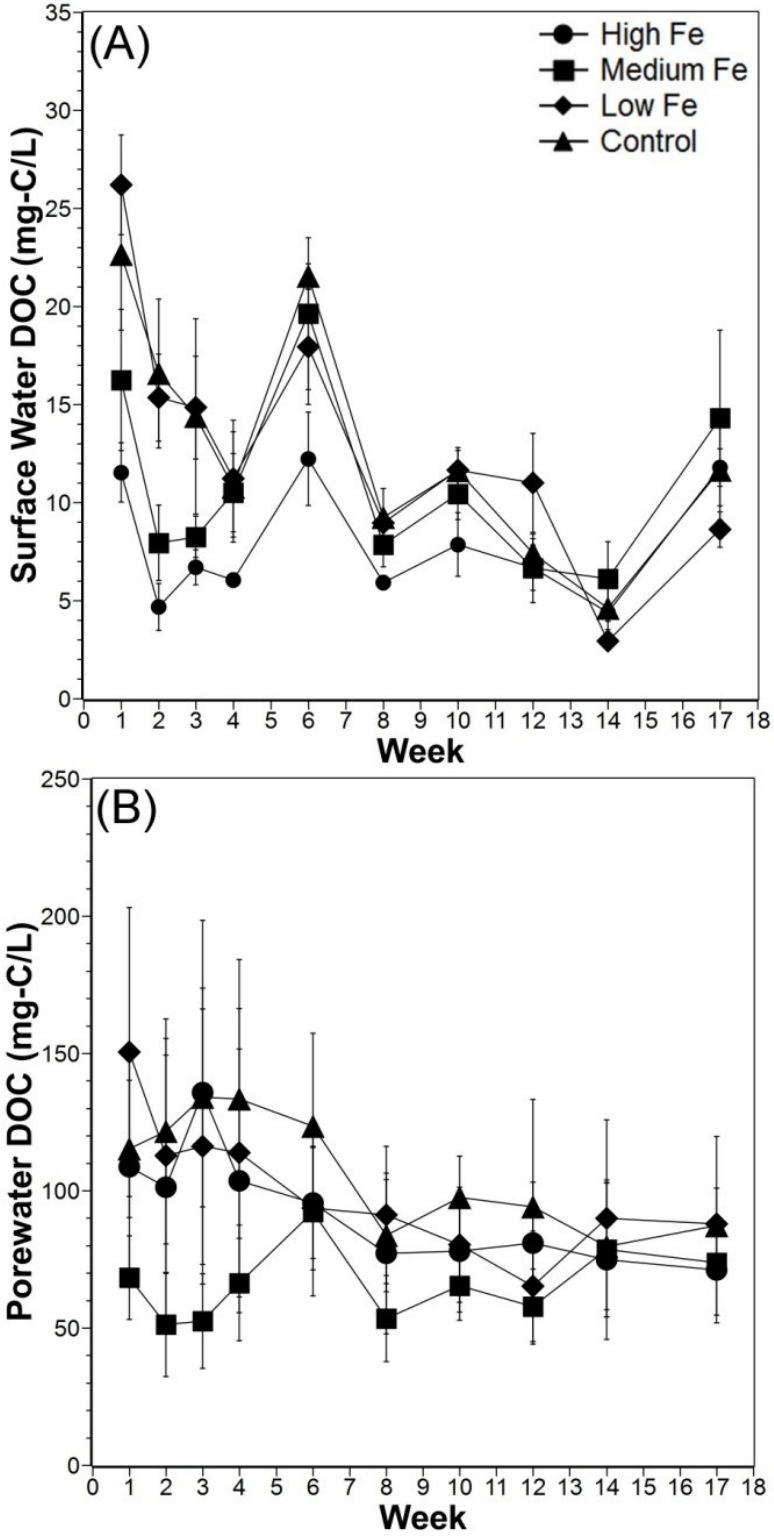

Figure 2-7. Concentrations of dissolved organic carbon (DOC) in (A) the surface water of the devegetated microcosms normalized to the 5 L reservoir volume, and (B) the devegetated microcosm porewater. Values are shown as average of the triplicate microcosms ± standard error.

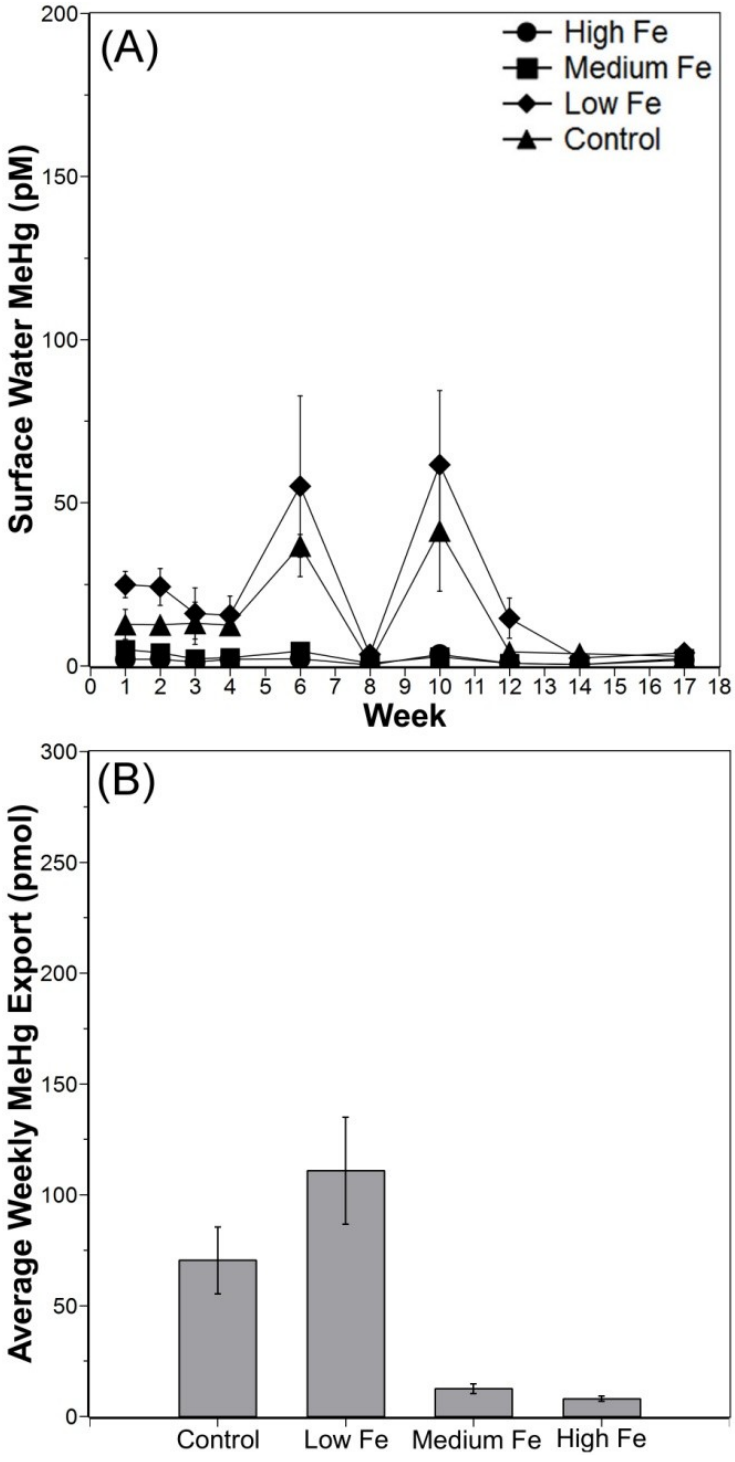

Figure 2-8. (A) Methylmercury measured in the surface water of the devegetated microcosms, normalized to the 5-L reservoir volume, after 7-day exposure to microcosm sediments. (B) Average mass of MeHg exported per week over the experimental period (n=30 per group). The medium and high dose groups were each significantly different (α=0.05, $p<0.001$) than the control, while the low dose group was not significantly different than the control. Values shown are average ± standard error.

Table 2-1. Surface water methylmercury (MeHg) concentrations are shown for the devegetated microcosms. Values are listed in pM, and represent the 5-L normalized concentration. For concentrations that were measured as zero or below quantification, the value used for averaging is listed in parentheses (one half of the quantification limit mass in the distilled sample volume, normalized to 5-L).

Treatment	Tank ID	Week 1	Week 2	Week 3	Week 4	Week 6	Week 8	Week 10	Week 12	Week 14	Week 17
Control	3	11.4	12.6	4.2	8.1	36.5	1.0	14.4	4.2	1.5	4.3
	6	5.4	13.1	9.3	12.8	30.9	0.7	33.0	5.9	6.8	2.5
	8	21.2	12.0	25.6	16.6	43.0	1.1	76.5	2.5	3.0	1.8
Low Fe	1	29.6	13.5	5.3	19.2	55.0	3.5	88.2	17.0	4.5	4.2
	2	16.9	32.8	31.3	23.3	103	5.7	80.2	23.8	2.2	2.1
	7	28.2	26.2	11.6	3.9	7.0	1.1	16.6	2.9	0.0 (0.4)	5.5
Medium Fe	5	4.3	3.3	0.8	1.9	2.3	0.8	1.7	0.0 (0.3)	0.0 (0.3)	4.2
	10	9.2	7.2	4.6	4.4	9.2	1.2	3.9	1.3	0.0 (0.3)	0.7
	11	1.3	1.6	1.0	1.1	1.8	0.3	2.4	0.7	0.4 (0.3)	1.8
High Fe	4	2.9	2.2	0.0 (0.5)	2.5	1.9	0.2 (0.2)	6.1	1.4	0.3 (0.3)	1.7
	9	0.0 (0.3)	1.3	0.0 (0.4)	1.2	1.9	0.0 (0.2)	2.4	0.0 (0.3)	0.0 (0.3)	0.0 (0.4)
	12	2.7	2.4	2.4	2.4	2.5	0.4	2.1	0.6	0.3 (0.3)	3.1

2.3.3 Sulfur Minerals in Devegetated Microcosms

The depth profiles of AVS and chromium reducible sulfur (CRS) concentrations at the end of the experimental period (Figure 2-9) indicated increased formation of AVS for the high dose group at the 2-3 cm depth relative to the other groups. Additionally, all three treatment groups showed elevated concentrations of CRS relative to the control dose over the 2-4 cm depth.

2.3.4 Dissolved Sulfur and Iron in Vegetated Microcosms

Samples were collected from the vegetated microcosms over an 8-week period following the iron amendment. Around Week 4, plants in many of the microcosms had lost their vibrant green color. By Week 8, almost all plants were dormant.

Sulfate concentrations remaining in the surface water after one week of tidal exposure decreased by approximately 6-7 mM, which was similar to the decrease observed in the devegetated experiment (Figure 2-10). Patterns in the porewater sulfide concentrations (Figure 2-11(a)) were not as evident in the vegetated experiment because substantial variability occurred among the triplicate microcosms. On average, the vegetated low and medium dose groups exhibited lower sulfide concentrations than the control, but the variability was large due to a single tank behaving markedly different than the other two. The low and medium dose groups had lower average sulfide concentrations than the vegetated control. The large standard error was caused by one microcosm behaving differently than the other two in the group. For example, in the medium dose group, two of the three microcosms had values below 0.01 mM throughout the 8 week observation period, while a single microcosm (Tank 3) had a sulfide concentration that stayed around 1.0 mM throughout. This trend was also found in the porewater iron data, as Tank 3 of the medium group was again found to behave differently than the other two microcosms, where it had concentrations that were two orders of magnitude smaller than the others. While it is difficult to infer the cause of this variability, the relationship between porewater iron and sulfide are consistent with expectations. Because the porewater iron availability in Tank 3 decreased below 10^{-5} M by Week 2 (similar to the iron concentration found in both control groups), the sulfide concentrations were able to build up in the porewater because there was not enough iron present to precipitate an iron-sulfur mineral.

Dissolved iron concentrations in the porewater (Figure 2-11(b)) exhibited trends similar to those observed in the first experiment with the highest iron doses having the highest concentrations. However, concentrations were around an order of magnitude higher than those measured for the corresponding dose in the devegetated experiment. The vegetated control generally showed lower average iron concentrations than the devegetated control.

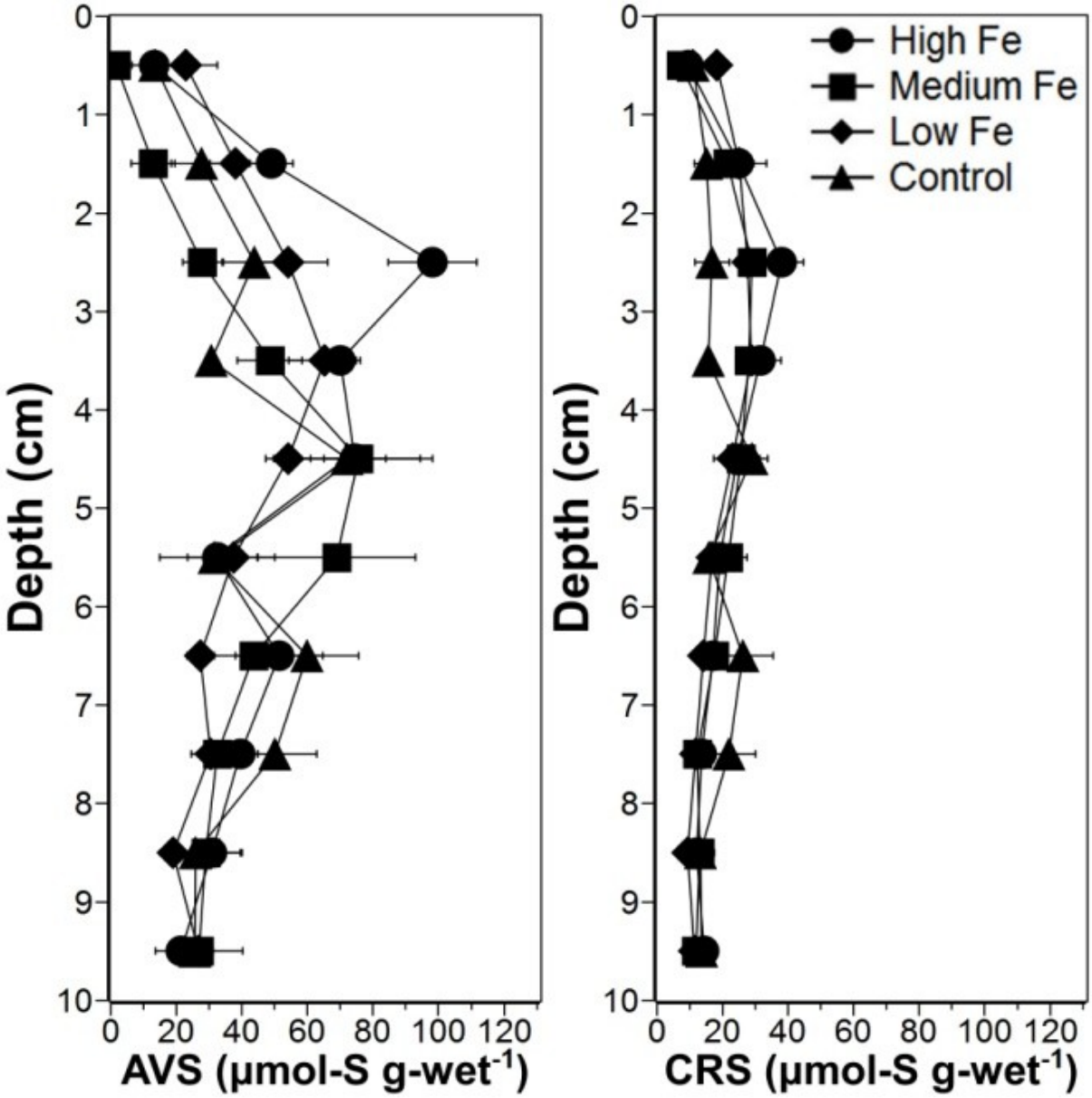

Figure 2-9. Depth profiles of reduced sulfur speciation in the devegetated microcosms collected at the end of the experiment for the top 10-cm of sediments from composite core samples. Values shown as average of triplicate microcosms ± standard error.

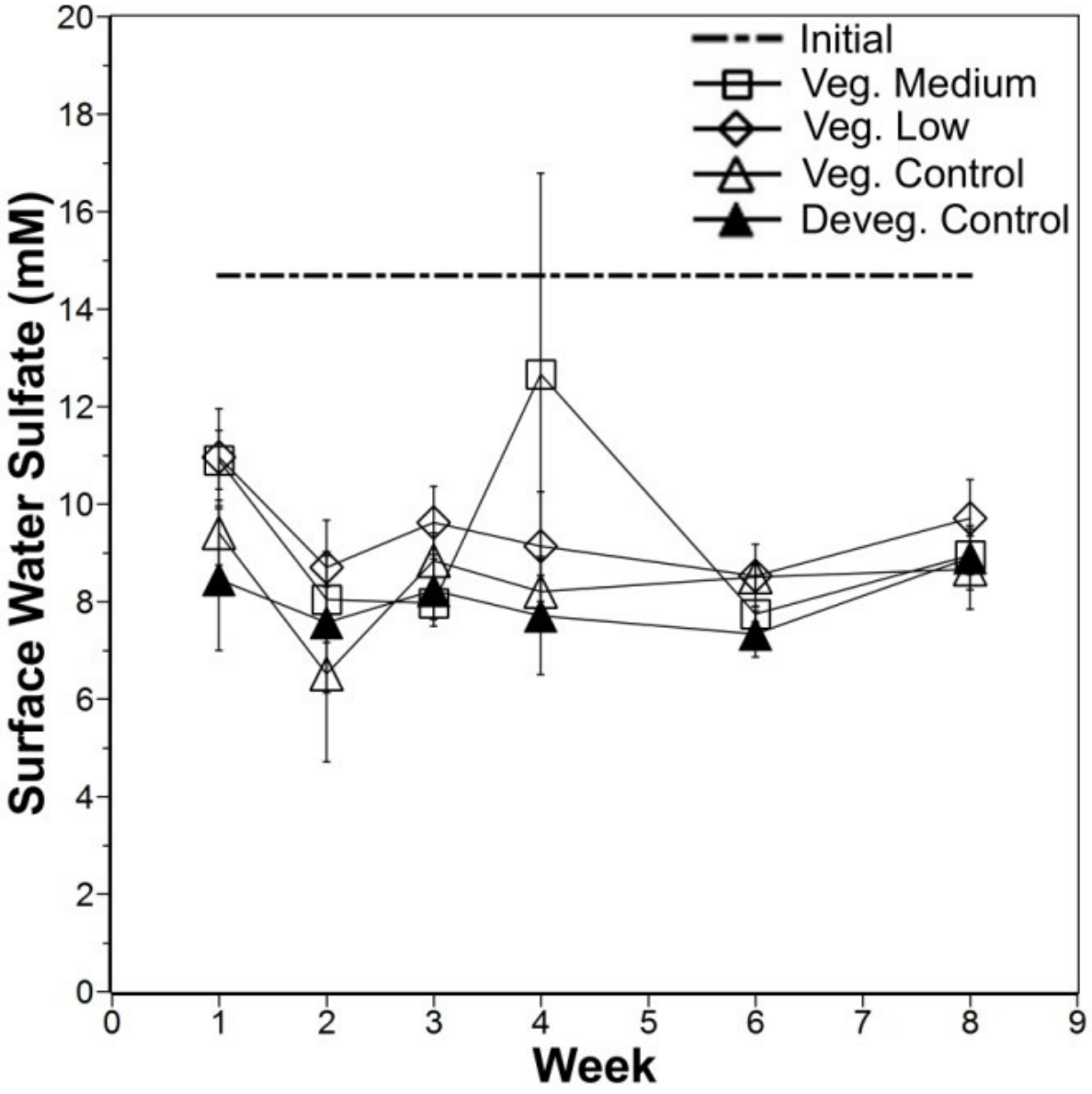

Figure 2-10. Concentration of sulfate remaining in vegetated microcosm reservoirs, normalized to the 5 L volume, after one week of tidal exposure. The dashed line represents the average initial sulfate concentration in the simulated estuarine water each week. Values are shown as average ± standard error for the triplicate microcosms in each group.

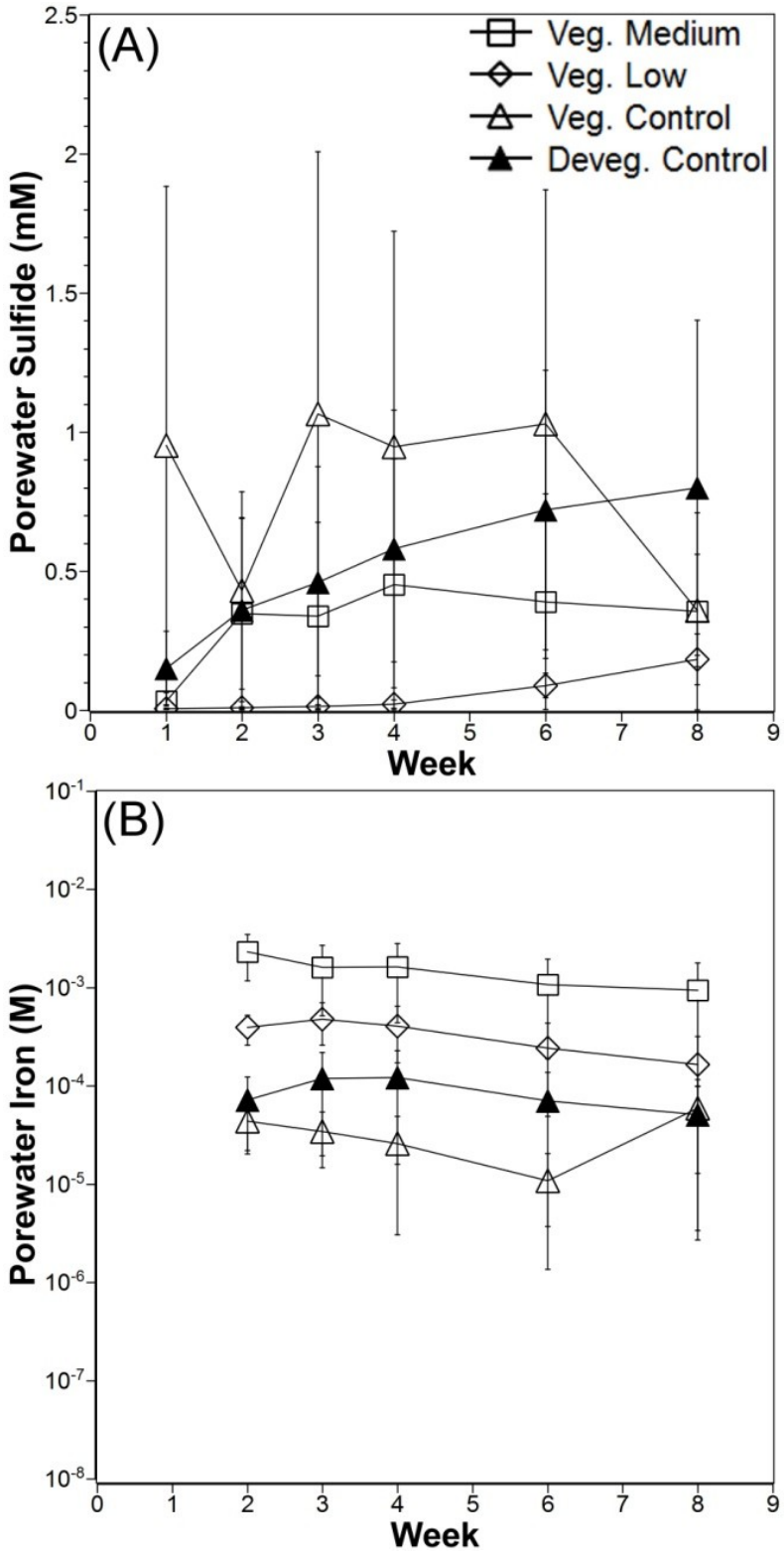

Figure 2-11. Average porewater concentrations in the vegetated microcosms for dissolved sulfide (A) and dissolved iron (B). Values shown are the average concentration of the triplicate microcosms ± standard error for each iron treatment group.

2.3.5 Mercury in Vegetated Microcosms

Inorganic mercury concentrations were similar among all groups with average concentrations ranging between 10 and 120 pM (Figure 2-12). During the initial three weeks of the experiment, the low and medium groups had lower average concentrations of MeHg in the surface water than the vegetated control (Figure 2-13(a)). However, the vegetated control showed considerable variability. The weekly averages for the control were brought up by very high concentrations of MeHg measured within a single microcosm during each week (see Table 2-2). For example, in Week 1, Tank 5 had a normalized surface water MeHg concentration of 250 pM, while Tanks 12 and 10 had values of 28 and 1 pM, respectively. Then in Week 2, Tank 12 had a concentration of 240 pM while Tanks 5 and 10 had values of 10 and 4 pM, respectively. This heterogeneity in the exported MeHg resulted in the large standard errors, and made it difficult to evaluate the efficacy of the amendment for the vegetated experiment. By Week 4, average MeHg concentrations were similar for all groups. No significant differences were found between the average weekly export of MeHg (Figure 2-13(b)) for any of the groups (one-way ANOVA with $\alpha = 0.05$, $p = 0.11$).

2.3.6 Sulfur Minerals in Vegetated Microcosms

Depth profiles analyzed for reduced sulfur speciation showed small increases in AVS for the vegetated treatment groups relative to the control over 2-4 cm depth. No differences were evident at any depth for CRS (Figure 2-14).

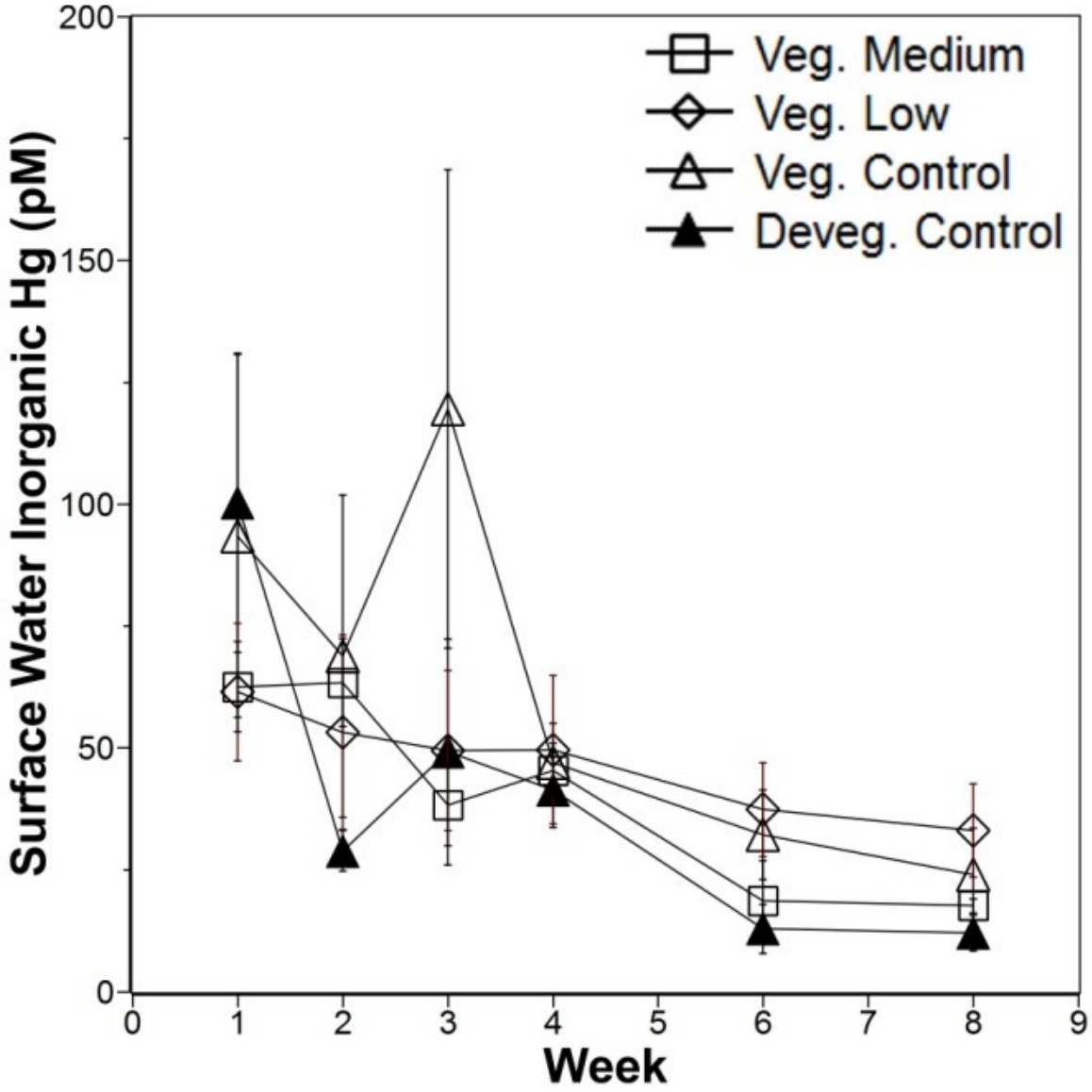

Figure 2-12. Inorganic mercury concentrations (normalized to the 5-L reservoir volume) in the surface water for the vegetated microcosms. Values are shown as average of the triplicate microcosms ± standard error.

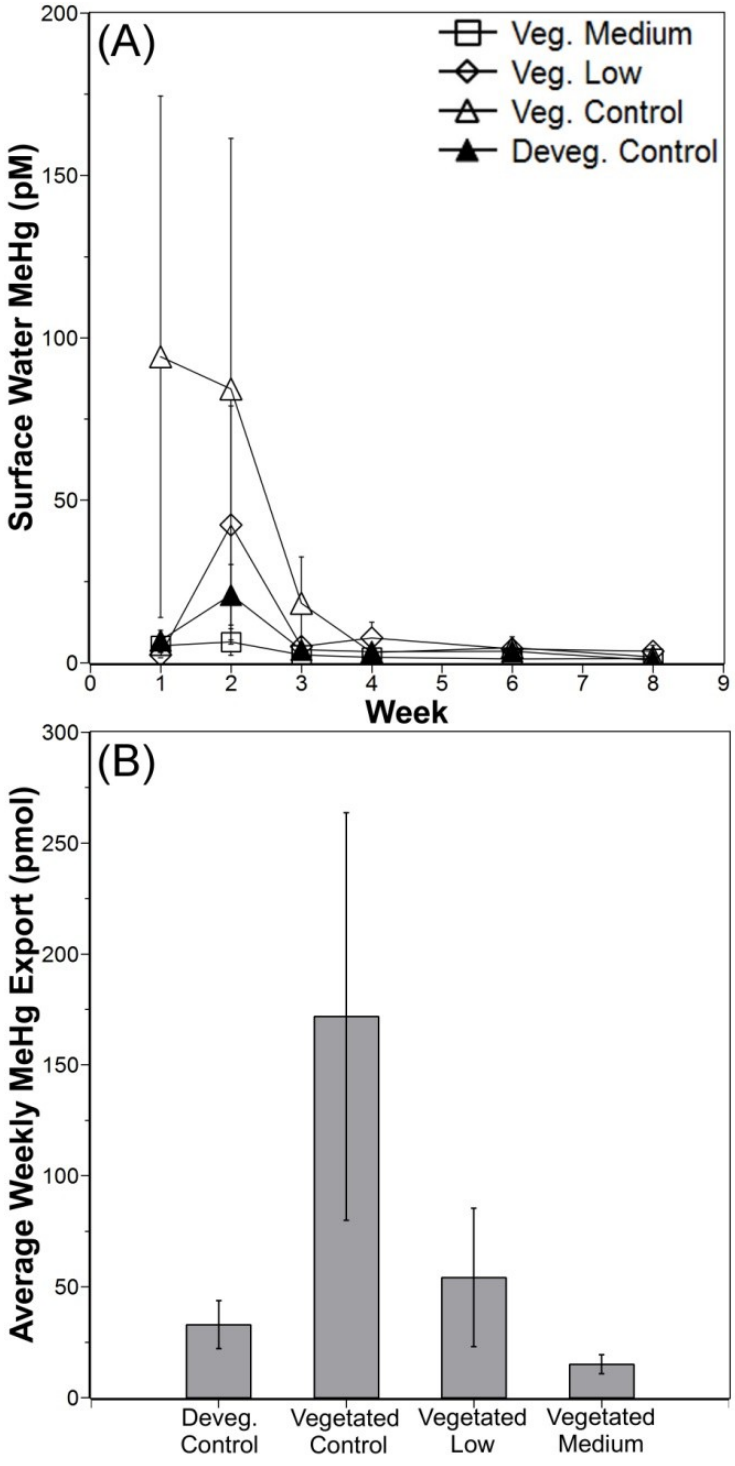

Figure 2-13. (A) Methylmercury measured in the surface water of the vegetated microcosms, normalized to the 5-L reservoir volume, after 7-day exposure to microcosm sediments. (B) Average mass of MeHg exported per week over the experimental period (n=18 per group). No statistical difference was found between the groups (p=0.11). Values shown are average ± standard error.

Table 2-2. Surface water methylmercury (MeHg) concentrations are shown for the vegetated microcosms. Values are listed in pM, and represent the 5-L normalized concentration. For concentrations that were measured as zero the value used for averaging is listed in parentheses (one half of the quantification limit mass in the distilled sample volume, normalized to 5-L).

Treatment	Tank ID	Week 1	Week 2	Week 3	Week 4	Week 6	Week 8
Deveg. Control	2	1.8	37.1	0.6	3.9	7.4	1.1
	6	6.2	20.8	5.0	3.4	2.3	0.7
	8	12.6	4.8	6.3	2.8	0.9	0.6
Control	5	254	10.1	46.6	2.3	11.2	4.0
	10	1.0	3.8	0.7	1.9	1.3	0.0 (0.3)
	12	27.6	239	7.3	5.2	1.4	0.9
Low Fe	4	1.5	8.1	2.0	2.4	0.0 (0.4)	1.3
	7	1.6	116	10.6	17.2	9.4	7.1
	9	3.8	3.4	2.3	3.1	2.8	2.1
Medium Fe	1	6.2	3.4	2.0	1.5	1.4	1.7
	3	1.5	1.2	0.0 (0.4)	0.8	1.5	1.7
	11	8.0	14.5	4.9	2.7	0.0 (0.4)	0.0 (0.4)

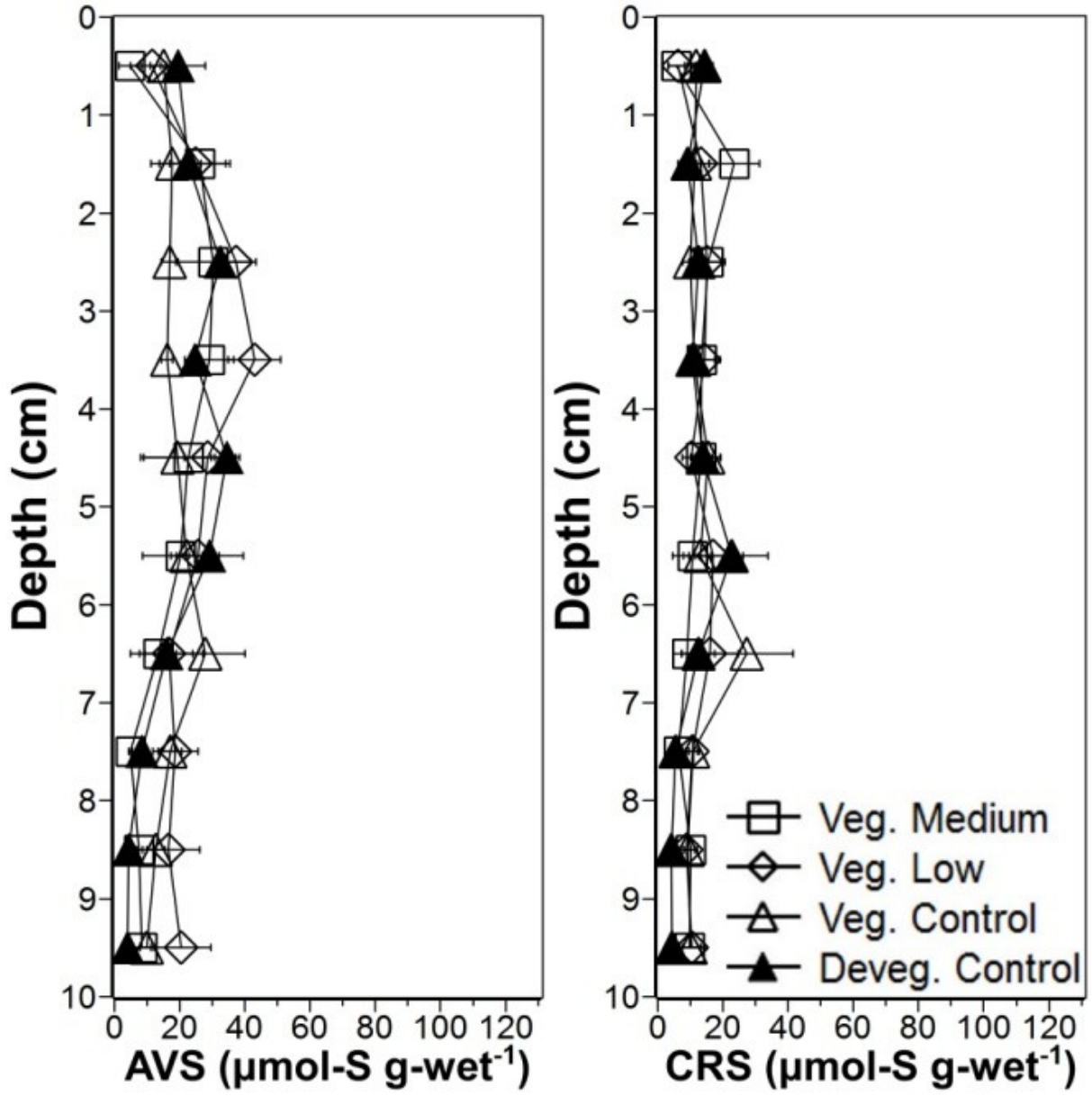

Figure 2-14. Depth profiles of reduced sulfur speciation in the vegetated microcosms collected at the end of the experiment for the top 10-cm of sediments from composite core samples. Values shown as average of triplicate microcosms ± standard error.

2.4 Discussion

These microcosm experiments demonstrated that the amendment of tidal wetland sediments with iron can reduce methylmercury concentrations under simulated field conditions. The findings are consistent with previous mechanistic studies that demonstrated this effect in short incubation experiments (Han et al. 2008; Liu et al. 2009; Mehrotra et al. 2003; Mehrotra & Sedlak 2005), and showed that an iron amendment can be effective for a period of at least 12 weeks under these conditions. This study also provided insight into the fate of iron and S[-II] within the sediments and the role of vegetation. Each of these issues is explored in the following sections.

The effect of iron on sediment biogeochemistry was most evident in the devegetated experiment. Iron addition increased porewater Fe[II] which subsequently lowered the concentration of porewater S[-II] for all of the treatment groups. Coupled with the decrease in porewater iron observed over the first 12 weeks for the medium and high dose groups, these findings suggest that there was a solid-phase sink for both iron and sulfur in the sediments (e.g., $FeS_{(s)}$ and $FeS_{2(s)}$) (King et al. 1985). The presence of these minerals was confirmed through the AVS/CRS measurements and by visual observation of the formation of black sediment layers characteristic of $FeS_{(s)}$. The formation of these minerals could also be important to Hg bioavailability since they can be important scavengers of Hg[II] (Jeong et al. 2007; Skyllberg & Drott 2010), and mercury can coprecipitate with authigenic pyrite in marine sediments (Huerta-Diaz & Morse 1992). In both cases, it is possible that mercury could be rendered less bioavailable. If this occurred following an iron amendment, it could provide a long-term means of reducing MeHg production, provided that the minerals are prevented from reoxidizing and releasing the associated mercury. However, it appears that iron-sulfur minerals did not affect the microcosms in this way, since the inorganic mercury concentrations were similar for all groups (Figure 2-6 & Figure 2-12). It is possible that the high concentrations of porewater DOC (Figure 2-7(b)) inhibited sorption to the minerals by forming complexes with Hg.

Due to the destructive nature of the sampling, sediment cores were collected only after the final water samples were collected, and it is unclear if larger differences in sulfur mineral concentrations existed earlier in the experiment. A mass balance on sulfur within the microcosms was estimated by using measured sulfur inputs and final concentrations within the sediment cores. Prior to the iron addition, a sediment sample was collected from each microcosm (composited 0-3 cm depth) for an AVS measurement; with an average concentration for all twelve microcosms of 36 ± 2 umol-S/g-wet sediment. For the mass balance, this value was assumed to be constant over the top 10-cm of depth, yielding an estimate of the initial mass of reduced sulfur in the microcosms (i.e., 512 mmol-S). The other sulfur input to the microcosms was the net amount of sulfate reduced each week. This value was calculated using the difference between the average initial sulfate concentration in the simulated estuarine surface water and the normalized value measured at the end of the weekly tidal period (Figure 2-2). For the weeks where surface water concentrations were not measured, the average of the previous and following weeks was used for the net sulfur input. Because the cores were collected 6 to 8 weeks following the Week 17 water measurements, two mass balances were calculated to account for this period of continued microcosm operation (e.g., continued daily tidal cycling and weekly water changes). Table 2-3 shows the mass balance for the case in which it is assumed that the only important sulfur inputs from the surface water came during the 17 week experimental period, and that the AVS and CRS had only negligible changes between this time and the core

collection. Table 2-4 shows the mass balance for the case where net sulfate reduction was assumed to continue for a period of seven weeks at the average net rate calculated over the first 17 weeks.

Loss terms for the mass balance were calculated using the difference between the Week 1 and Week 17 porewater sulfate concentrations (assuming a uniform concentration throughout the entire porewater volume within the top 10-cm depth, Figure 2-4) and the AVS and CRS concentrations measured in the 10-cm sediment cores. Additionally, the potential loss of H_2S through volatilization was calculated using measured porewater pH (Figure 2-5) and sulfide concentrations. It was assumed that all of the porewater in the microcosm had a uniform concentration equal to the value measured in the porewater samplers over a one week period, and that the sediments had 70% porosity.

The flux of H_2S from the porewater to the atmosphere was calculated using a two-layer model (Reese et al. 2008):

$$F = k\left(C_w - \frac{C_a}{H}\right) \quad (1)$$

where C_w is the concentration of H_2S in the porewater, C_a is the concentration of H_2S in the air (assumed to be the average for ambient urban air: 0.009 µM m^{-3} (Robinson & Robbins 1970)), H is the unitless Henry's constant, and k is the film transfer coefficient. The film transfer coefficient is defined by (Balls & Liss 1983):

$$\frac{1}{k} = \frac{1}{\alpha k_w} + \frac{1}{H k_a} \quad (2)$$

where k_w and k_a are the transfer velocities for the water and gas phases, respectively, and α is a correction factor specific to H_2S that reflects an enhancement of k_w due to chemical reactivity of the H_2S in the liquid phase. Values of these constants used in the calculation were obtained for pH 7 from reference (Balls & Liss 1983).

The concentration of H_2S in the porewater (C_w) was calculated using the porewater pH and measured total sulfide (S_T) for each week using:

$$C_W = \left(\frac{[H^+]}{[H^+]+K_{a1}}\right) S_T \quad (3)$$

where K_{a1} is the first dissociation constant for H_2S ($K_{a1} = 1.0\text{x}10^{-7}$). This value was then plugged into (1) to yield the flux for each dose group during that week in mol cm^{-2} h^{-1}. To obtain the weekly potential flux of sulfide out of the porewater, this value was multiplied by the surface area of the microcosms (1290 cm^2) and by the timescale of exposure to the atmosphere (18 hours of low tide per day for 7 days in each week). An example of this calculation for Week 1 is shown in Table 2-5.

Table 2-3. Values calculated for mass balance of sulfur inputs and final concentrations in the microcosms, assuming no changes occurred in acid volatile sulfides (AVS) and chromium reducible sulfur (CRS) between the Week 17 water sampling and the sediment core collection. Values are listed as mmol-S.

	Initial AVS (10 cm)	Net SO_4 Reduced (17 wks)	Δ Porewater Sulfate	Total Inputs	AVS + CRS (10cm)	Mass Out, No H_2S	Unacc-ounted	Potential H_2S Volatilzed	% Recovered
Control	512	571	49.4	1080	796	845	238	11500	78%
Low	512	660	105	1170	800	905	267	3980	77%
Medium	512	566	143	1080	791	934	145	589	87%
High	512	485	78.9	1000	971	1050	-52	2250	105%

Table 2-4. Values calculated for mass balance of sulfur inputs and final concentrations in the microcosms, assuming an additional seven weeks of sulfur inputs due to continued sulfate reduction between the final water sampling and sediment core collection. Measured sulfur minerals include acid-volatile sulfides (AVS) and chromium reducible sulfur (CRS). Values are listed as mmol-S.

	Initial AVS (10 cm)	Net SO_4 Reduced (24 wks)	Δ Porewater Sulfate	Total Inputs	AVS + CRS (10cm)	Mass Out, No H_2S	Unacc-ounted	Potential H_2S Volatilized	% Recovered
Control	512	805	49.4	1320	796	845	472	11500	64%
Low	512	927	105	1440	800	905	534	3980	63%
Medium	512	802	143	1320	791	934	381	589	71%
High	512	686	78.9	1200	971	1050	149	2250	88%

Table 2-5. An example of the values computed for the potential loss of H_2S due to volatilization from the porewater for Week 1.

Week	Fe Dose	pH	Total Sulfide (mM)	$[H^+]$ (M)	$\left(\frac{[H^+]}{[H^+]+K_{a1}}\right)$	Porewater $[H_2S]$ (M)	Flux (mol cm^{-2} h^{-1})	Weekly Flux (mmol)
1	Control	7.3	1.58	4.90E-08	0.32	5.12E-04	5.60E-06	910
1	Low	7.4	0.18	4.01E-08	0.28	5.16E-05	5.64E-07	91.7
1	Medium	7.0	0.02	1.01E-07	0.50	8.73E-06	9.54E-08	15.5
1	High	6.6	0.02	2.45E-07	0.71	1.52E-05	1.66E-07	27.0

The mass balance on sulfur in the devegetated experiment indicated between 77 and 105% of the sulfur added during the 17-week experimental period could be accounted for as AVS/CRS in the top 10-cm of the sediment and porewater sulfate. If it was assumed that sulfate reduction continued at its average rate within the microcosms over the 6-8 week period between the final water measurement and the sediment core collection, between 63 and 84% of the sulfur was recovered. A calculation of potential volatilization of H_2S from the porewater during the daily exposure of the sediment to the air, based on porewater pH and sulfide concentrations, suggests that H_2S volatilization likely accounted for the remaining sulfur. However, it is possible that a portion of the S[-II] in the porewater could have been oxidized by iron (oxyhydr)oxide minerals to S[0] (Poulton et al. 2004), which was not detected by our analytical methods.

An approximate mass balance for iron was also calculated by assuming that all of the measured AVS and CRS consisted of $FeS_{(s)}$ and $FeS_{2(s)}$, respectively (Table 2-6). This calculation yields between 38-72% recovery of the added iron as iron-sulfur minerals. It is likely that some of the remaining iron was present in the sediments as $FeCO_{3(s)}$ or as an Fe[II]/Fe[III] mineral phase not detected by the AVS/CRS extraction methods. Reoxidation of a portion of the Fe[II] to Fe[III] was possible at the sediment-water interface, and was evident for the medium and high iron doses by the presence of red solids on the sediment surface.

Addition of iron to the devegetated sediments at both the medium and high dose levels significantly reduced the concentrations of MeHg that were exported from the porewater to the surface water (Figure 2-8). Because the export of inorganic mercury was similar among all of the treatments, it appears that the addition of iron did not substantially inhibit the exchange of mercury species to the surface water. This suggests that the reduction in MeHg export was related to the net production of MeHg in the sediments. In-situ methylation rates were not directly measured; however, the percent of total mercury that is MeHg (%-MeHg), which has been considered an approximation of net MeHg production in coastal sediments (Sunderland et al. 2006), provides further evidence that iron addition decreased net methylation rates. Consistent with this assumption, weekly average %-MeHg values in the surface water of the devegetated microcosms over the first 12 weeks (excluding the Week 8 pump failure) were higher in the control and low groups than in the medium and high dose groups (Figure 2-15). These values likely reflect porewater concentrations since there were no other sources of mercury in our system. The average %-MeHg values, typically between 5 to 40%, were consistent with porewater values reported in other wetland mesocosm studies (Harmon et al. 2004; King et al. 2002) and in contaminated bay sediments (Bloom et al. 1999).

Table 2-6. Average values estimated for a mass balance of iron inputs and final concentrations as iron-sulfur minerals (acid-volatile sulfides, AVS, and chromium reducible sulfur, CRS) in the microcosms. Values are listed as mmol-Fe.

	Initial AVS (10 cm)	Iron Dose	Mass In	Final AVS+CRS as Fe (10-cm)	Unaccounted For	% Recovered
Control	512	0	512	669	-156	131%
Low	512	416	928	667	261	72%
Medium	512	832	1340	657	688	49%
High	512	1660	2180	827	1350	38%

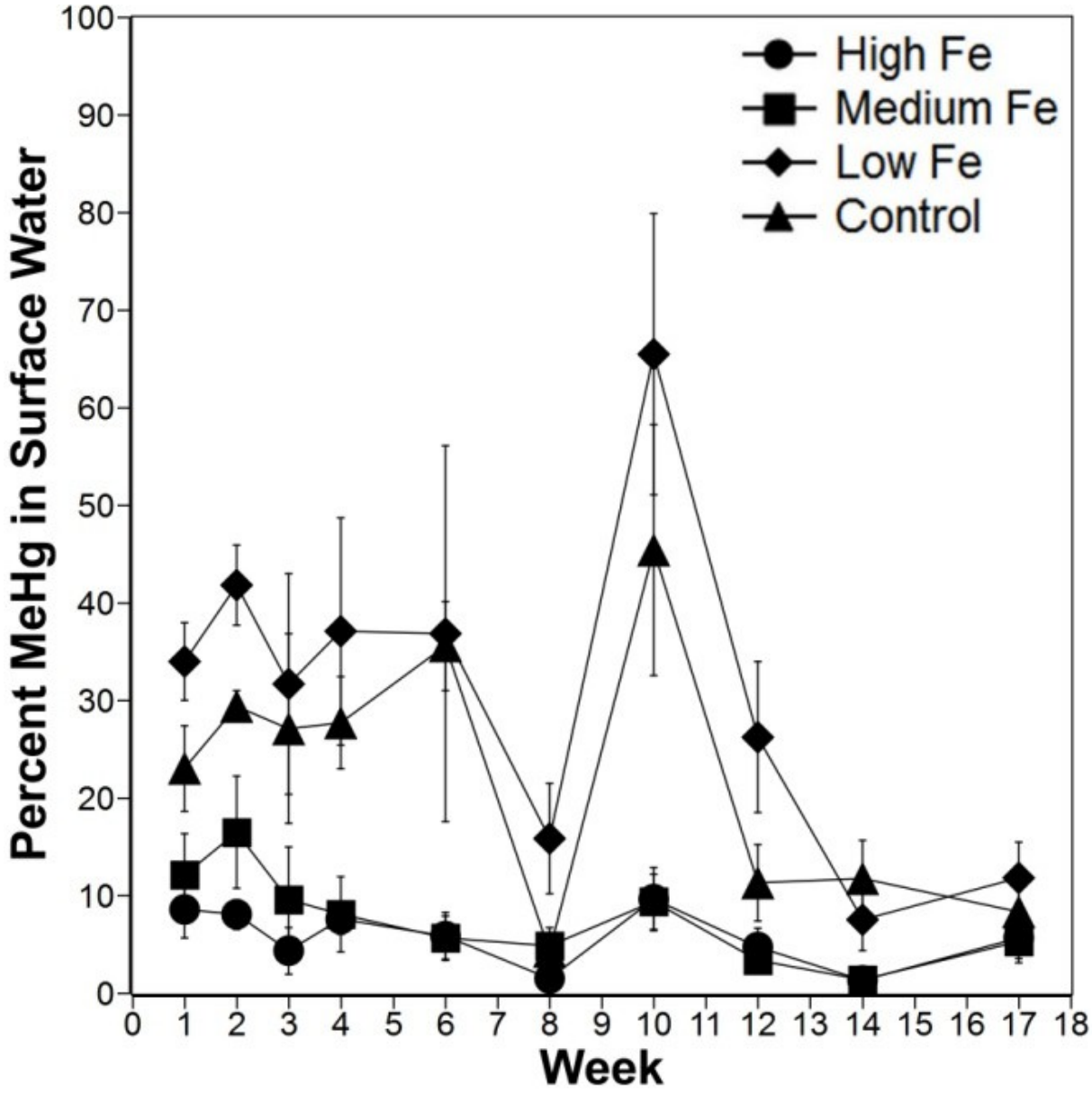

Figure 2-15. The percent of surface water total mercury that was measured as methylmercury (%-MeHg) for the devegetated microcosms. Values are shown as average of the triplicate microcosms ± standard error.

The net export of MeHg decreased after approximately 12 weeks in the devegetated microcosms, and after around 3 weeks in the vegetated microcosms, until there was no difference between the control and treatment groups. The decrease in net MeHg export that occurred after the first 12 or 3 weeks may have been due to the experimental limitations of the microcosms to act as proxies of field conditions over extended periods of time. In the lab, the microcosms were subjected to conditions unlike those encountered in the field. For example, the microcosms were supplied with simulated estuarine water that contained negligible concentrations of DOM and dissolved mercury. Additionally, the movement of tidal water occurred only on the surface of the microcosms, while under field conditions the water table varies vertically in the sediments as the tides change. Over time, this could have limited advective flushing of reduced species in the microcosms and affected the redox stratification. By disturbing the sediments, we also may have induced a period of high net MeHg production early in the experiment. Field studies have shown pulses of MeHg can occur when reservoirs (St Louis et al. 2004) or tidal marshes (Miles & Ricca 2010) are subjected to new hydraulic conditions. If this was the case for our microcosms, these results suggest that an iron amendment may be able to reduce the size of the MeHg pulses that occur when natural systems are inundated.

The reason for the increased variability in porewater sulfide and MeHg export in the vegetated experiment is unclear, however several factors could have contributed. The laboratory equilibration time to the new hydraulic conditions was reduced from 4 months for the devegetated sediment experiment to only 3 weeks for the vegetated experiment. Additionally, plants can significantly alter the biogeochemistry of salt marsh sediments through the production of organic acids that can stimulate microbial activity (Windham-Myers et al. 2009) and release of oxygen into the rhizosphere (Maricle & Lee 2007). Therefore, the presence of plants may have introduced extra heterogeneity into the system. While care was taken to select similarly vegetated plots in the field during microcosm collection, the amount of living roots in each microcosm was not quantified. Additionally, the health of individual plants within the microcosms could have contributed to the variability. By around 3 to 4 weeks into the experimental period, most of the plants had gone dormant, but individual plants declined at different times, which could have resulted in increased variability due to the decreased subsurface activity of the plants.

Even with the increased variability in the vegetated experiment, the trends observed were similar to that of the devegetated sediments, and suggest that an iron amendment could be an effective means of controlling net MeHg export in restored tidal wetlands. Research at the field scale is needed to determine the efficacy of an iron amendment under field conditions, and if an amendment is effective for longer than 12 weeks or if repetitive dosing would be needed. Additionally, unintended consequences of adding iron to the ecosystem, including toxicity to wetland vegetation, must be taken into account to ensure that changes that alter habitat quality do not occur.

Chapter 3. Incubation Studies of Pickleweed-Dominated High Marsh Sediments

3.1 Introduction

Wetland sediments are highly productive environments where biomass produced by aquatic plants is oxidized by an abundant microbial community (Figure 3-1). Because diffusion of O_2 through sediment porewater is slow, aerobic microbes near the surface rapidly consume oxygen leading to anaerobic conditions at depths of just a few millimeters below the sediment surface (Mitsch & Gosselink 2007). Thus, a large amount of organic carbon is oxidized under anaerobic conditions in wetland sediments. The typical view of anaerobic processes in wetland sediments involves vertical stratification of terminal electron acceptors since microbes will preferentially use the electron acceptors that yield the most energy. According to this conceptual model, as sediment samples are collected at increasing depths it should be possible to identify zones where microbes use oxygen, nitrate, manganese, iron, sulfur and then CO_2 as terminal electron acceptors.

Due to the high availability of sulfate in seawater, sulfate is often the predominant terminal electron acceptor in salt marsh sediments (Howarth 1984, Howarth & Giblin 1983, King et al. 1985). However, recent research has demonstrated that microbial processes and redox cycling in salt marsh sediments can be much more dynamic than originally thought, with iron-reducing bacteria accounting for a significant portion of total carbon oxidation in surficial sediments (Gribsholt et al. 2003, Hyun et al. 2007, Koretsky et al. 2003). Furthermore, sediment biogeochemical conditions can vary substantially between seasons in some salt marsh environments (Koretsky & Miller 2008, Koretsky et al. 2003, Kostka & Luther 1995, Neubauer et al. 2005). Seasonal changes reflect changes in redox processes that are primarily driven by the activity of the salt marsh vegetation. For example, some active wetland plants can cause more oxidizing conditions by releasing oxygen from their roots (Holmer et al. 2002), which rapidly oxidizes reduced iron and sulfur species in the sediments (Lee 1999). Alternatively, wetland macrophytes often secrete labile organic acids from their roots, which can increase microbial respiration rates and more rapid consumption of electron acceptors (Hines et al. 1989). While these important processes have been described in several salt marsh ecosystems, there is only limited information about biogeochemical cycles in salt marshes dominated by pickleweed (*Sarcocornia pacifica*), such as those in the San Francisco Bay-Delta.

It is important to understand the complex redox processes in the tidal wetlands of the Bay-Delta because MeHg production is related to the activity of different microbial communities in salt marsh sediments. Pickleweed wetlands are especially important because they frequently have elevated concentrations of MeHg in the sediments (Marvin-DiPasquale et al. 2003, Windham-Myers et al. 2009).

While methylmercury production is primarily driven by sulfate-reducing bacteria (Compeau & Bartha 1985, Gilmour et al. 1992), recent research has demonstrated that some iron-reducing bacteria can also methylate mercury (Fleming et al. 2006, Kerin et al. 2006). Furthermore, iron reduction rates have been correlated with MeHg production in a Chesapeake Bay salt marsh (Mitchell & Gilmour 2008) and a tidal lagoon in southern California (Rothenberg et al. 2008). However, these correlations might only serve as a surrogate for redox conditions or overall biological activity in the sediments. Thus, a direct link between iron-reducers and *in situ* MeHg production in tidal wetlands has not been established. Ultimately, iron reduction could play an important direct or indirect role in the net production of MeHg in wetland sediments. In light of these recent findings, it is possible that iron amendments could inadvertently stimulate

iron-reducing bacteria or alter the microbial community in a manner that results in the production of higher concentrations of MeHg.

This chapter describes our use of sediment incubation experiments to gain insight into the complex biogeochemical cycling of iron, sulfur, and mercury occurring within sediments from Gambinini Marsh in Petaluma, CA. Sediment incubation experiments are commonly used to assess short-term microbial activity and the accumulation of end-products of microbial respiration (Hyun et al. 2007, Koretsky et al. 2003, Lovley & Phillips 1987, Roden & Wetzel 1996), as well as mercury methylation rates (Avramescu et al. 2011, Hammerschmidt & Fitzgerald 2004, Heyes et al. 2006). Short incubations provide a means of evaluating site specific rates under controlled conditions. Anoxic incubation experiments of salt marsh sediments run for between 3 and 7 days have demonstrated a substantial increase in concentrations of Fe[II] (Hyun et al. 2007), MeHg (Mehrotra & Sedlak 2005), and reduced sulfur minerals (King 1983). While incubation experiments provide useful information about redox processes occurring at a site, care needs to be taken when interpreting results because the act of collecting samples and preventing exchange of gases and water with the surrounding environment perturbs the system. Specifically, rates measured in incubation experiments may overestimate the importance of reactions that occur under reducing conditions.

The closed, anoxic incubation experiments described in this chapter provided insight into the redox processes occurring within the sediments of Gambinini Marsh, including the microbial production of MeHg under iron-reducing and sulfate-reducing conditions. Additionally, the *in situ* core incubations, conducted with open and closed systems, allowed us to observe short-term changes in redox-active species under field conditions, as well as to compare seasonal differences between summer and winter conditions.

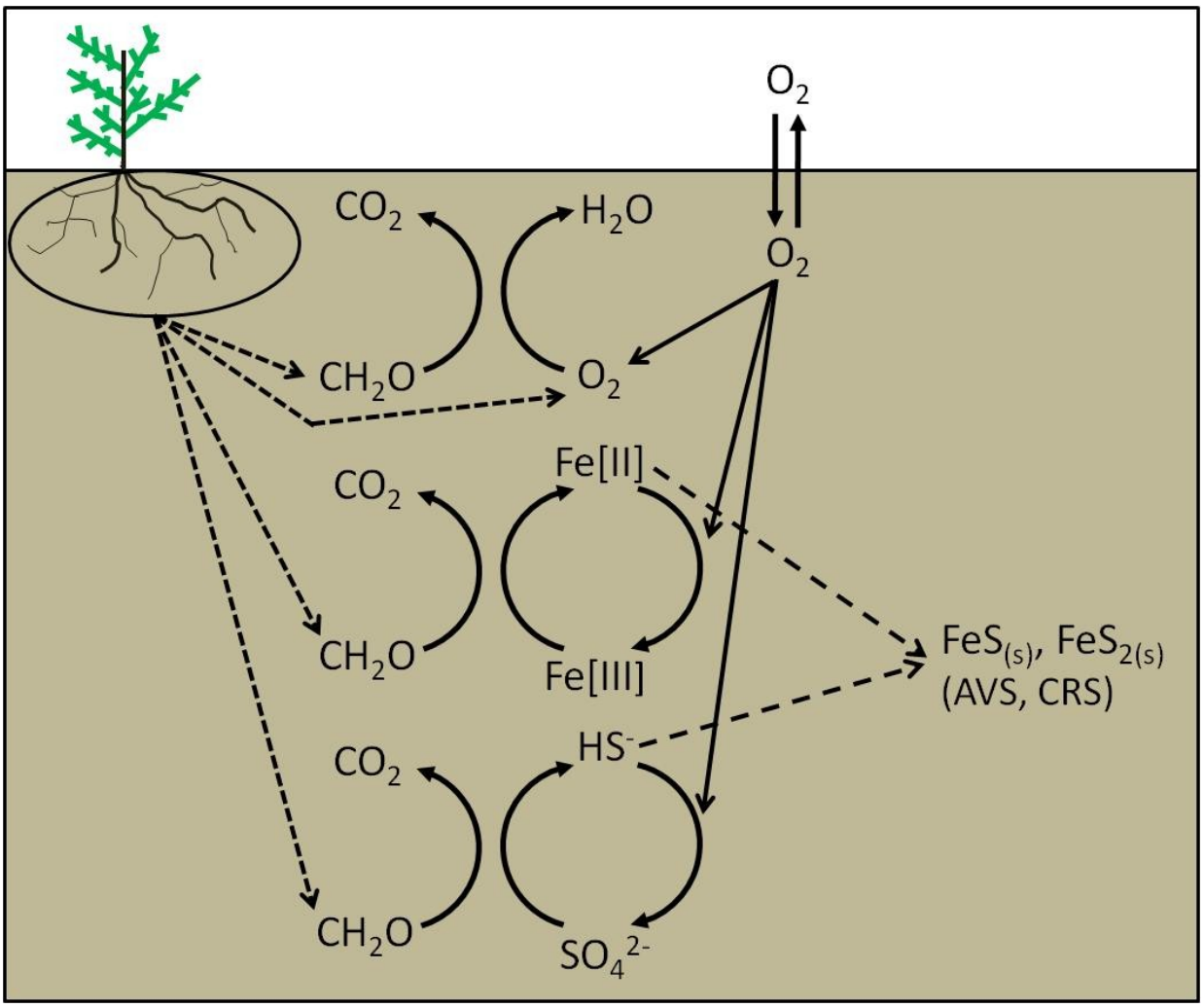

Figure 3-1.Schematic of select redox processes involving oxygen, iron, and sulfur that typically occur in wetland sediments.

3.2 Methods

3.2.1 San Francisco Bay Pickleweed Marsh Characterization

Sediments were collected from the Gambinini Marsh, a tidal salt marsh along the Petaluma River. Sediments from this location also were used for the laboratory microcosms described in Chapter 2, as well as the field study described in Chapter 4.

Sediment geochemistry and redox conditions of salt marshes can vary considerably even at similar elevation ranges and vegetation types within a limited geographic area (Gardner et al. 1988, Heim et al. 2007, King et al. 1982, Koretsky et al. 2008). To gain insight into the relevance of studies conducted in the Gambinini Marsh, sediment concentrations of iron and sulfur species were measured in sediments collected from pickleweed-dominated marshes in northern San Francisco Bay. Sediment cores were collected from Gambinini Marsh in July and August of 2009 (see section 3.2.2 for details) and from four public-access sites around northern San Francisco Bay in August 2009. At Point Isabel Regional Shoreline (37.908192°N, 122.326863°W), Richmond, CA, sediments were collected from a low-marsh area dominated by pickleweed, as well as an unvegetated slough that drained the marsh plain. Two different areas of pickleweed marsh were sampled at Point Pinole Regional Shoreline, Richmond, CA. From the southwestern area of the park (37.992776°N, 122.359114°W), samples were collected from a mid-marsh plain in areas dominated by pickleweed, as well as an adjacent low marsh dominated by cordgrass (*Spartina spp.)*. Separate samples were collected from the northeastern area of the park (38.007166°N, 122.351818°W), which includes a high marsh plain dominated by pickleweed, as well as an adjacent intertidal mudflat area. The marsh plain is around 0.5 m higher in elevation than the mudflat, which is apparent from the abrupt drop that occurs at the transition between the two regions. Samples also were collected from a small area of marsh bordering a large slough at Las Gallinas Valley Sanitation District Facility (38.033670°N,122.502891°W) near San Rafael, CA. The fringe marsh was approximately 5 meters wide between the tidal channel and the berm, and samples were collected from the middle of the vegetated area. Finally, samples were collected from the interior of a high marsh area dominated by pickleweed at Bothin Marsh (37.886768°N, 122.521205°W) in Mill Valley, CA.

Surficial sediment samples were collected using acid-cleaned 10-mL plastic syringes with the tip cut off approximately 2 mm from the top. To collect a sample, the syringe was inserted into the ground to around a 4-cm depth. After removing the sediment it was immediately transferred into a pre-cleaned 20-mL glass jar with a Teflon-lined lid. The syringe was inserted into the sampling area four times to collect enough sediment to fill the jar and minimize headspace. After collection, the samples were frozen on dry-ice, and were kept frozen until analysis, which occurred within 24 hrs.

3.2.2 Gambinini Marsh Cores

Sediment cores were collected from an area of Gambinini Marsh adjacent to the test plots used to collect porewater samples (see Chapter 4). Two 20-cm cores (Cores #1 and #2) were collected in August 2009 and were sectioned at 2-cm resolution. A 5-cm core was collected in July 2009 and sectioned at 1-cm resolution (Core #3). An acid-cleaned acrylic coring tube (6.3

cm i.d.) with a beveled leading edge was pressed into the marsh sediments by hand during low tide (i.e., no surface water was present on the surface of the marsh during collection). A rubber stopper was pressed into the open core top, and the tube was pulled from the ground. A second rubber stopper was immediately placed on the bottom of the core, and the ends were wrapped in parafilm. The coring tubes were then double-bagged in plastic zipper-lock bags, and placed vertically into a cooler full of ice until they were sectioned using plastic tools in the laboratory later that day.

3.2.3 Laboratory Incubation Experiments

To determine if iron-reducing bacteria had the potential to be important sources of MeHg in the high-marsh sediments of Gambinini Marsh, sediment incubation experiments were conducted. Sodium molybdate, a specific inhibitor of sulfate reduction (Oremland & Taylor 1978), was added to one set of the incubation vessels to stop the activity of the sulfate-reducing bacteria. This allowed us to compare the accumulation of reduced iron species, reduced sulfur species, and MeHg under conditions where the native iron-reducing microbial community was growing with and without competition from the sulfate-reducing community.

Surficial sediments were collected from a pickleweed-dominated area near the porewater sampling test plots in August 2009. Aboveground vegetation was clipped at the sediment surface and removed before a hand trowel was used to collect sediments from the 0-4 cm depth range. Five acid clean glass jars with Teflon-lined lids (500-mL) were packed until no headspace remained above the sediment. The jars were placed on ice in a cooler until sub-sampling occurred in the laboratory later that day. Surface water was collected from a 0.25 m depth in the middle of the largest slough in the vicinity of the sampling area in pre-cleaned 500-mL FEP bottles. The bottles were kept in a cooler on ice until used in the laboratory later that day.

In a nitrogen filled glovebag, sediments were transferred from the collection jar to 60-mL serum bottles using acid-rinsed stainless steel spatulas. The serum bottles were filled with approximately 35 g of wet sediment, and then they were completely filled with slough water that had been purged by N_2 for at least 60 min. This provided a 1:1 ratio by weight of wet sediment to slough water for the slurries. Each bottle was spiked with 15 nmol of Hg(II) from a diluted HNO_3-acidified standard to provide a source of labile mercury. Once the jars were filled, they were capped with rubber septas, sealed using aluminum crimp-caps, and mixed on a rotary vortexer.

The serum bottles were incubated in the dark at room temperature for a period of up to one week, with triplicate bottles collected at 12, 60, 108, and 180 hours. At the time of collection, bottles to be sacrificed were removed from the box and placed into a nitrogen-filled glove bag. The bottles were opened inside of the bag, and a 15-mL plastic centrifuge tube was filled with the sediment slurry. The serum bottles were recapped inside of the glove bag, and then were frozen until analysis for methylmercury. The sealed centrifuge tubes were removed from the glove bag, wrapped in parafilm and centrifuged to separate the sediment and water. Subsamples of the porewater and sediment were then collected and immediately analyzed for iron and sulfur speciation, with the exception of porewater samples for sulfate analysis, which were placed into plastic test tubes and frozen until analysis, which occurred within 5 days.

Three experimental conditions were evaluated for this experiment, with 12 serum bottles receiving each treatment (n=3 bottles for each time point for each condition). The untreated

incubation was a 1:1 mix of slough water and marsh sediment. Twelve of the jars were given a sodium-molybdate amendment to inhibit sulfate reduction. For the Mo-amended condition, the deaerated slough water was amended with $NaMoO_4$ at a final concentration of 20 mM, which was approximately equal to the estimated concentration of sulfate in the slough water. Previous research suggests strong inhibition of sulfate reduction when concentrations of sulfate and molybdate are near equimolar (Oremland & Capone 1988). The third condition consisted of sediment and slough water amended with 3% formaldehyde as an abiotic control.

3.2.4 Field Core Incubation Experiments

To assess the effect of exposure of the surficial sediments to the atmosphere on iron, sulfur, and methylmercury, an *in situ* incubation experiment was carried out using cores located in the high marsh plain of Gambinini Marsh. The experiment was conducted during both the summer (July 2010) and fall (November 2010) seasons to compare seasonal variations in mercury biogeochemistry.

For the experiment, pre-cleaned 25-cm acrylic cores (6.3 cm i.d.) were installed in the marsh adjacent to the porewater collection plots. Six cores were pressed 15 cm into the sediment within a 0.5 m by 0.5 m area. Three of the coring tubes were left with an open top, and three were capped with a rubber stopper wrapped in parafilm to minimize gas exchange with the atmosphere. The cores were left in the marsh for one week until sample collection. On the core collection day, triplicate fresh cores were collected from random positions within the same plot, to assess any changes due to the presence of the acrylic tube.

On the date of sample collection, the cores were pulled from the ground one at a time and sectioned immediately in the field at depths of 0-1 cm, 3-4 cm and 6-7 cm. For the capped cores, the entire tube was pulled from the ground and the bottom was capped with a rubber stopper. For the open-top cores and the freshly collected cores, a rubber stopper was fitted into the top of the tube, just before pulling the core out of the ground.

The core was immediately sectioned in the field by extruding the core from the top of the coring tube, using a rod to slide the sediments. Plastic 5-mL syringes with the tips cut off (1-cm i.d.) were used to subsample the extruded core section at the respective depths. The subsamples were combined inside of a 15-mL plastic centrifuge tube. Enough subsamples were collected from a core depth to fill the centrifuge tube with no headspace. The tube was then capped, wrapped in Parafilm, and kept on ice until analysis in the lab within 4 hours. Care was taken to minimize the exposure time of the sediments to the air. An entire core could be collected and sectioned at the three depths in less than 5 minutes.

During the July field incubation, the open cores had approximately 5 cm of water on the surface of the sediments inside of the core tube at the time of sample collection. The sediments outside of the tube had no standing water on the surface due to tidal flushing. It is unknown how long the water was in the tube prior to sample collection.

3.2.5 Analytical Methods

Water and sediment samples were analyzed using established methods. Method detection limits were defined as three times the standard deviation of the blanks, unless otherwise noted.

For samples with concentrations below the detection limit, one-half of the detection limit was used for calculations.

Fe[II] and total iron concentrations were measured in porewater by modified version of a porewater analysis method for small sample volumes (Viollier et al. 2000). The modification included using separately prepared aliquots for direct reaction with ferrozine (Fe[II]) and for reduction of Fe[III] to Fe[II] by hydroxylamine hydrochloride followed by reaction with ferrozine and measurement of absorbance at 562 nm (Stookey 1970). Detection limits for Fe[II] and Fe_{total} were 2.2 µM and 1.7 µM, respectively. Concentrations of Fe[II] and microbially-reducible Fe[III] (i.e., the difference between measured total 0.5 N HCl-extractable iron and Fe[II]) were measured in sediments following the method of Lovely & Phillips (1987) with colorimetric quantification with ferrozine. Sulfate was measured by ion chromatography (Dionex DX-120, average daily detection limit of 19 µM). Porewater sulfide was measured with the methylene blue colorimetric method (detection limit of 0.43 µM) (Cline 1969). Reduced sulfur speciation in sediments was measured using a modified diffusion method for the sequential extraction of acid volatile sulfides (AVS) and chromium reducible sulfur (CRS) (Hsieh & Shieh 1997) with addition of ascorbic acid to improve recovery in the presence of ferric minerals (Hsieh et al. 2002), followed by quantification of trapped sulfide by methylene blue (recovery of a spiked Na_2S standard was 94 ± 20% , n=10).

MeHg in porewater and sediments was measured by acidic chloride distillation (Horvat et al. 1993, Olson et al. 1997), aqueous phase ethylation, collection on Tenax traps, thermal desorption, GC separation, and detection by CVAFS (Bloom 1989). Percent recovery of MeHg spiked into a distillation blank averaged 91 ± 20% (n=47), recovery of MeHg spikes into duplicate sediment samples averaged 92 ± 25% (n=15), and recovery of distilled NIST mussel tissue standard (NIST SRM 2976) was 85 ± 12% (n=44). The detection limit was 0.76 pM, and was determined by distillation and analysis of 17 samples of a 0.5 pM solution (USEPA 2001).

3.3 Results

3.3.1 North Bay High Marsh Characterization

The concentration and speciation of iron and sulfur in the sediments collected at sites around San Francisco Bay indicate that the geochemistry of pickleweed-dominated high marsh plains were consistent among sites. There were distinct differences between iron and sulfur speciation in low-marsh and mudflat areas relative to the high-marsh, pickleweed areas.

While samples collected from the same site often had similar concentrations of total Fe, samples from high marsh areas had higher concentrations of reducible Fe[III] than the low marsh areas and mudflats (Figure 3-2). This observation suggests that more Fe[III] was available for iron-reducing bacteria in the high marsh. Additionally, in the two pickleweed-dominated low marsh areas (Point Isabel Pickleweed and Bothin Marsh), nearly all of the iron in the sediment was present in the reduced form.

Lower concentrations of reducible Fe[III] were observed at depth in the cores collected in Gambinini Marsh (Figure 3-3). Sediments from surficial layers (0-2 cm) contained between 19 and 72 µmol-Fe[III]/g-dry, whereas sediments from deeper layers below the root zone (14-16 cm depth) consisted almost entirely of Fe[II].

Solid-phase reduced sulfur species (Figure 3-4) were present at concentrations that were lower than those of iron. With the exception of the Point Isabel Slough and the vegetated low marsh, the concentrations of AVS were below the detection limit. CRS was detected in almost all samples, with the highest observed concentrations occurring in the low marsh area dominated by *Spartina* and the adjacent slough bottom. The concentrations measured at the pickleweed sites were consistent with concentrations measured in the Gambinini Marsh sediment cores (Figure 3-6).

Sediment MeHg concentrations for the 20 cm cores (Figure 3-7) were consistent with reported patterns from other Bay-Delta locations with the highest concentrations for each core occurring near the sediment surface (Bloom et al. 1999, Marvin-DiPasquale & Agee 2003, Merritt & Amirbahman 2008, Zelewski et al. 2001). Concentrations in the upper sediment layers were similar to levels reported in pickleweed marshes in the Bay-Delta (Marvin-DiPasquale et al. 2003, Windham-Myers et al. 2009).

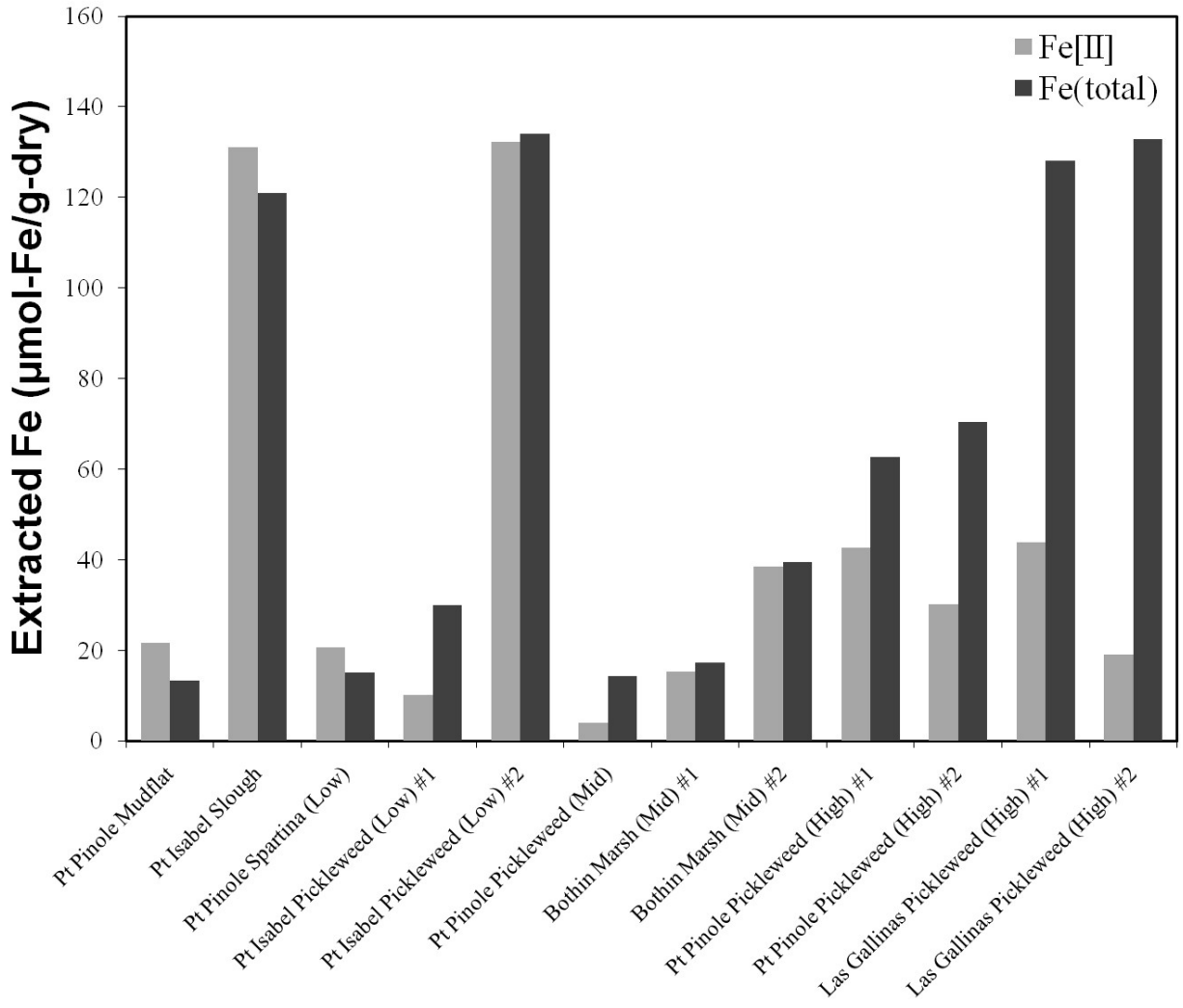

Figure 3-2. Measured iron concentrations in salt marsh sediment samples collected around Northern San Francisco Bay. Low, Mid, or High designations in the label refer to the marsh elevation in the area sampled.

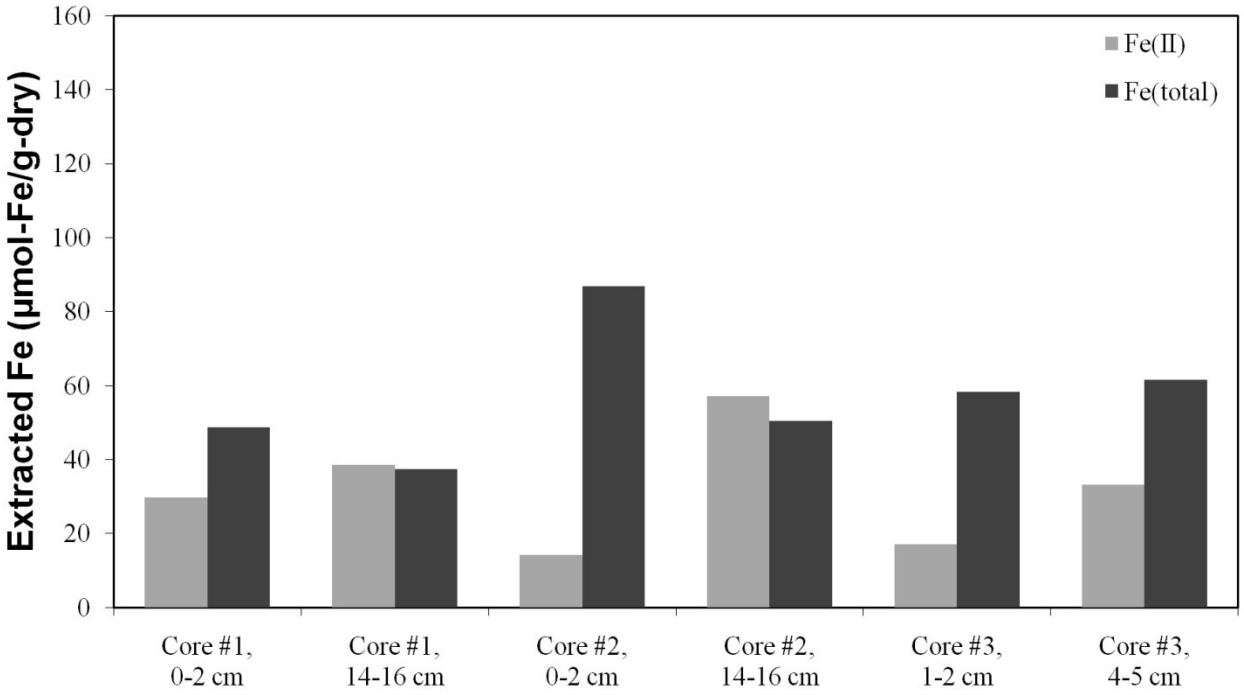

Figure 3-3. Measured sediment iron concentrations in from two depths in cores collected in Gambinini Marsh during July and August 2009.

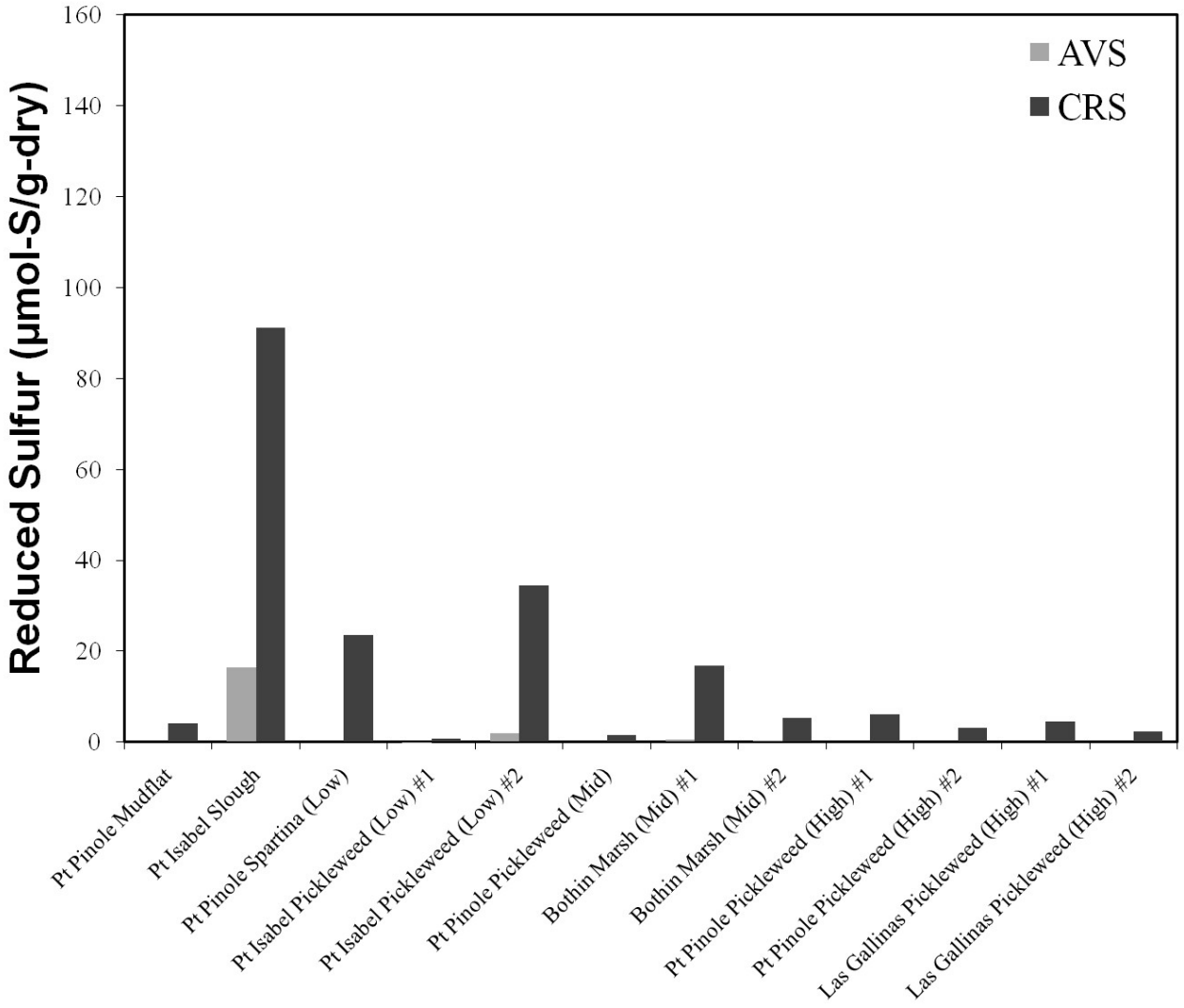

Figure 3-4. Measured acid volatile sulfide (AVS) and chromium reducible sulfur (CRS) concentrations in salt marsh sediment samples collected around Northern San Francisco Bay. Low, Mid, or High designations in the label refer to the marsh elevation in the area sampled.

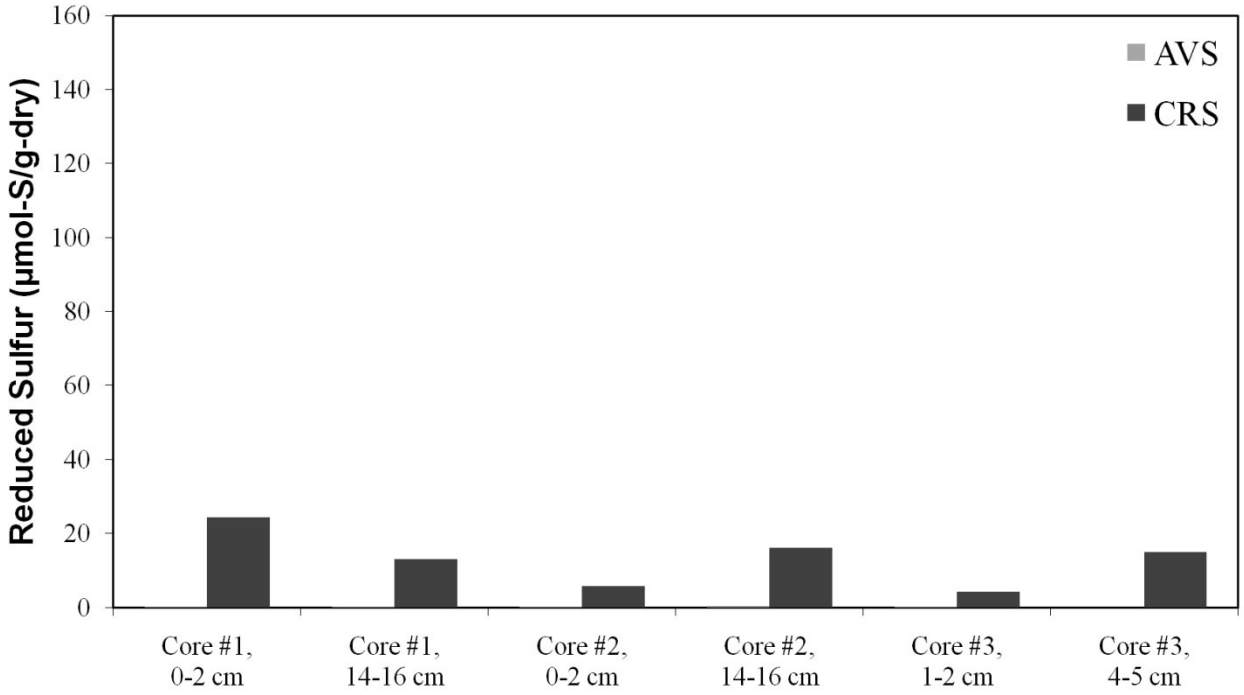

Figure 3-5. Measured sediment acid volatile sulfide (AVS) and chromium reducible sulfur (CRS) concentrations in from two depths in cores collected in Gambinini Marsh during July and August 2009.

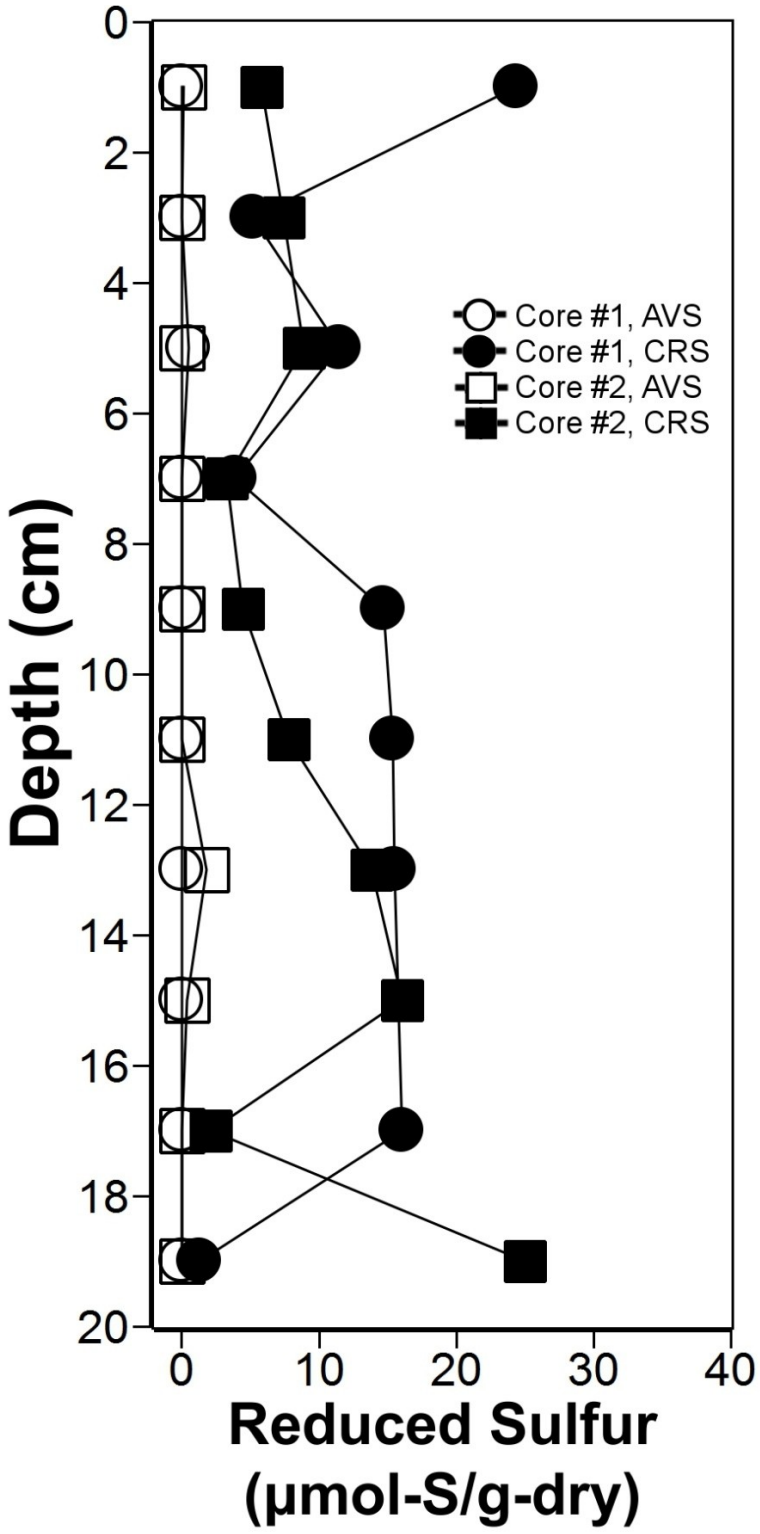

Figure 3-6. Acid volatile sulfide (AVS) and chromium reducible sulfur (CRS) depth profile from two 20-cm cores collected in Gambinini Marsh in August 2009.

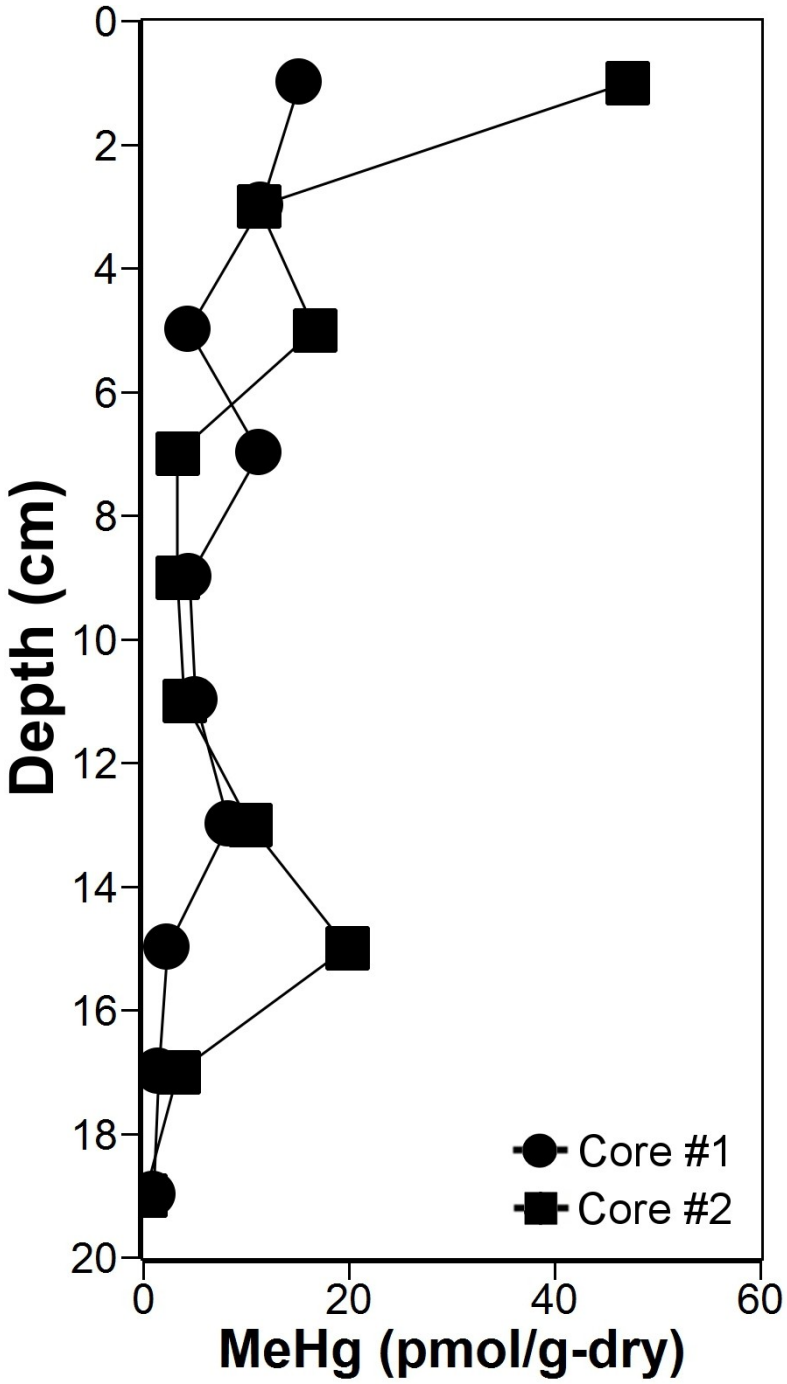

Figure 3-7. Depth profile of sediment MeHg in two sediment cores collected from Gambinini Marsh in August 2009.

3.3.2 Laboratory Sediment Incubation

The concentration of Fe[II] in the sediments (Figure 3-8) increased over time with nearly identical concentrations observed for both the untreated and the Mo-amended treatments. No production of Fe[II] was observed in the abiotic control. Total iron concentrations were stable over time (data not shown) with an average initial concentration of 84±8.4 μmol/g-dry. Concentrations of Fe[II] in the porewater (Figure 3-9) also increased over time for both the ambient and Mo-amended incubations, with higher average concentrations occurring in the Mo-amended treatment. Porewater Fe[II] concentrations were unchanged in the abiotic control over the 7-day incubation period.

Sulfate concentrations in the porewater (Figure 3-10) were constant throughout the incubation for both the Mo-amended and abiotic treatments whereas the untreated sediments exhibited a slow decrease throughout the 7-day incubation period. Sulfide was not detected in the porewater at concentrations above 0.01 mM for any treatment condition. No increase in AVS or CRS concentrations were observed for the Mo-amended and abiotic treatments. For the untreated sediments, both AVS and CRS increased from values near the detection limit 12 hours after initiation of the experiment to average concentrations of 4.5 and 5.1 μmol-S/g-dry, respectively, on day 7 (Figure 3-11). The increases in concentrations of AVS and CRS minerals accounted for 23% of the sulfate lost in the untreated sediment. The presence of reduced sulfur minerals in only the untreated incubation was further supported by the observation of areas of black sediment in the untreated jars after 7 days.

Initial concentrations of methylmercury in the slurries were approximately 5 pmol/g-dry for all three treatment conditions (Figure 3-12). The average concentration of MeHg in the Mo-amended incubation increased slightly to approximately 18 pmol/g-dry by Day 7. Concentrations of MeHg in the untreated slurry increased throughout the incubation to a final average concentration of 141 pmol/g-dry.

3.3.3 Field Core Incubations

For the July experiment, daily high air temperatures in Petaluma were between 23 and 33° C, with nightly lows between 9 and 13 °C. In November, daily high temperatures were between 12 and 14 °C, with overnight lows between -2 and 5 °C.

During the July experiment, average concentrations of Fe[II] increased with depth for all three conditions, but concentrations in the 0-1 cm intervals were not significantly different from Fe[II] concentrations in the deeper layers (Figure 3-13, One-way ANOVA with $\alpha = 0.05$ followed by Tukey's HSD). In the November experiment, the trends observed in the Fe[II] concentrations were less distinct than in July. The seasonal differences become more apparent when the data were expressed in terms of the fraction of extracted iron as Fe[II] (Figure 3-14). During July, the average fraction of Fe[II] was below 0.5 for the 0-1 cm depth for each condition, which was statistically different than the 3-4 cm and 6-7 cm depths for both the capped and open core condition, and the 0-1 cm depth was statistically different than the 6-7 cm depth in the fresh sediment (One-way ANOVA with $\alpha = 0.05$ followed by Tukey's HSD). In contrast, during November, the average fraction of Fe[II] stayed above 0.8 for all conditions, and were statistically similar for all depths under all conditions.

While AVS was not detected in any of the cores (data not shown), CRS concentrations (Figure 3-15) showed similar patterns to those observed for Fe[II]. During July, the surface layer of each core exhibited lower average concentrations of CRS than the deeper layers. However, the differences were not statistically significant (One-way ANOVA with $\alpha = 0.05$ followed by Tukey's HSD performed on log-transformed data). During November, the average CRS concentrations were similar at all depths. Additionally, concentrations in both the July and November experiments showed a range of average CRS concentrations that were similar to those observed in the 20 cm cores collected in August 2009 (Figure 3-6).

Concentrations of sediment MeHg (Figure 3-16) did not exhibit strong trends with depth or season. The exception was the Open Core in July, which exhibited higher average MeHg concentrations. However, there were no statistical differences among samples of any depth or season (One-way ANOVA with $\alpha = 0.05$ followed by Tukey's HSD performed on log-transformed data).

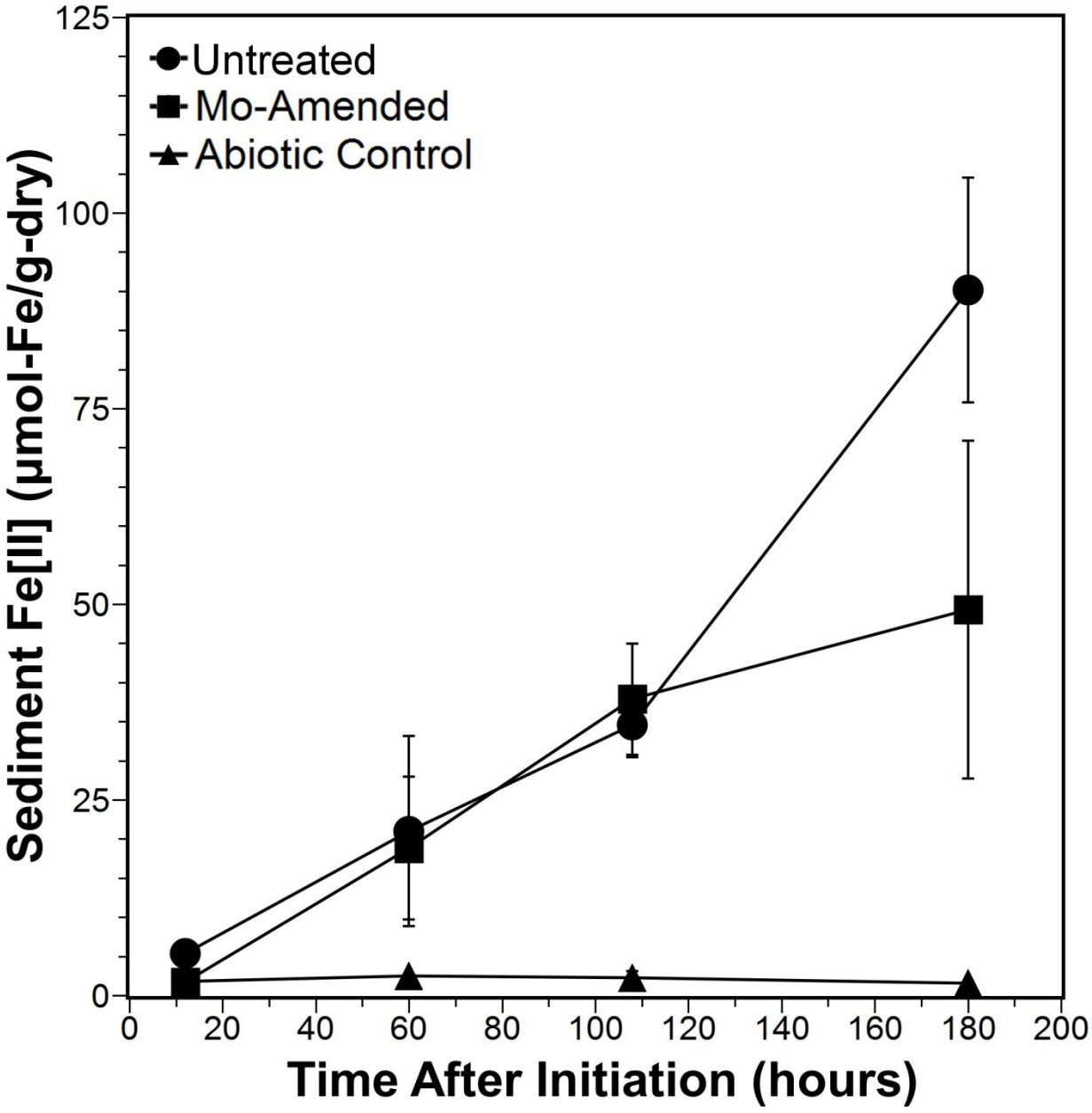

Figure 3-8. Average sediment Fe[II] concentrations measured during the incubation of sediments from the pickleweed-dominated high marsh plain of Gambinini Marsh. Values are shown as average ± S.E of the triplicate incubation bottles.

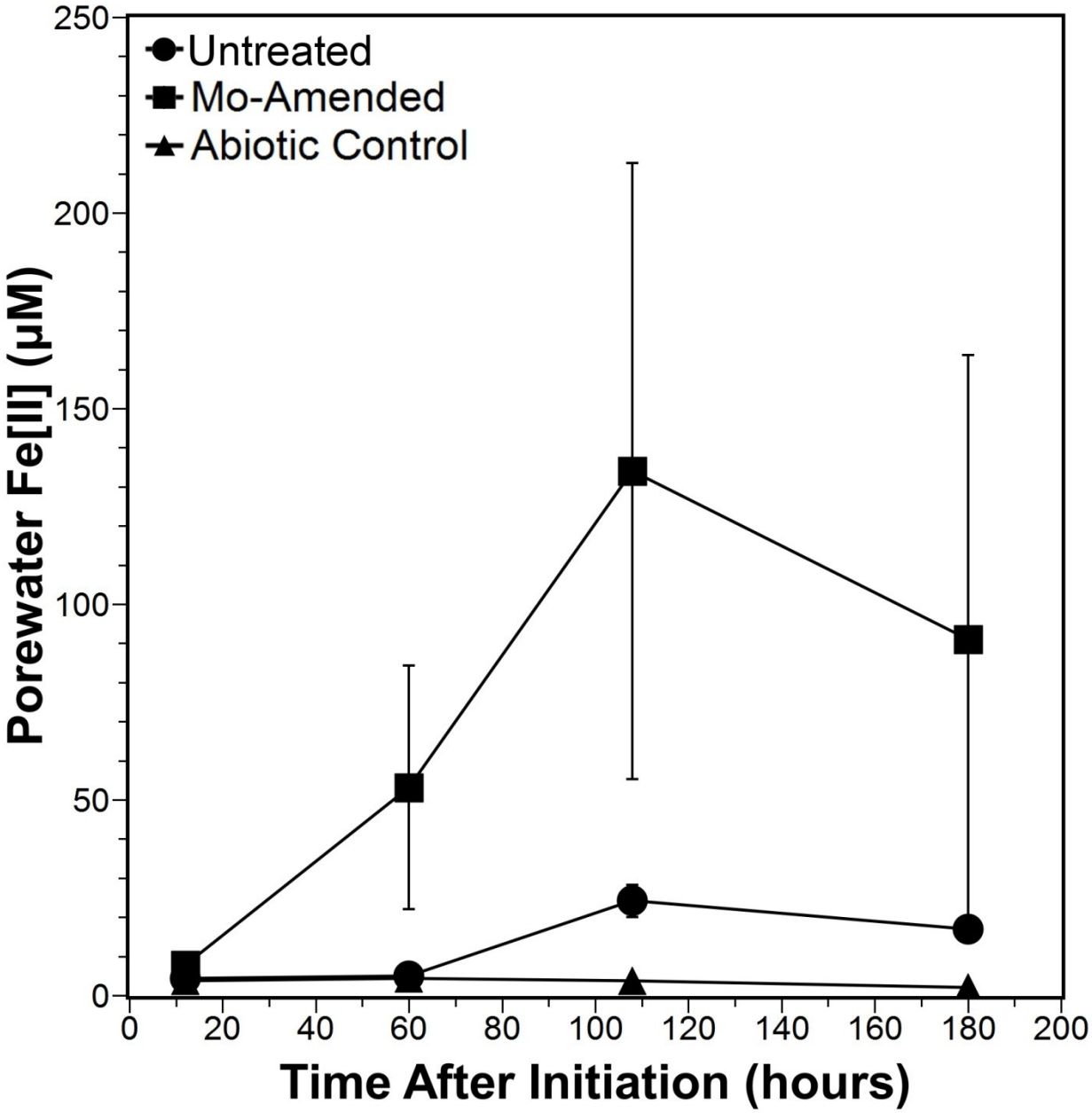

Figure 3-9. Average porewater Fe[II] concentrations measured during the incubation of sediments from the pickleweed-dominated high marsh plain of Gambinini Marsh. Values are shown as average ± S.E of the triplicate incubation bottles.

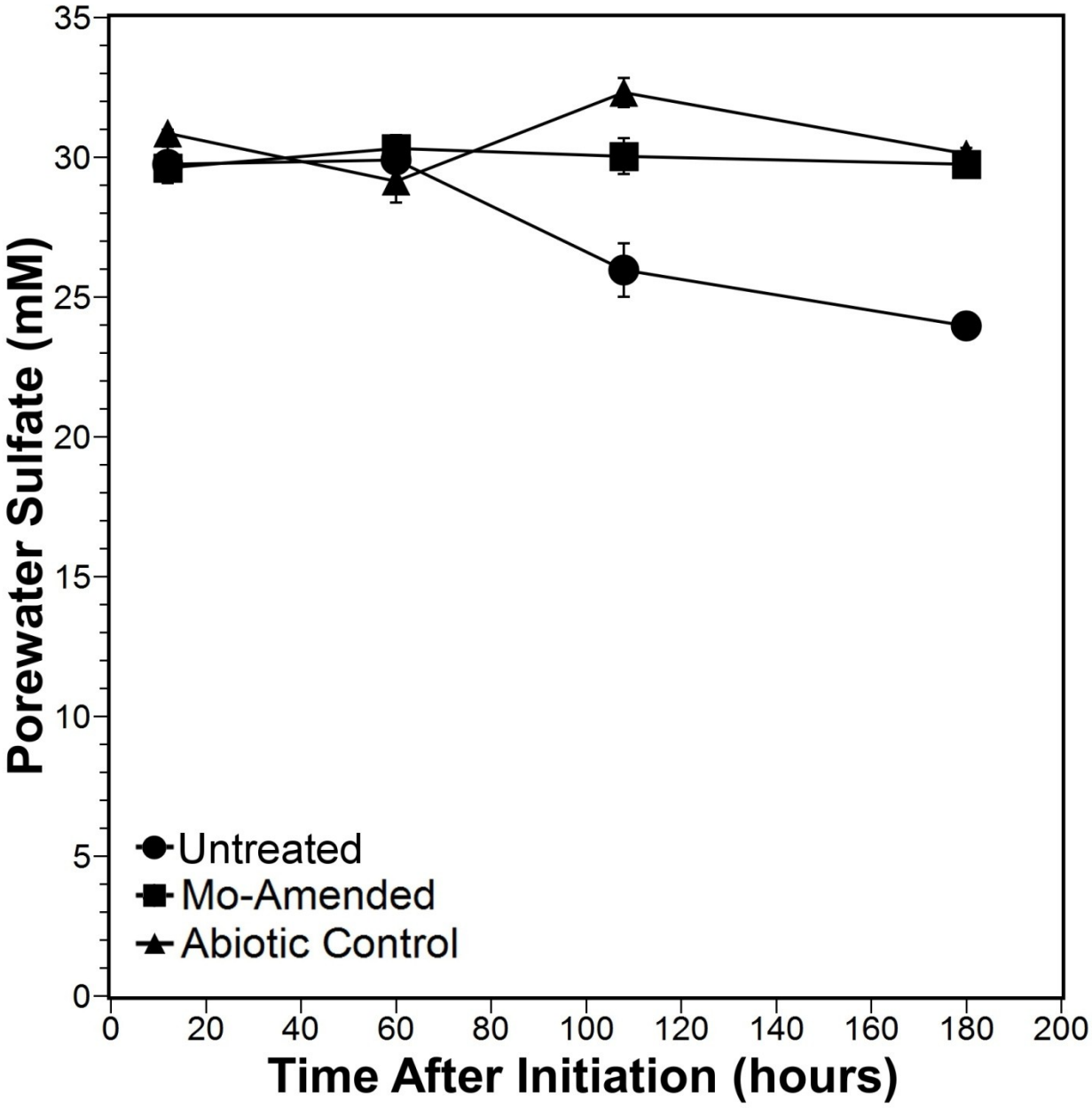

Figure 3-10. Average porewater sulfate concentrations measured during the incubation of sediments from the pickleweed-dominated high marsh plain of Gambinini Marsh. Values are shown as average ± S.E of the triplicate incubation bottles.

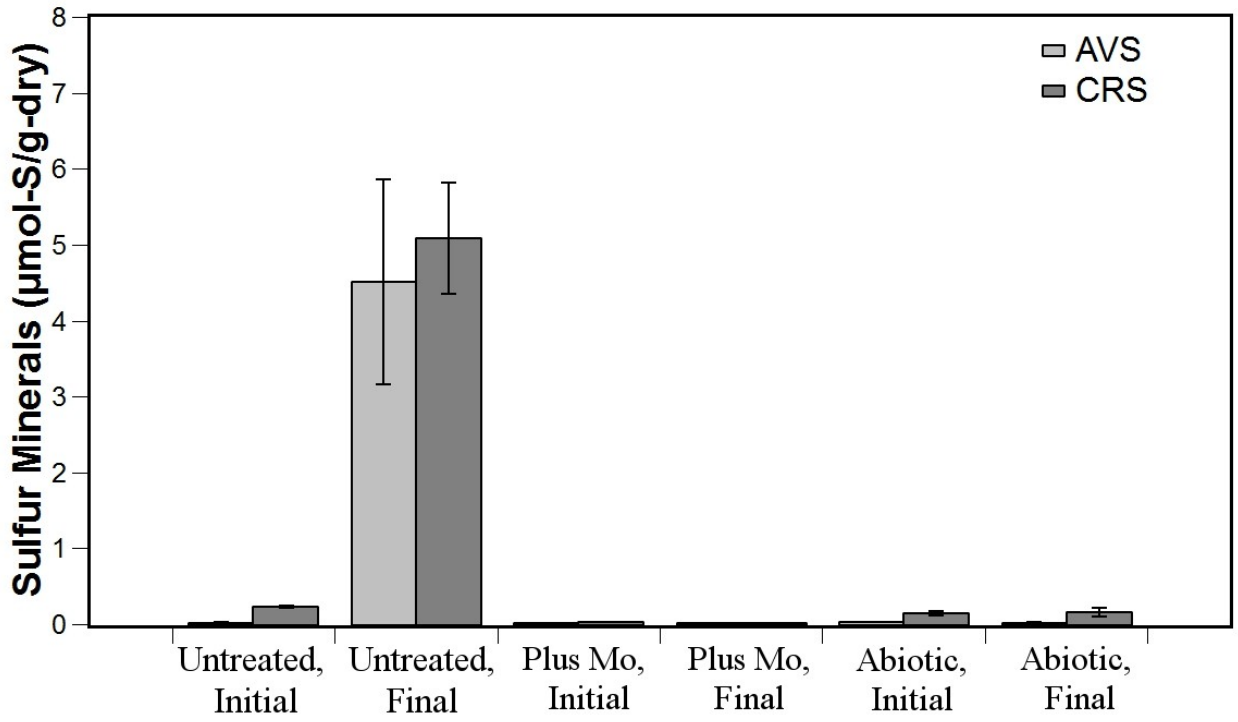

Figure 3-11. Average acid-volatile sulfide (AVS) and chromium-reducible sulfur (CRS) concentrations measured during the incubation of sediments from the pickleweed-dominated high marsh plain of Gambinini Marsh. Initial represents the values measured in the samples collected 12 hours after the initiation of the experiment, and "Final" represents samples collected at hour 180. Values are shown as average ± S.E of the triplicate bottles.

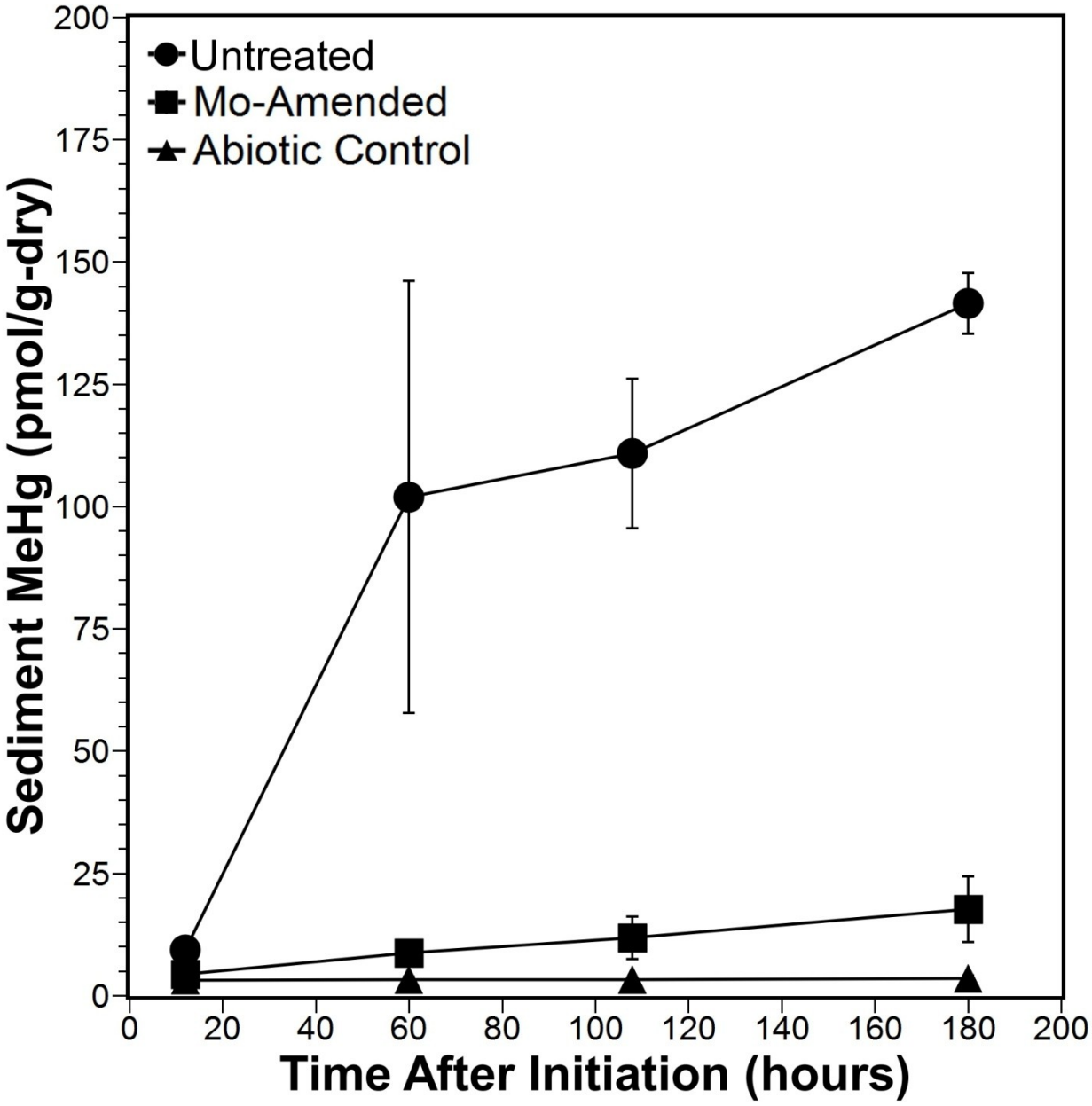

Figure 3-12. Average slurry methylmercury (MeHg) concentration measured during the incubation of sediments from the pickleweed-dominated high marsh plain of Gambinini Marsh. Values are shown as average ± S.E of the triplicate incubation bottles.

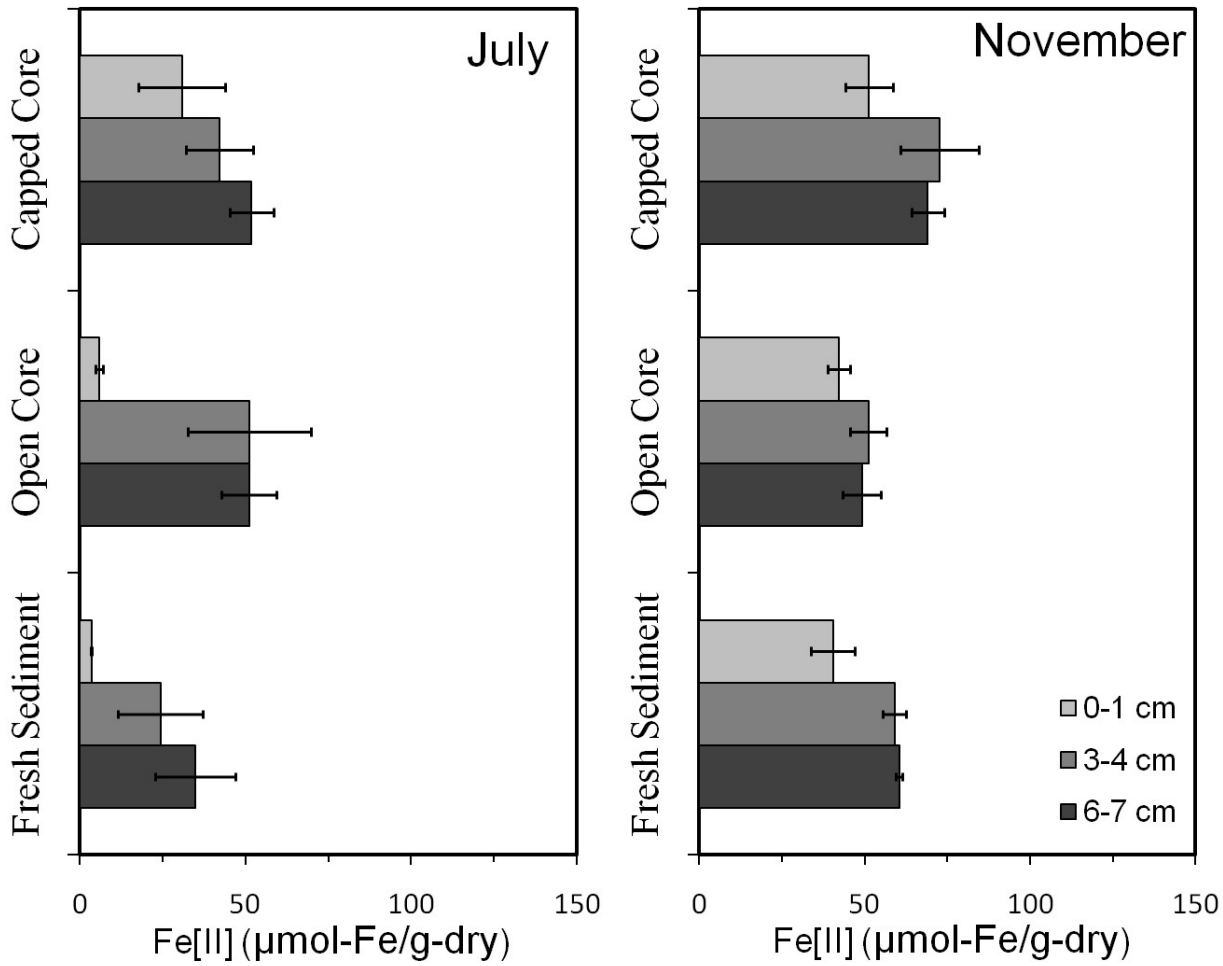

Figure 3-13. Sediment Fe[II] concentrations measured in *in situ* field core incubations in Gambinini Marsh. Values are shown as average ± S.E of the triplicate cores.

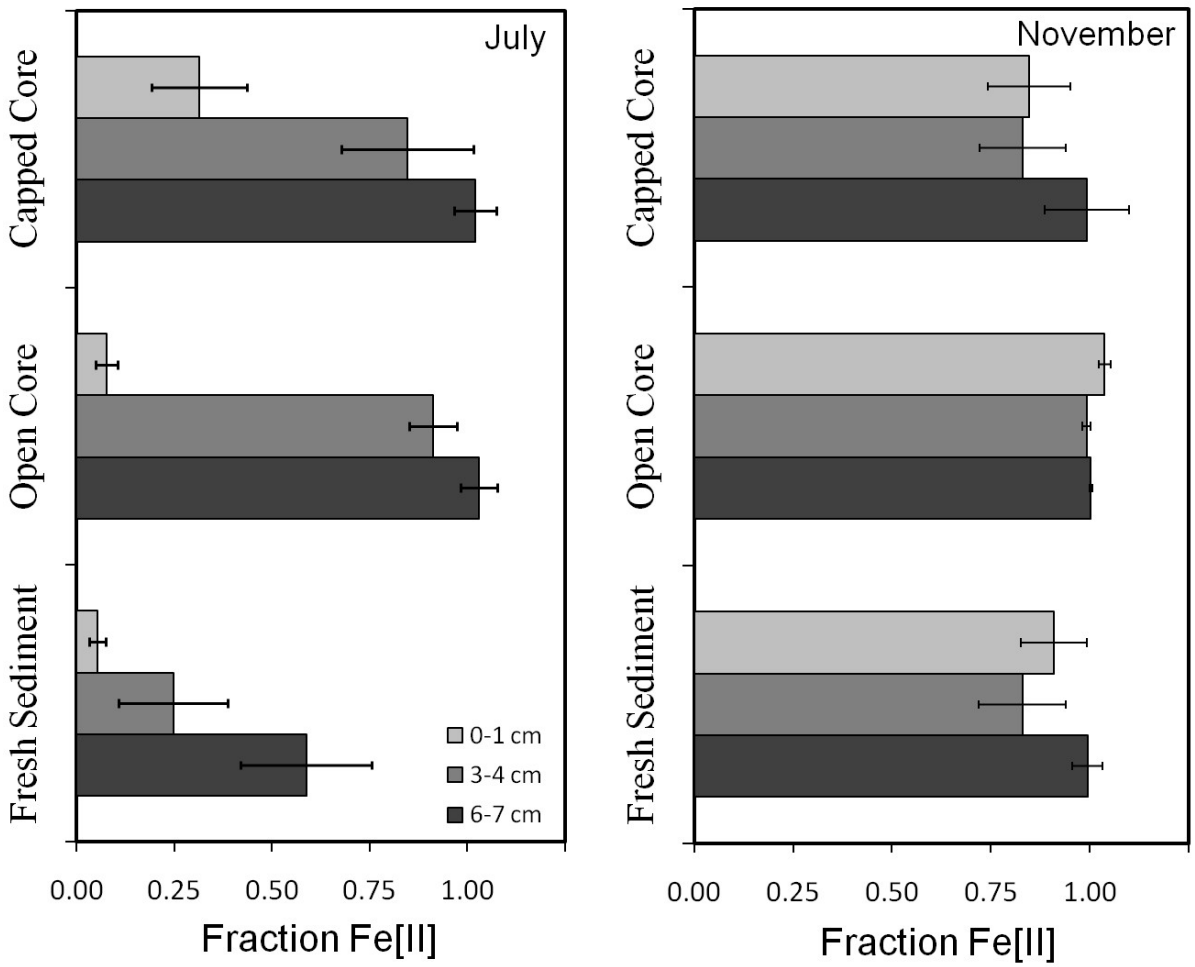

Figure 3-14. The fraction (Fe[II]/Fe[total]) of total extracted iron that was measured as Fe[II] in the *in situ* field core incubations in Gambinini Marsh. Values are shown as average ± S.E of the triplicate cores.

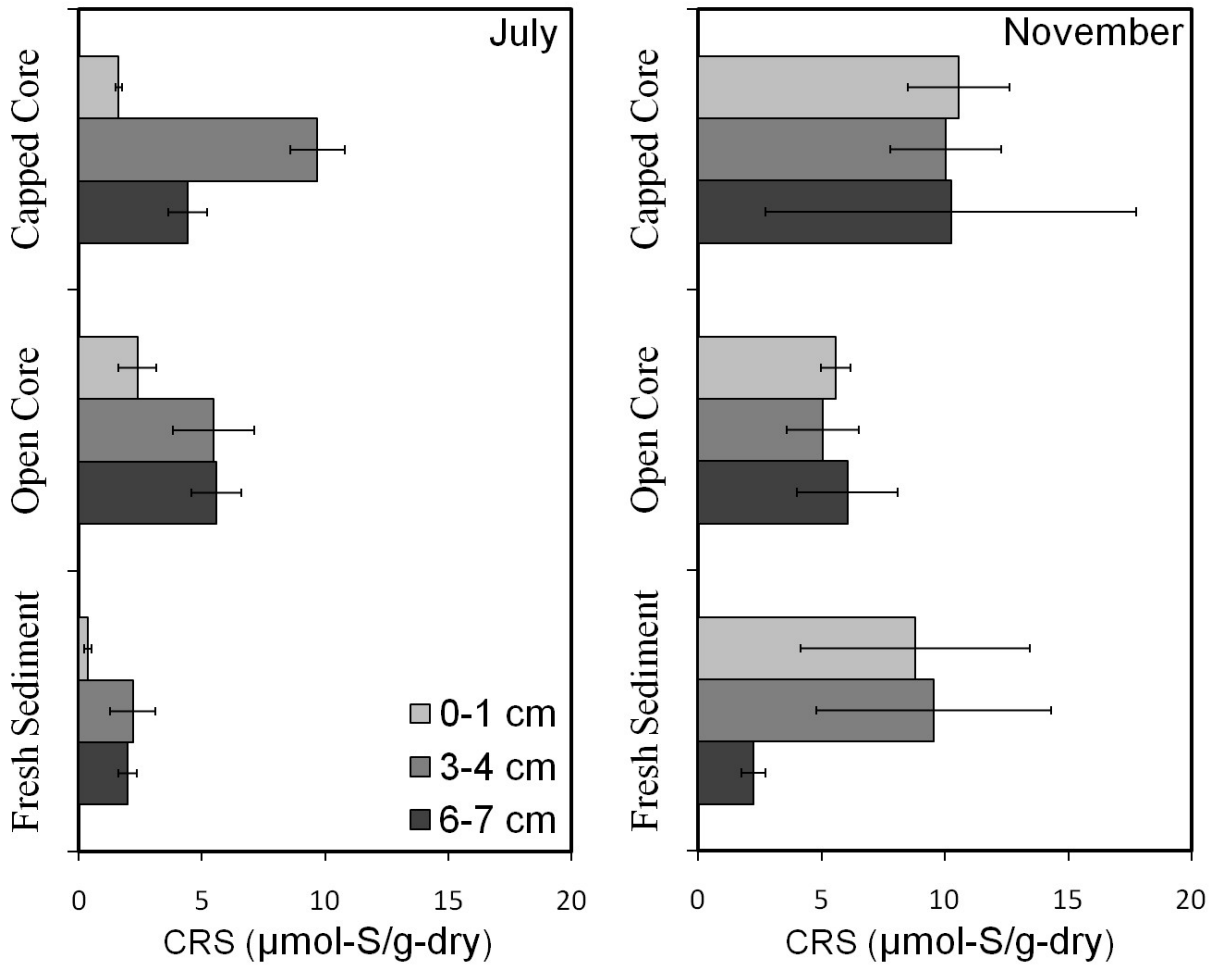

Figure 3-15. Sediment chromium reducible sulfur (CRS) concentrations measured in *in situ* field core incubations in Gambinini Marsh. Acid volatile sulfide (AVS) was not measured in the cores. Values are shown as average ± S.E of the triplicate cores.

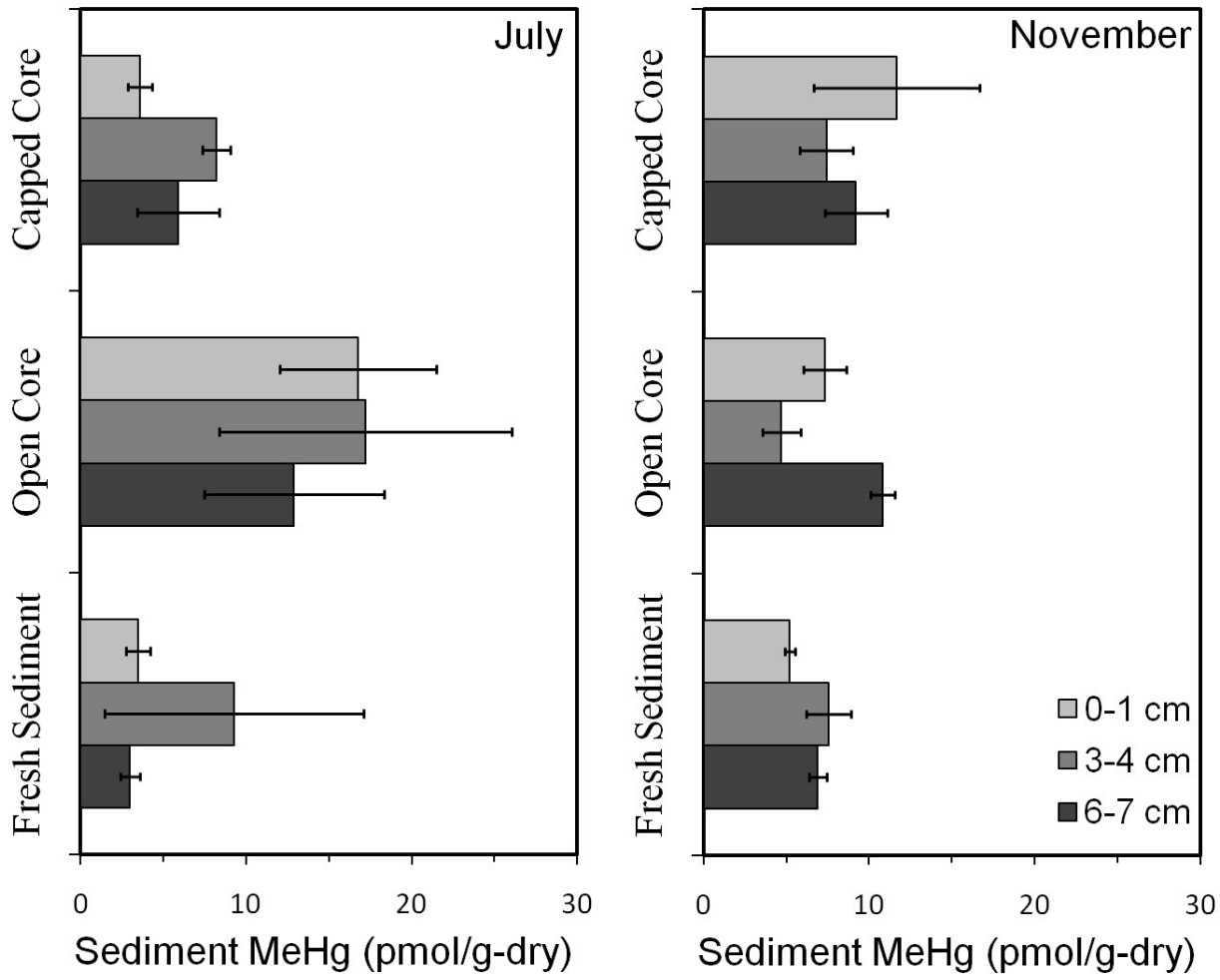

Figure 3-16. Sediment methylmercury (MeHg) concentrations measured in *in situ* field core incubations in Gambinini Marsh. Values are shown as average ± S.E of the triplicate cores.

3.4 Discussion

3.4.1 Tidal Salt Marsh Sediment Redox Conditions

3.4.1.1 Influence of Oxygen on Redox Cycling

Oxygen is the most energetically favorable terminal electron acceptor, and when O_2 is available, aerobic organisms outcompete other species. In saturated sediments, oxygen penetration is limited due to slow diffusion rates and rapid utilization by aerobic organisms as well as abiotic reactions with reduced species such as Fe[II]. As a result, quiescent sediments will often exhibit depletion of O_2 within a few millimeters of the sediment surface (Brendel & Luther 1995). However, diffusion from the atmosphere or overlying oxygenated water is not the only mechanism for transfer of oxygen to the subsurface sediments in tidal wetlands. The exchange of porewater with tidal sloughs also can introduce oxygen into the sediments, as oxygenated surface water infiltrates through creek bank walls during high tides. Seepage of porewater into tidal slough channels during low tide can also allow enhanced rates of infiltration of oxygen into the surficial sediments. While potentially important locally, these effects are most prominent within a few meters of tidal slough channels (Gardner 2005, Li et al. 2005, Ursino et al. 2004). Salt marsh plants can introduce oxygen into sediments as well, as they decrease the level of the water table during low tide via evapotranspiration (Dacey & Howes 1984) and release oxygen through their root systems. While most of the oxygen present in the roots is used for respiration, some leaks into the surrounding rhizosphere, a process known as radial oxygen loss. This process can help plants to counteract sulfide toxicity (Lee 1999) and can cause vegetated sediments to exhibit increased concentrations of oxidized species relative to nearby unvegetated sediments (Howes et al. 1981, Koretsky & Miller 2008). Different wetland plant species are capable of introducing oxygen into the sediments to varied degrees (Koretsky et al. 2008). While we are unaware of a study directly on radial oxygen loss from *S. pacifica* roots, other high marsh species are capable of seasonally oxygenating the root zones of sediments (Canario et al. 2007, Otero & Macias 2002).

The introduction of oxygen into the anaerobic subsurface can have a profound effect on the geochemistry of reduced wetland sediments. Sulfide is readily oxidized in the presence of oxygen, with half lives in seawater at pH 8 reported to be around 26 hours (Millero et al. 1987a). The presence of reduced transition metals like Fe[II] can catalyze the sulfide oxidation reaction (Vazquez et al. 1989) with reported half lives less than 23 minutes in iron-rich deep waters of Chesapeake Bay (Millero 1991). Dissolved Fe[II] also undergoes rapid oxidation when oxygen is present, with reported half lives of less than 10 minutes in seawater at pH 8 (Millero et al. 1987b). Amorphous $FeS_{(s)}$ minerals are also oxidized quickly upon exposure to oxygen with half-lives on the order of 30 minutes under conditions typical of estuarine waters (Simpson et al. 2000).

In the pickleweed-dominated high marsh sediments analyzed in this chapter, relatively low concentrations of reduced compounds (i.e, less than 30 μmol/g Fe[II] and less than 2 μmol/g AVS) were measured in the surficial sediments during the summer months. In contrast, when devegetated microcosms from the same site (Chapter 2) were subjected to a simulated tidal cycle in the laboratory, average porewater sulfide concentrations as high as 1.5 mM, and average AVS

concentrations as high as 35 μmol-S/g were observed at 0-3 cm depth. Furthermore, when the sediments from Gambinini Marsh were incubated in the absence of oxygen in a closed container (Section 3.3.2), Fe[II] concentrations increased starting shortly after initiation of the 7-day experiment. This suggests that the sediments are populated by a microbial community that includes both sulfate and iron reducers. The absence of Fe[II] and S[-II] in porewater samplers installed at the wetland but not in the microcosms or incubation experiments may have been attributable to higher fluxes of oxygen into the sediments under field conditions and not the absence of microbial activity.

When the exchange of gases with the atmosphere was prevented in the capped core experiment, an increased fraction of Fe[II] was observed in the 0-1cm layer compared to the fresh, uncapped sediment core. The effect was also apparent at depth, where around 80% of the extracted iron was Fe[II] in the 3-4 cm layer of the capped core, while only around 25% of the iron was Fe[II] in the fresh sediment core. This suggests that oxygen may be reaching a depth of at least 3-4 cm in the wetland. In addition to separating the surface of the sediments from the atmosphere, the capped tube physically separated the entrapped sediment from the lateral movement of porewater during tidal events and severed the connection of the sediments to the nearby live plant roots. Pickleweed has a dense and relatively shallow (maximum depth of 14 cm, (Windham-Myers et al. 2009)) system of thin roots, and they were easily cut by the beveled edge of the coring tube. Thus, the increased fraction of reduced species in the coring tubes could also have been attributable to decreased inputs of oxygen from the pickleweed roots. This interpretation is strengthened by the results of the November experiment, which took place after the pickleweed had undergone senescence. In these experiments, high proportions of Fe[II] (typically greater than 80%) were observed in both the incubated and fresh cores.

3.4.1.2 Iron Cycling

Iron reduction is an important process for carbon oxidation in tidal salt marsh systems dominated by many plant species (Hyun et al. 2009, Hyun et al. 2007, Kostka et al. 2002). Our results suggest that it also occurs in the pickleweed-dominated sediments of Gambinini Marsh. There is a substantial pool of reducible Fe[III] in the surficial sediments, which could be used by iron-reducing bacteria. Our measurements of sediment Fe[II] and Fe[III] concentrations were comparable in magnitude to those reported in sediments collected from tidal marshes in the Chesapeake Bay (Mitchell & Gilmour 2008), coastal Georgia (Hyun et al. 2007), and Delaware Bay (Kostka & Luther 1995). Previous published research suggests that all forms of easily extractable and reducible Fe[III] minerals in the sediments are part of the reactive pool of Fe[III] utilized by microbial respirators (Kostka & Luther 1995, Lovley & Phillips 1987).

Our *ex situ* incubation experiments showed similar rates of accumulation of Fe[II] in the sediments of both the untreated and the Mo-amended samples, demonstrating that iron reduction and sulfate reduction occurred simultaneously within the incubation bottle. Therefore, it is possible that these two processes occur simultaneously in the sediments of Gambinini Marsh. It is also possible that heterogeneity in the intact sediment cores results in microenvironments where SO_4^{2-} is reduced because Fe[III] has been depleted (Jorgensen 1977, Sundby et al. 2003). A previous study of incubated surficial sediments (0-3 cm) from a stand of tall-form *Spartina alterniflora* in a Georgia salt marsh (Hyun et al. 2007) showed similar rates of Fe[II] production as those observed in our experiment. They also found that inhibiting sulfate reduction with

molybdate did not alter Fe[III] reduction rates. However, inhibition of sulfate reduction did reduce the total respiration rate by approximately 60%, as measured by the total production of CO_2 during the incubation. The generation of CO_2 was not measured in our experiment, but based on the comparable rates of Fe[II] generated in both sets of sediments, it seems likely that both iron and sulfate reduction occur simultaneously in the upper 4 cm of the Gambinini Marsh.

Additionally, the *in situ* core incubation experiment exhibited seasonal variations in the proportion of reduced iron in the sediments. In the fresh sediment cores, the percent of extracted iron present as Fe[II] in the 0-1 cm and 3-4 cm layers increased from below 25% in July to greater than 80% in November. Seasonal changes of this nature, with a higher percentage of Fe[III] species present in salt marsh sediments during summer months, and higher concentrations of reduced iron minerals during winter months have been reported previously in *Spartina*-dominated salt marshes (Kostka & Luther 1995, Sundby et al. 2003).

3.4.1.3 Sulfur Cycling

Sulfate is often the predominant electron acceptor in salt marsh sediments. While Fe[III] reduction was evident in the surficial sediments, sulfate reduction was likely an important process in Gambinini Marsh. When the sediments were incubated under anaerobic conditions, sulfate reduction readily occurred in the untreated condition, which was evidenced by the decrease in sulfate concentration after 7 days for only the untreated condition, as well as an accumulation of AVS and CRS. For the untreated incubation, there was a net loss of approximately 350 µmol of sulfate, compared to a net production of approximately 570 µmol of Fe[II]. In terms of total electron transfer, however, sulfate was more dominant. With 8 electrons transferred for each sulfate reduced to S[-II], a total of 2800 µmol of electrons were transferred via sulfate reduction, compared to 570 µmol of electrons transferred via iron reduction (a one electron transfer during the reduction of Fe[III] to Fe[II]). This suggests that sulfate reducers are an important part of the microbial community in Gambinini Marsh sediments, and may exist in concert with iron-reducing bacteria in microenvironments suited to sulfate reduction.

It is difficult to assess the relative rates of sulfate reduction in the marsh sediments based on measurements of sediment concentrations, because the end product of sulfate reduction (sulfide) is highly reactive, and is rapidly oxidized by oxygen. Additionally, as mentioned above, sulfide reacts rapidly with Fe[III] minerals, which are prevalent in the sediments of Gambinini Marsh. For example, ferrihydrite has been shown to have a half life of around 4 hours in the presence of 1 mM sulfide (Canfield et al. 1992). This means that as sulfide was produced during sulfate reduction, it reacted quickly with the available pool of Fe[III] minerals to form Fe[II] and oxidized sulfur species, leaving only a very low-level steady state concentration of sulfide in the porewater until the entire pool of reactive Fe[III] minerals were consumed (Canfield 1989). In fact, it has been estimated that in salt marsh and intertidal sediments, as little as 0.15% to 7.5% of the total reduced sulfate is accrued in the sediments as reduced sulfur species (Howarth 1984) with the remainder being reoxidized or lost from the system via diffusion or advection. Thus, the small accumulation of reduced sulfur species in Gambinini Marsh sediments should not be regarded as indicative of a lack of sulfate-reduction. Rather, sulfide likely reacted with Fe[III]-containing minerals and oxygen.

This rapid oxidation of sulfide can play an important role in the formation of iron-sulfur minerals in salt marsh sediments as well. For example, the formation of pyrite is often reported

to be slow due to an intermediate step in which H_2S or S^0 reacts with iron monosulfide minerals ($FeS_{(s)}$) (Rickard & Morse 2005). However, in salt marsh sediments, where dissolved sulfide concentrations remain low and the pH is between 5.5 and 7, it is possible for the porewater to be oversaturated with respect to pyrite and undersaturated with respect to $FeS_{(s)}$. This allows for the direct formation of $FeS_{2(s)}$ on the timescale of hours to days (Howarth 1979). This process may explain the rapid accumulation of CRS in the *ex situ* incubations (Figure 3-11), as well as the detection of CRS but not AVS in Gambinini Marsh cores and surficial sediments collected from other high marshes around Northern San Francisco Bay.

3.4.2 Methylmercury Production

The increase in MeHg concentrations during the laboratory incubation experiment (Figure 3-12) demonstrated that sulfate-reducers produced most of the methylmercury in the Gambinini Marsh sediments. MeHg concentrations for the Mo-amended incubation also increased, with a final concentration that was about 5 times higher than the abiotic control. While it is possible that iron-reducing bacteria produced MeHg, the MeHg production also could have been due to sulfate reduction occurring within small microenvironments in the jars. For the unamended incubation, there was a net decrease of approximately 350 µmol sulfate (corresponding to 5.8 mM decrease in porewater concentration) and a net increase of approximately 1200 pmol MeHg during the 7-day incubation. For the Mo-amended condition, an increase of approximately 125 pmol MeHg was observed. Based on the rate of production of MeHg in the unamended experiment, this would require a net reduction of around 35 µmol sulfate, which would correspond to a decrease of around 0.6 mM sulfate in the porewater. This value is within the error of the triplicate samples from 12 hour and 180 hour samples for the Mo-amended condition. Regardless of the source of MeHg in the Mo-amended samples, the concentration of MeHg produced after 7-days in the Mo-amended condition was 10 times lower than the untreated condition.

Estuarine sediments in locations inundated with high salinity water have often been described as being less important sources of MeHg than locations with intermediate salinity because high rates of sulfate reduction can result in the generation of high concentrations of sulfide (Gilmour & Henry 1991). The accumulation of sulfide can limit the production of MeHg by lowering the concentration of bioavailable inorganic mercury species (Benoit et al. 1999, Benoit et al. 1998). However, in a tidal salt marsh like Gambinini Marsh, sulfide does not accumulate in the sediments. Thus, the high salinity water would not inhibit further mercury methylation. On the contrary, high tidal salt marsh plains have the potential to be significant sources of MeHg due to the potentially high rates of sulfate reduction, which are often correlated with mercury methylation rates (Avramescu et al. 2011, Choi & Bartha 1994, King et al. 1999). This inference is consistent with the observation of relatively high MeHg concentrations in the surficial sediments of Gambinini Marsh (see Chapter 4 for a more detailed comparison).

While the laboratory incubation experiment showed that the microbial community in the sediments can rapidly produce MeHg during a closed-container incubation, dynamic iron cycling in the surficial sediments may limit the efficacy of iron amendments for the control of MeHg production. The iron amendment hypothesis is based on the potential for Fe[II] to decrease the concentration of dissolved sulfide in porewater, and to remove sulfide from solution to form $FeS_{(s)}$. In the high marsh of Gambinini Marsh, $FeS_{(s)}$ (as AVS) was not detected in surficial sediments, and Fe[III] minerals were abundant. Since it is likely that iron was cycled between

Fe[II] and Fe[III] forms in the sediments, a ferrous iron amendment may not have much impact on Hg speciation or sulfate-reducing organisms. However, it is also possible that additional iron added to the system could favor microbial respiration by Fe[III] reducers or alter speciation in microenvironments. To better understand the long-term cycling of redox active species in the marsh sediments, as well as to evaluate the potential efficacy of an iron amendment under field conditions, further research is necessary to study these processes *in situ*.

Chapter 4. Methylmercury Production in the Gambinini Marsh

4.1 Introduction

Wetlands are highly productive ecosystems in terms of primary productivity and carbon mineralization. Due to limited oxygen transport in saturated wetland sediments, most microbial oxidation of carbon occurs under anoxic conditions. This creates an environment that is conducive to the production of methylmercury (MeHg). Consistent with this observation, previous studies have demonstrated that MeHg concentrations in freshwater systems are correlated with the amount of wetland acreage within a watershed (Babiarz et al. 1998, Guentzel 2009, Hurley et al. 1995, St Louis et al. 1994). Tidal wetlands, including tidal freshwater and salt marsh habitats, also exhibit characteristics conducive to MeHg production. However, relatively few studies have been conducted to assess the MeHg contribution of wetlands receiving inputs of inorganic Hg from the atmosphere (Hall et al. 2008, Kongchum et al. 2006, Langer et al. 2001, Mitchell & Gilmour 2008) or point sources of mercury pollution (Canario et al. 2007, Valega et al. 2008).

Historic mining activities have resulted in elevated concentrations of mercury in the San Francisco Bay-Delta (Conaway et al. 2007), which has negatively impacted wildlife in the estuary (Eagles-Smith et al. 2009, Schwarzbach et al. 2006, Tsao et al. 2009) and led to fish consumption advisories to protect human health (EPA 2009). However, while tidal wetlands are believed to contribute substantially to MeHg loading in the estuary, only a few studies have included data on MeHg concentrations in the tidal freshwater marshes of the Delta (Choe et al. 2004, Heim et al. 2007) and the tidal salt marshes around San Francisco Bay (Clarisse et al. 2011, Marvin-DiPasquale et al. 2003, Windham-Myers et al. 2009).

Seasonal studies of sediment biogeochemistry (Koretsky & Miller 2008, Neubauer et al. 2005, Otero & Macias 2002) and MeHg concentrations (Langer et al. 2001, Mitchell & Gilmour 2008) have been reported for other salt marsh environments. In general, the studies indicate seasonal fluctuations in MeHg and redox-active inorganic species due to changes in the activity of wetland vegetation as plants alter the redox conditions of the rhizosphere by releasing oxygen (Howes et al. 1981, Lee 1999, 2003) and organic acids (Mucha et al. 2005, Windham-Myers et al. 2009). In the Bay-Delta, tidal freshwater wetlands have also been shown to have higher MeHg concentrations during the late spring and early summer than during the late summer and fall (Choe et al. 2004, Heim et al. 2007), which may be attributable to increased mercury methylation rates at higher water temperatures (Gilmour et al. 1998). This pattern has also been reported in open-water sediments of the Bay-Delta, where methylation rates increased during February and March, and demethylation rates increased in May and October (Marvin-DiPasquale & Agee 2003). However, no studies of temporal MeHg production have been reported for tidal salt marshes in the Bay-Delta.

Previous research conducted in a tidal freshwater marsh in Frank's Tract (Choe et al. 2004), located in the Delta near Oakley, California, indicated higher MeHg concentrations in the surface water of the marsh as the tide was ebbing (1.5 pM) relative to water flowing into the wetland at high tide (0.75 pM). This demonstrated that the marsh was a net exporter of MeHg, and suggests that tidal freshwater marshes could be important sources of MeHg to the Bay-Delta. The potential for tidal marshes to act as sources of MeHg to the estuary may hinder current restoration objectives of increasing the acreage of these important ecosystems (CSWRCB 2006). To remedy this conflict between the need for increased tidal wetland habitat and concern over increased MeHg concentrations, it is important to evaluate landscape-scale controls that could be effective in preventing the production and export of MeHg from restored tidal wetlands.

In Chapter 2, it was demonstrated that adding Fe[II] to the sediments of tidal wetland microcosms made from intact sediment cores from Gambinini Marsh altered the geochemistry of iron, sulfur, and mercury in a manner than reduced the export of MeHg in the surface water by as much as 80-90%. While these results suggested the potential for using iron addition as a means of controlling MeHg production in tidal wetlands, the sediment conditions in the microcosms did not fully mimic encountered at the field site. Specifically, the microcosms had sulfidic sediments, with 1.0-1.5 mM of dissolved sulfide in the porewater and concentrations of acid-volatile sulfides (AVS) ranging from 13 to 72 μmol-S/g-wet in the top 10 cm of the sediments. In contrast, the cores collected from the Gambinini Marsh in July 2009 (Chapter 3) showed an absence of porewater sulfide and less than 4.5 μmol/g-wet of AVS throughout the top 20-cm of the sediments. Furthermore, acid-extractable Fe[III] was detected in the surficial sediments, which is consistent with an absence of sulfide (Canfield et al. 1992).

Incubation experiments described in Chapter 3 demonstrated that iron reduction occurs in the sediments under anaerobic conditions, and that MeHg production was attributable to sulfate reduction, and not iron reduction. These findings suggest that addition of iron would not promote mercury methylation via the stimulation of the activity of iron-reducing bacteria, but the presence of Fe[II] in the sediments suggests that increasing iron concentrations via an iron amendment might have little effect on MeHg production in the system. The observation of simultaneous iron and sulfate reduction in the incubation experiments suggests the presence of microenvironments within the sediments where sulfate reduction occurs due to local depletion of Fe[III] (Jorgensen 1977). Bulk scale measurements of marine and coastal sediments sometimes show more oxidized overall conditions, but sub-millimeter microenvironments with increased rates of microbial metabolism and increased concentrations of reduced species can exist within discrete zones of the more oxidized bulk sediment (Stockdale et al. 2009). For example, microenvironments with increased sulfate reduction rates have been identified around organic deposits like decaying plant roots and burrowing organism fecal material (Stockdale et al. 2010) or near oxic/anoxic boundaries of macrofaunal burrows (Bertics & Ziebis 2010). Therefore, it is possible that iron addition might still result in decreased MeHg production if it is able to alter the mercury speciation within the sulfate-reducing microenvironments where mercury methylation occurs.

To better understand temporal variations in mercury biogeochemistry and the efficacy of sediment iron addition, a 17-month field study was conducted in the Gambinini Marsh. By employing test plots in the pickleweed-dominated high marsh plain, from which porewater and surficial sediments could be readily sampled, it was possible to gain insight into the role of iron and sulfur on MeHg production. Additionally, an iron amendment was conducted in two of the test plots provided information on the effect of Fe[II] addition on MeHg concentrations, as well as the long-term fate of the added iron.

4.2 Methods

4.2.1 Gambinini Marsh Description

Gambinini Marsh (38.207°N,122.584°W) is a historic salt marsh with a high marsh plain dominated by pickleweed. The marsh is along the western edge of the Petaluma River, just south

of Petaluma, CA, and is part of the Bay-Delta estuary. The Bay-Delta region experiences a Mediterranean climate, with warm, dry summers and cool, wet winters. Daily average high air temperatures in Petaluma are highest during July through September (28°C) and lowest in December and January (14°C). Petaluma receives an average of 0.66 m of rainfall each year, with over 90% occurring from November to April. The marsh experiences the mixed semidiurnal tidal cycle of the Petaluma River, which is connected to northern San Francisco Bay and is a fully tidal river (mean tidal range of 1.5 m, with a mean spring tide range of 1.9 m) with seasonal flow. This means that there is no net outflow during the dry season (i.e., all water movement is due to the tidal cycle), and wet season discharge is driven by precipitation in the 378 km^2 watershed.

4.2.2 Test Plots

Test plots were established in the high marsh plain of Gambinini Marsh in June 2009. A 10 m by 10 m area was identified that had a similar density and height of actively growing pickleweed. Within this area, a total of six, 1 m by 1 m plots were established using wooden dowel rods pressed into the sediments with a rope wrapped around the poles at a height of approximately 25 cm above the vegetation (Figure 4-1). While six plots were initially established, only four were sampled throughout the course of the study (Plots A, D, E, and F).

Three porewater samplers (10-cm Rhizon Soil Moisture Sampler; Rhizosphere Research Products, Netherlands) were installed at a depth of 2.5 cm below the sediment surface at randomly selected locations in each plot. A stainless steel putty knife was used to open a 10-cm long slit in the sediments, and the porewater sampler was gently pressed into the hole. The slit was then pressed closed by hand to prevent water from pooling around the sampler. The porewater samplers were equilibrated for 10 days before porewater was sampled.

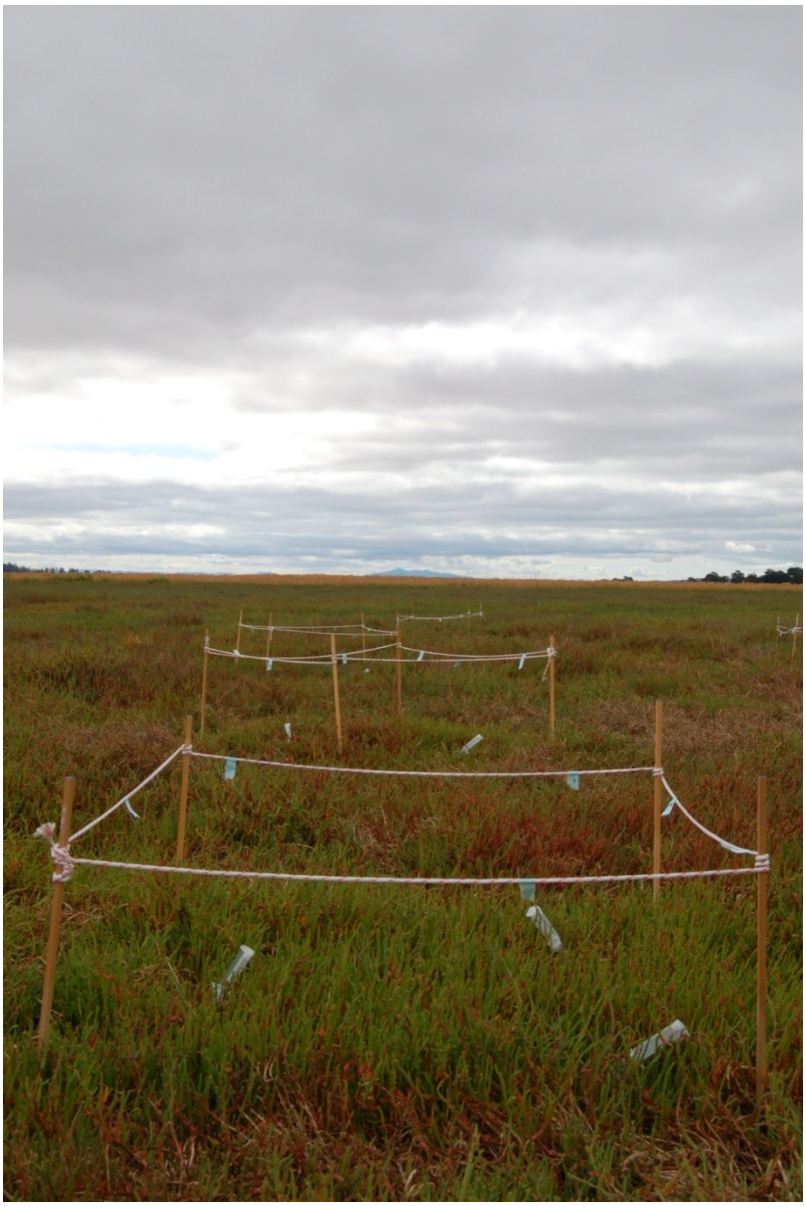

Figure 4-1. Test plots in the Gambinini Marsh with syringes attached to the porewater samplers during sample collection.

4.2.3 Iron Addition to Field Plots

Two of the four experimental test plots were amended with iron on October 30, 2009. The amendments were added in a similar manner to the microcosm experiment (see Chapter 2). The amendment was administered as a de-aerated solution of 1.4 M $FeCl_2$ in 1.5 M $NaHCO_3/Na_2CO_3$ buffer, with a total injection volume of 1.0 L. Plots D and F received an amendment of 1.0 L of a control solution of 1.4 M $CaCl_2$ in 1.5 M $NaHCO_3/Na_2CO_3$ buffer. The solution was injected at a depth of 2.5 cm using a 20 mL plastic syringe in a random pattern across the surface of each test plot to assure uniform distribution of the added iron. The amendment solutions were prepared on the morning of the amendment and were stored in plastic bottles wrapped in parafilm and double-bagged in plastic zipper-lock bags for travel to the field site. It was assumed that little oxidation of Fe[II] occurred during transit because the iron solutions stayed the same grey color during travel, and only began to turn red (characteristic of the Fe[III]-oxides produced by oxidation from atmospheric oxygen) after the bottles had been opened in the field.

Plots A and E were amended with iron to a concentration of 77 g-Fe/m^2, which was calculated to approximately double the existing concentrations of HCl-extractable iron measured in the top 5-cm of sediment. It is notable that this concentration was between 3 and 10 times lower than the doses employed in the microcosm experiment (180, 360, and 720 g-Fe/m^2). Both amendment doses were intended to double the existing iron concentrations. However, the test plot dose was based on measured concentrations of HCl-extractable iron in the sediment, while the microcosm dose was calculated based on measured concentrations of acid volatile sulfides (assumed to consist entirely of $FeS_{(s)}$) after being subjected to laboratory conditions for four months. Since the microcosms were very sulfidic at the time of analysis, it is likely that the AVS measurement overestimated the concentration of iron in the sediments, however, no direct measurement of sediment iron concentrations was made for the microcosms.

4.2.4 Collection of Porewater and Sediment Samples

Samples were collected from the test plots every two or four weeks between July 2009 and November 2010, with the exception of September 2009 and a three month period between December 2009 and March 2010. To ensure that sediments were wetted during the high tide and that a large volume of porewater would be available for sampling, samples were collected on dates coinciding with the spring-tide portion of the tidal cycle.

Porewater samples were collected using air-tight plastic syringes connected to the outlet ports of the porewater samplers. Early in the morning on the day of sampling, an acid-cleaned syringe was attached to the luer-lock connector of the sampler, and a vacuum was applied to the syringe. The syringes were then wrapped in aluminum foil to prevent possible photo-demethylation of the samples during the collection period. The syringe was kept under vacuum until a sufficient volume of porewater was collected (typically a total of 35-55 mL). For the first 4 sampling dates (Days 190, 204, 218, and 280) a 20-mL syringe was connected and filled twice, and for all other dates a single 60-mL syringe was used. The sampling process typically required 6 to 8 hours.

After a sufficient sample volume was obtained, the syringe was disconnected from the porewater sampler, and a 22-gauge stainless steel needle was attached. The sample was

immediately split between two pre-cleaned glass vials with a PTFE septa. For samples to be analyzed for mercury species, approximately 35 mL of sample was transferred to a 40-mL amber glass vial that contained 0.05 mL of 1+1 H_2SO_4 as a preservative. The remainder of the collected porewater (typically 10-15 mL) was then transferred to a 20-mL clear glass vial to be analyzed for dissolved sulfide, sulfate, iron, dissolved organic carbon (DOC) and pH. On each sampling date three blanks consisting of reagent water were collected and analyzed in the same manner as the samples: a bottle blank, a travel blank, and a field blank.

Before sampling, the vials were filled with N_2 and wrapped with parafilm to maintain an O_2-free atmosphere to prevent the oxidation of reduced species in the samples. In the field, the sample needle was pressed through the septa to begin the transfer of the porewater and then a second needle of smaller diameter (25 gauge) was used to vent the N_2 headspace. After the sample was transferred to each vial, the bottles were wrapped with parafilm, double-bagged in zipper-lock plastic bags, and kept on ice in a cooler until analysis.

Analysis of Fe[II], S[-II] and pH was typically completed within 3 hours of sample collection. Aliquots of around 1-4 mL were transferred to plastic tubes which were frozen until analysis for sulfate and DOC. The DOC tube included an addition of 0.025 mL concentrated HCl as a preservative before freezing, and the blanks stored in plastic tubes did not produce DOC. Samples for mercury analysis were kept refrigerated in the sealed vials until analysis.

Surficial sediment samples were also collected from the plots on some sampling dates. 10-mL plastic syringes with the tips cut off were used to collect a composite sample from each plot. The syringe was pushed into the sediment to a 3-cm depth and the sample was transferred to a pre-cleaned 20-mL glass vial with a Teflon lined lid. Samples were collected from four random locations in the test plot to obtain enough sediment to ensure no headspace in the glass vial. The sample vials were then double-bagged in the field and kept on ice in a cooler until they were returned to the laboratory. The samples were frozen until analysis, which occurred within one year.

4.2.5 Analytical Methods

Water and sediment samples were analyzed using established methods. Method detection limits were defined as three times the standard deviation of the blanks, unless otherwise noted. For samples with concentrations below the detection limit, one-half of the detection limit was used for calculations. Analyses for iron, sulfur, and mercury are described in Section 3.2.5 of Chapter 3. Organic carbon in porewater was measured via combustion and infrared detection (Shimadzu TOC-5000A, average daily detection limit 0.42 mg-C/L). Organic content of sediments was assessed by calculating the percent of mass lost on ignition (%-LOI), where dried sediment samples were baked in a muffle furnace at 550 °C for three hours.

4.3 Results

The field data presented in this chapter cover a 17-month period beginning in July 2009 and ending in November 2010, and include 21 sampling events. The data are presented on a Day of Year basis, where Day 1 is January 1, 2009, and Day 700 is December 1, 2010. A list of significant dates is provided in Table 4-1.

4.3.1 Porewater Samples

The concentration of iron in the porewater (Figure 4-2) exhibited seasonal variation with highest concentrations occurring during late summer and early fall. Both the control and treatment plots had average porewater Fe[II] concentrations below 900 μM during the first four months prior to the iron amendment. The amendment plots increased to 4600 μM and 6000 μM for plots A and E, respectively, following iron addition. Assuming a uniform porewater concentration for the top 5 cm of the sediments, the porewater concentrations accounted for 14.5% of the amended iron in Plot A and 19% in Plot E. The concentrations decreased during the six weeks following the amendment, but still remained higher than the control plots throughout the sampling period. In March 2010 (Day 440), iron concentrations were low for both the amended and control plots, with average concentrations less than 50 μM. Porewater iron concentrations in all four plots increased over a six-week period from July to early August 2010, and reached values that were as much as 5 times greater than in July 2009. Additionally, the iron-amended plots had higher average concentrations than the control plots throughout this period.

Methylmercury concentrations measured in the porewater (Figure 4-3) were highest during July and August 2009 and then decreased until October. From October 2009 through the end of the experiment, concentrations were approximately 10 times lower than those observed during Summer 2009. During the periods after October 2009, porewater MeHg concentration were often below the detection limit: At least half of the samples were below detection on October 21, 2009 and on each date from April through October 2010, with the exception of July 27 and August 11. The concentrations measured in the porewater during much of the experiment were in agreement with values reported in other salt marshes (typically 1 to 35 pM) in San Francisco Bay (Clarisse et al. 2011), Louisiana (Hall et al. 2008), and Connecticut (Langer et al. 2001), as well as freshwater environments in the Bay-Delta (Choe et al. 2004).

A small but insignificant ($p > 0.48$) decrease in the average MeHg concentrations was observed in the six weeks after the iron amendment Figure 4-3(B). However, a similar decrease was also observed in the control plots.

DOC concentrations (Figure 4-4) were initially highest in July 2009 and decreased during the winter and stayed fairly constant with concentrations ranging from approximately 20 to 40 mg-C/L over the remainder of the measurement period, which is typical of other tidal marsh (10-23 mg-C/L, (Hall et al. 2008)) and estuarine sediment environments (9 mg/L in Maine (Merritt & Amirbahman 2008)). In contrast, porewater sulfate concentrations (Figure 4-5) exhibited a more pronounced seasonal pattern, with concentrations up to twice those detected in seawater during the summer months due to evapotranspiration in the high marsh plain. During the winter and spring months, sulfate concentrations were near freshwater levels, due to increased freshwater flows of the Petaluma River and direct inputs of precipitation to the marsh. Porewater sulfide was not detected in any sample during the observation period, and porewater pH (Figure 4-6) typically ranged between 5.5 and 7.5, and showed the highest values for all groups in March 2010.

Table 4-1. Day of Year number equivalents for a selection of significant dates during the field sampling experiment.

Day of Year	Date	Event
1	1-Jan-09	Start Day
180	29-Jun-09	Test plots are established, porewater samplers installed
190	9-Jul-09	First day of porewater sampling
303	30-Oct-09	Iron amendment carried out
352	18-Dec-09	Last 2009 sampling date
440	16-Mar-10	First 2010 sampling date
677	08-Nov-10	Final sampling date

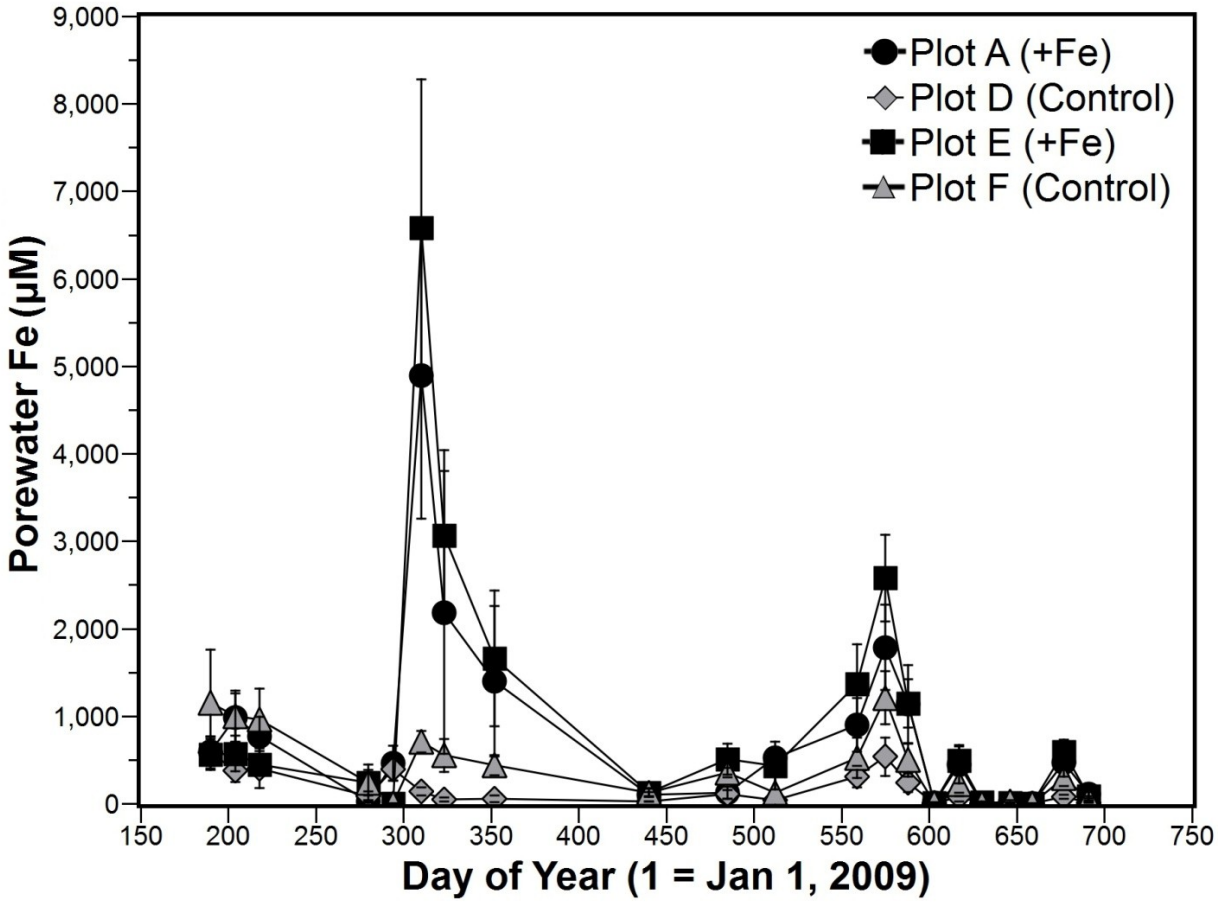

Figure 4-2. Concentration total dissolved iron measured in porewater samples collected from the Gambinini Marsh. Values are shown as average ± S.E. for the triplicate porewater samplers in each plot.

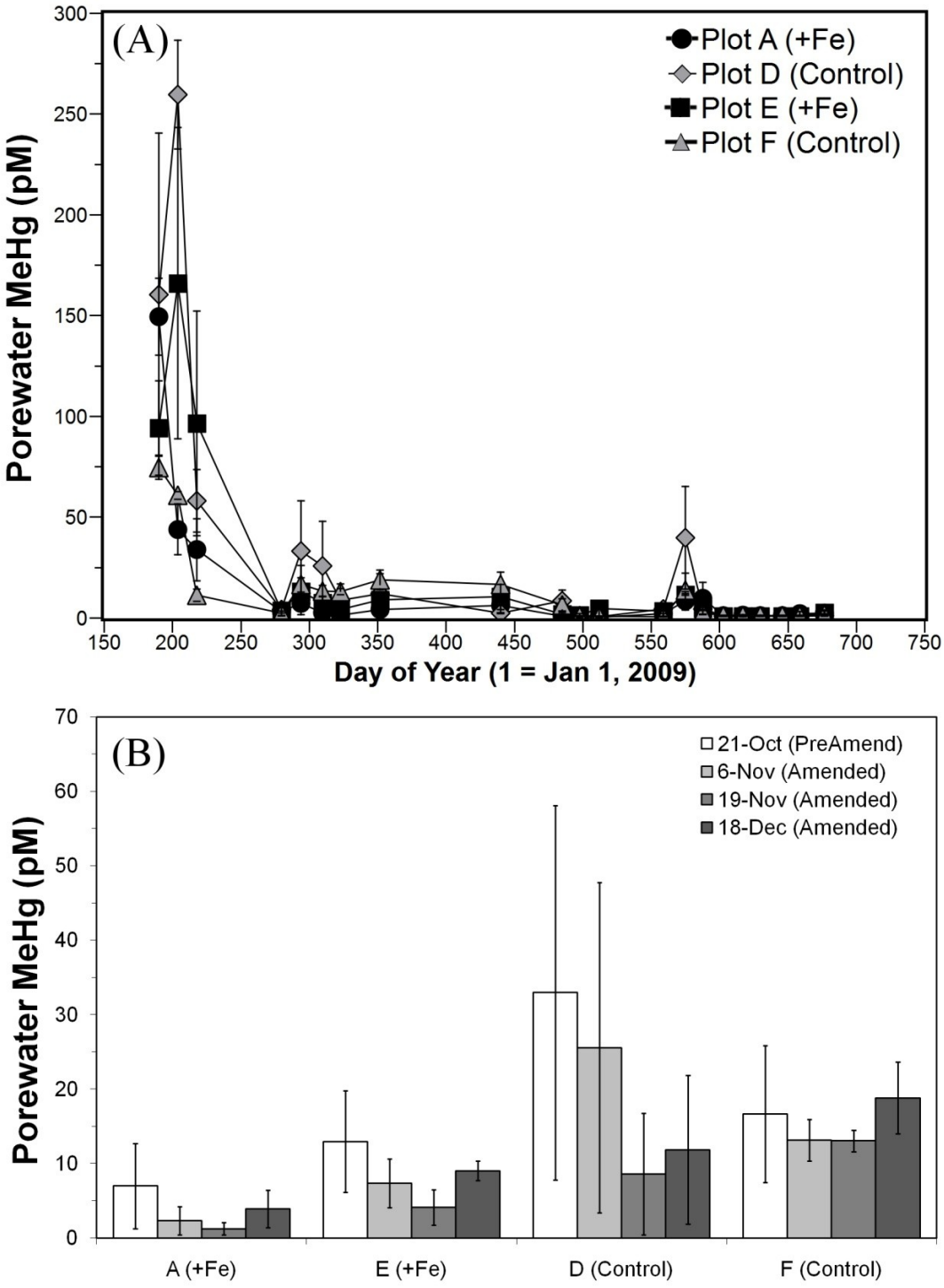

Figure 4-3. Porewater MeHg concentrations measured in Gambinini Marsh for (A) the entire sampling period and the data are rescaled (B) to show the concentrations immediately following the iron amendment. Values are shown as average ± S.E. for the triplicate porewater samplers in each plot.

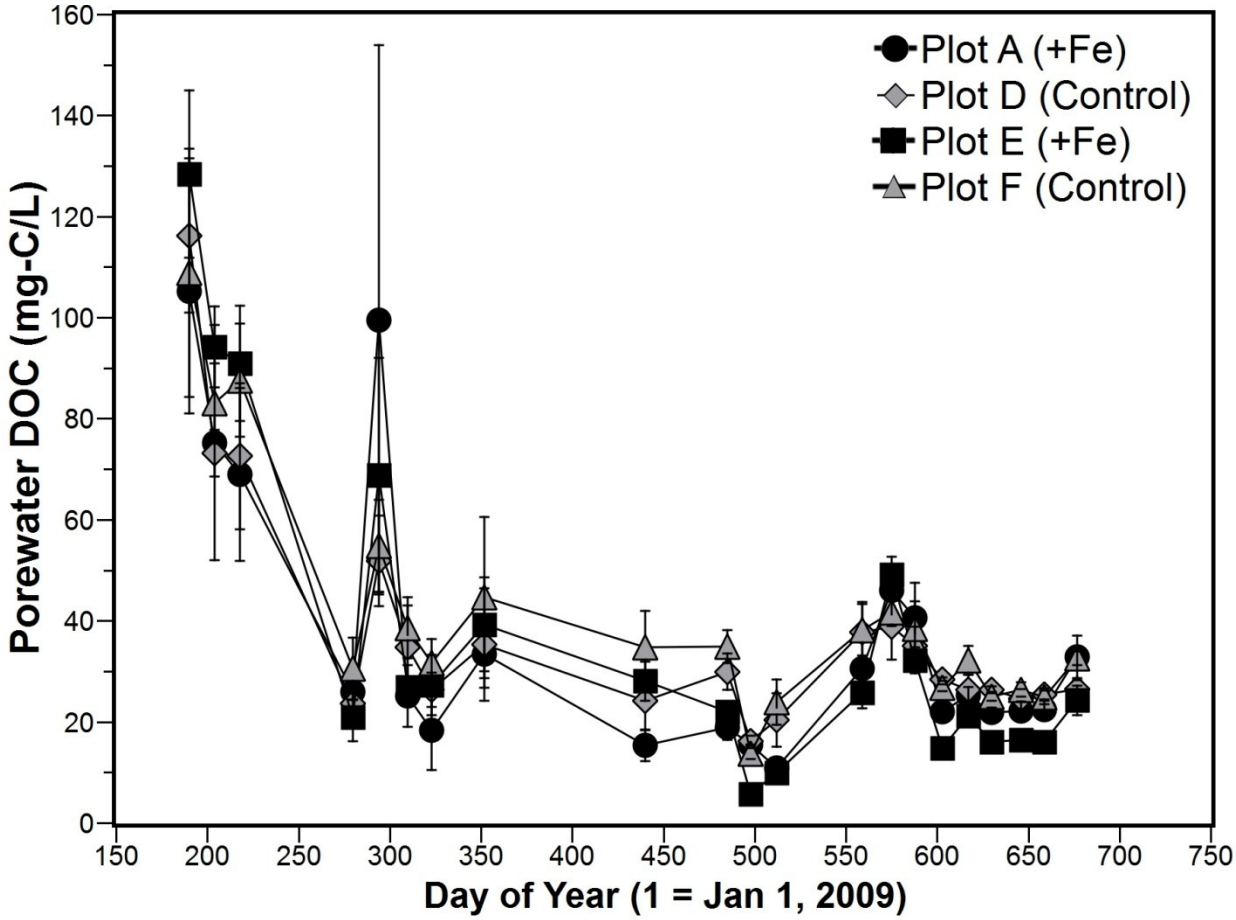

Figure 4-4. Concentrations of dissolved organic carbon (DOC) measured in porewater samples collected from the Gambinini Marsh. Values are shown as average ± S.E. for the triplicate porewater samplers in each plot.

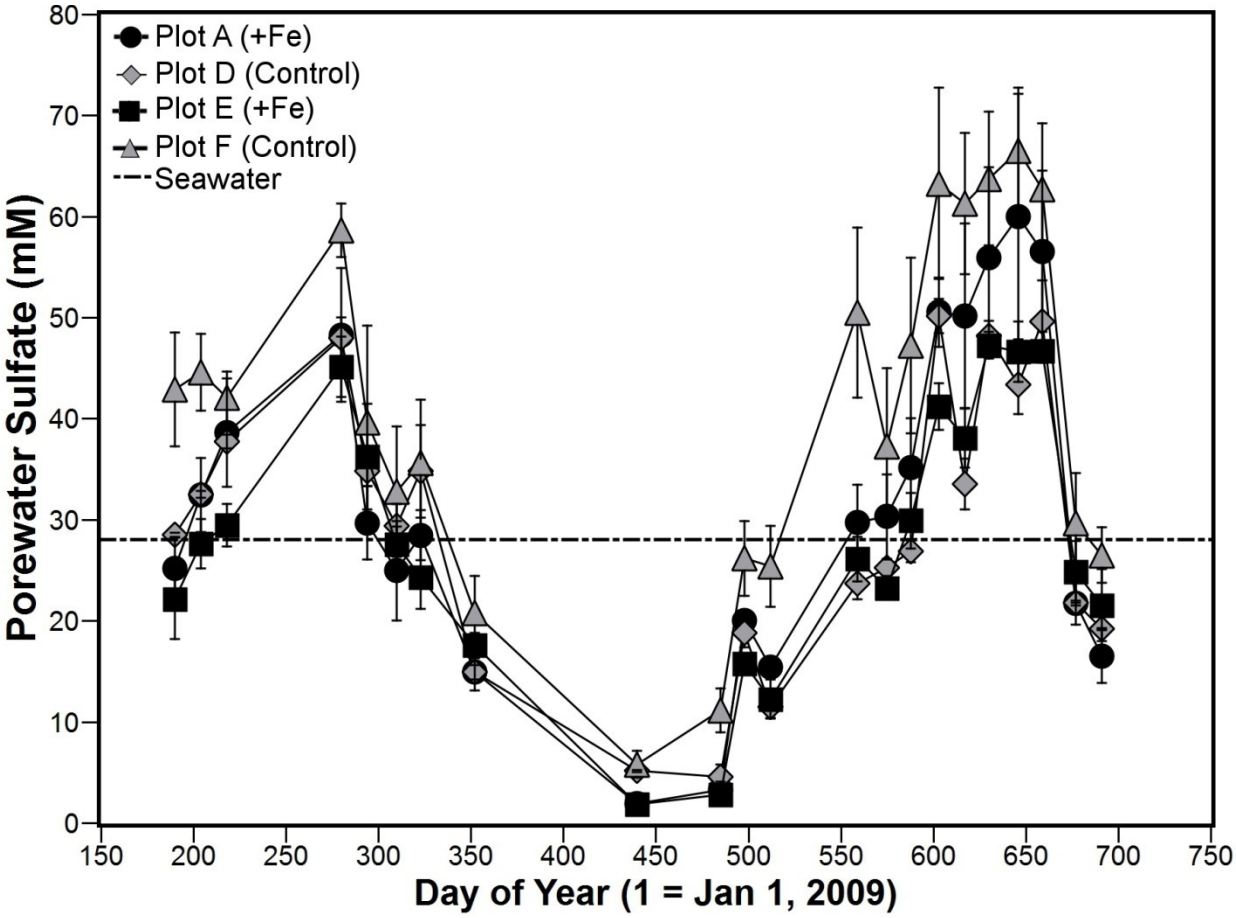

Figure 4-5. Concentrations of sulfate in the porewater samples collected from the Gambinini Marsh. Values are shown as average ± S.E. for the triplicate porewater samplers in each plot.

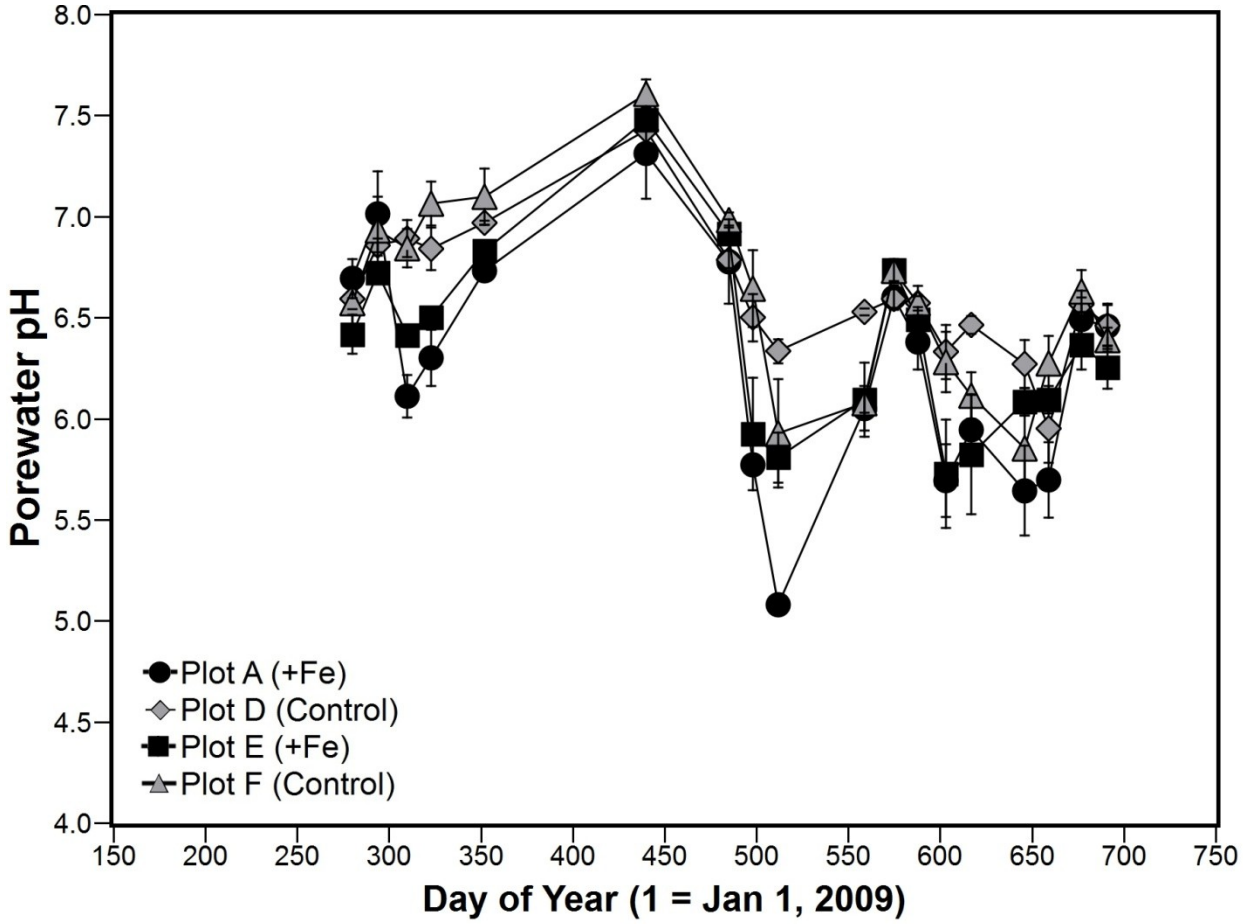

Figure 4-6. Porewater pH for samples collected from the Gambinini Marsh. Values are shown as average ± S.E. for the triplicate porewater samplers in each plot.

4.3.2 Sediment Concentrations

No clear temporal patterns were observed in the sediment iron concentrations. As observed in surficial sediments from around northern San Francisco Bay (see Chapter 3), the high marsh plain of Gambinini Marsh had a high relatively high concentrations of HCl-extractable Fe[III] (Figure 4-7(B)). Average concentrations of sediment Fe[II] were typically much lower with concentrations around 50 μmol-Fe/g-dry throughout the observation period (Figure 4-7(A)). One notable exception to this pattern was the elevated concentrations of Fe[II] measured in Plot A following the iron addition. While the concentration did not increase in the November 6, 2009 sample, collected 7 days after iron addition, approximately 70% of the added Fe was detected in the top 4 cm of the sediment for the sample collected on December 18, 2009. Sediment-associated iron returned to background levels by May 2010. Increased iron was not observed in the other amended plot (Plot E).

Average sediment concentrations of MeHg (Figure 4-8) were between 3 to 47 pmol-MeHg/g-dry, and showed a general trend of higher concentrations during late 2009 and March/May 2010 compared with July through October 2010. The measured concentrations were in general agreement with other reported values for tidal marshes in the Bay-Delta (Table 4-2). Sediment MeHg concentrations did not appear to be affected by the addition of iron in October 2009. The concentrations measured in November and December were very similar for Plots A, E, and D (the two amended and one control plot, respectively), with higher concentrations detected in Plot F. Porewater MeHg accounted for between 0.03% and 4.7% of the MeHg measured in the top 5-cm of the sediments, assuming uniform MeHg concentrations in the porewater and sediments over that depth interval (Table 4-3).

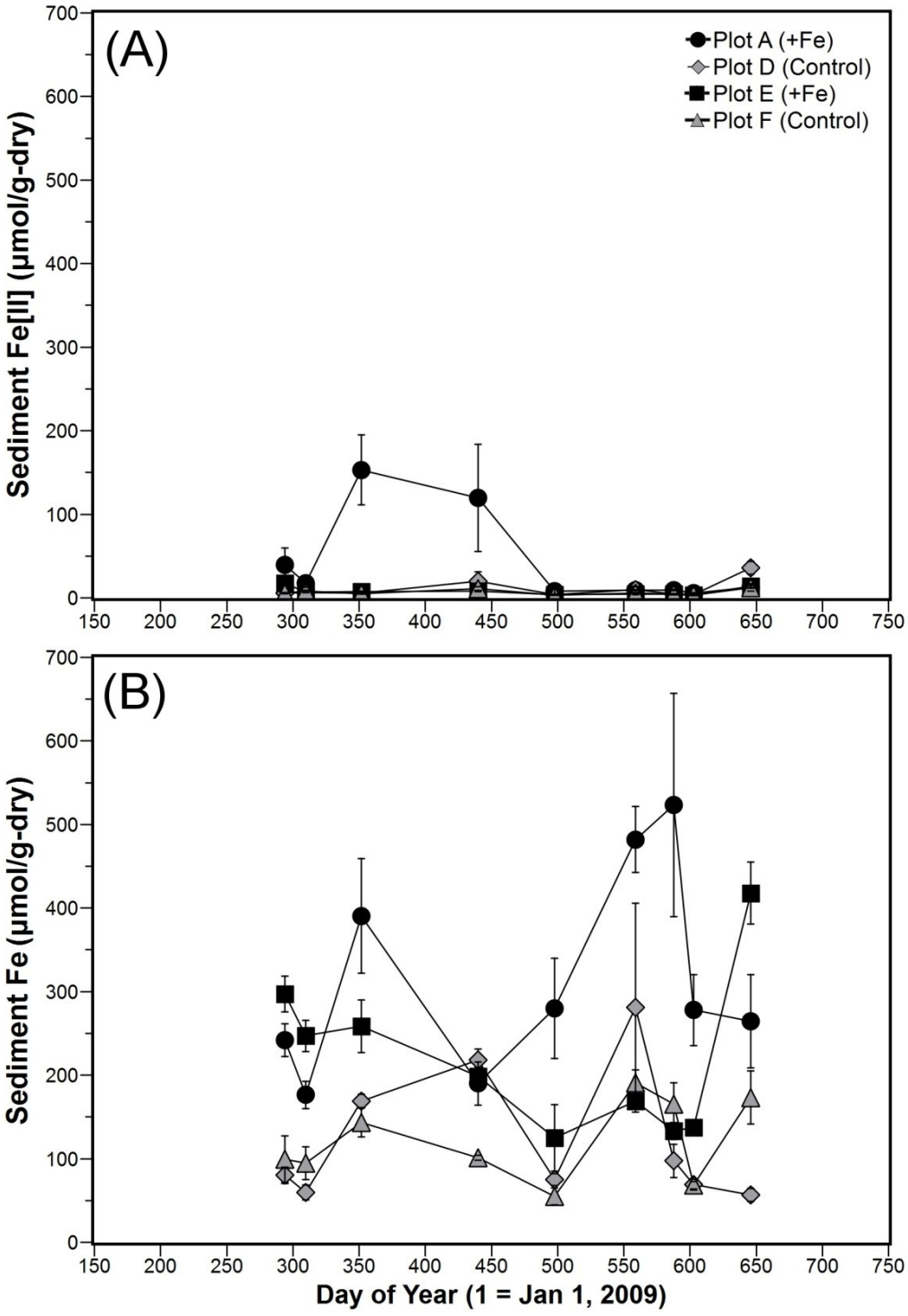

Figure 4-7. Concentration of (A) Fe[II] and (B) total extractable iron in surficial sediment samples from Gambinini Marsh on select dates during the sampling period. Values are shown as average ± S.E. for the triplicate measurements of the composite plot sediment samples.

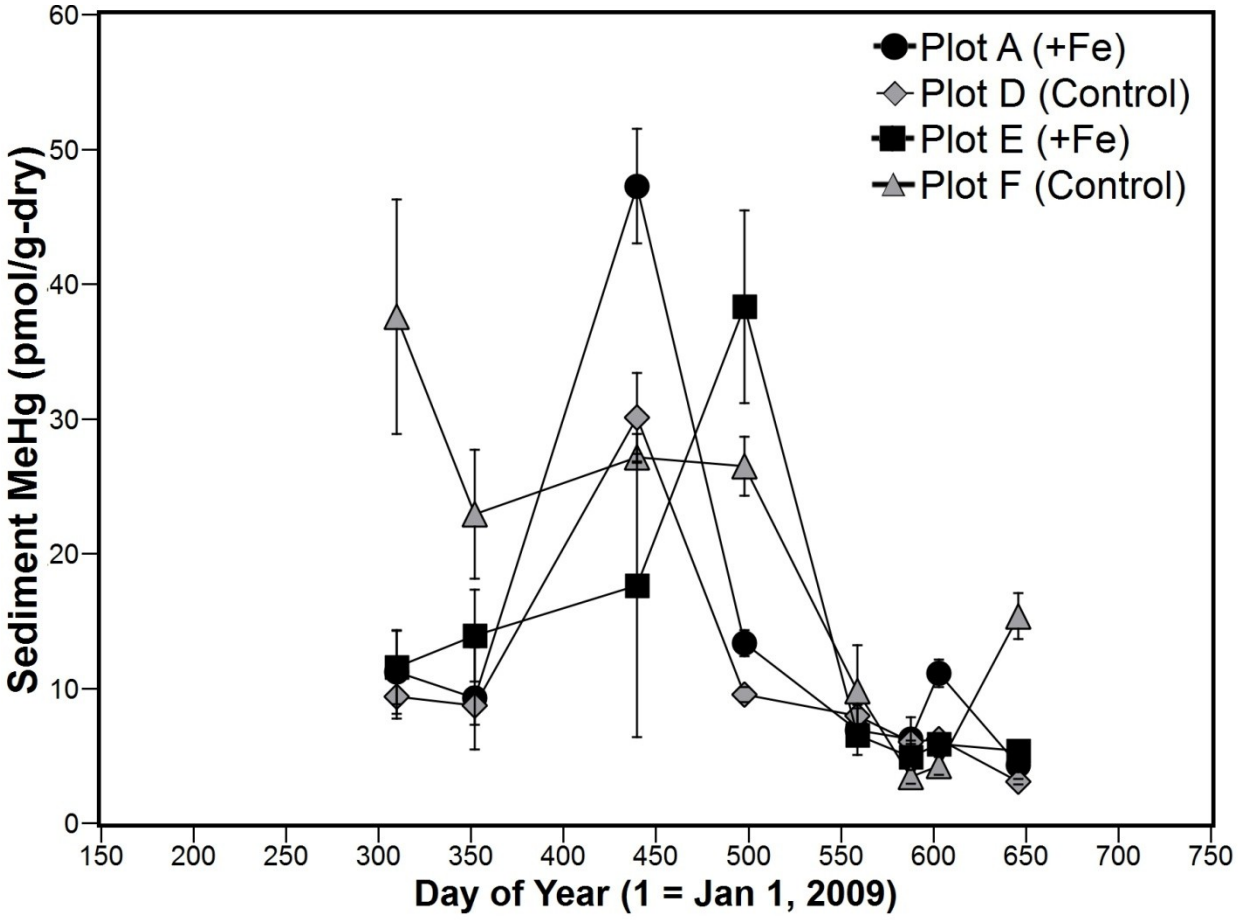

Figure 4-8. Concentration of methylmercury (MeHg) in surficial sediment samples from Gambinini Marsh on select dates during the sampling period. Values are shown as average ± S.E. for the triplicate measurements of the composite plot sediment samples.

Table 4-2. Sediment methylmercury (MeHg) concentrations reported for tidal freshwater and salt marsh habitats in the San Francisco Bay-Delta estuary.

Marsh Type	Elevation, Vegetation	Location	Sediment MeHg (pmol/g)	Study
Salt marsh	High, Pickleweed	San Pablo Bay	27 ± 17	Marvin-Dipasquale et al. 2003
Salt marsh	High, Pickleweed	Petaluma River	18 ± 7.5	Windham-Myers et al. 2009
Salt marsh	Edge, Gumplant	Petaluma River	10 ± 2.5	Windham-Myers et al. 2009
Salt marsh	Low, Cordgrass	Alviso	4 ± 1.5	Windham-Myers et al. 2009
Salt marsh	Mid, Bulrush	Alviso	4 ± 3	Windham-Myers et al. 2009
Salt marsh	High, Pickleweed	Alviso	8.5 ± 6	Windham-Myers et al. 2009
Salt marsh	--	China Camp S.P.	2 to 4.5	Clarisse et al. 2011
Salt marsh	High, Pickleweed	Petaluma River	3 to 47	*This study*
Tidal fresh	--	Frank's Tract	13 to 66	Choe et al. 2004
Tidal fresh	Interior	Frank's Tract	19 to 39	Heim et al. 2007
Tidal fresh	Exterior	Frank's Tract	6.8 to 10	Heim et al. 2007

Table 4-3. The percentage of methylmercury in the sediments that was measured in the porewater fraction for the dates when sediment samples were analyzed.

Day	310	352	440	498	559	588	603	646
A (+Fe)	0.35%	0.72%	0.22%	0.03%	0.47%	2.7%	0.11%	0.27%
E (+Fe)	1.1%	1.1%	1.0%	0.05%	0.85%	1.6%	0.17%	0.18%
D (Control)	4.7%	2.3%	0.13%	0.11%	0.90%	1.2%	0.16%	0.48%
F (Control)	0.60%	1.4%	1.0%	0.03%	0.08%	1.3%	0.29%	0.07%

4.4 Discussion

4.4.1 Redox Cycling

Measurements made throughout the 17-month observation period considered in conjunction with the results of Chapter 3 indicate that the sediments of Gambinini Marsh exhibit complicated redox conditions with multiple electron acceptors being important in different areas of the sediments.

The importance of oxygen as an oxidant is evident from the presence of reducible Fe[III] minerals in the top 4 cm of the sediments (Figure 4-7(B)) and the absence of sulfide, a species that is readily oxidized by O_2^-, in the sediment porewater.

Iron was present in porewater sampled at a depth of 2.5 cm throughout much of the year (Figure 4-2), and based on the low solubility of Fe[III] at circumneutral pH values, it is likely that nearly all of the iron in the porewater was Fe[II]. This suggests that there is a cycle of Fe[III]-mineral reduction to produce dissolved Fe[II]. Alternatively, it is possible that the sulfide produced by sulfate reduction reduced the Fe[III] minerals, which would explain why porewater sulfide was not detected. If a uniform porewater iron concentration is assumed over the top 5-cm of the sediments, a mass balance calculation demonstrates that the mass of dissolved iron was small relative to the mass of sediment Fe[III]: Porewater iron typically accounted for less than 3% of the iron in the top 5-cm of the sediments of the test plots. Immediately following the iron amendment, porewater iron concentrations in November (Day 310) accounted for as much as 10.5% of the measured iron in the amended plots. In both the control and iron-amended plots Fe[II] accounted for less than 3% of the iron by December (Day 352).

Salt marsh sediments often exhibit high rates of sulfate and iron reduction due to the availability of labile carbon and terminal electron acceptors, and while microbial respiration rates were not directly measured in this study, it is expected that they were high based on the availability of sulfate in the porewater and Fe[III] in the sediments as well as the rapid production of Fe[II] and loss of sulfate observed during the 7-day anoxic incubation experiments described in Chapter 3. A lack of detectable sulfide concentrations in the sediment porewater is not necessarily indicative of an absence of sulfate reduction within the sediments due to the high reactivity of sulfide toward oxygen and Fe[III] minerals (Koretsky et al. 2005). Thus, sulfide produced by sulfate-reducing organisms would not be detected in porewater or sediment samples. The presence of elevated concentrations of MeHg in the sediments of Gambinini Marsh, which was demonstrated to be a related to sulfate reduction in Chapter 3, is further evidence for active populations of sulfate-reducing bacteria in the system.

Iron reduction and sulfate reduction can occur simultaneously in the same vertical layers of surficial salt marsh sediments (Hyun et al. 2007, Koretsky et al. 2005, Kostka et al. 2002). For example, Lowe et al. (2000) used cell culture to identify iron-reducing and sulfate-reducing bacteria throughout the top 6-cm of a salt marsh in Georgia. The sediments exhibited the highest densities of iron-reducing bacteria at shallow depths where extractable Fe[III] concentrations were highest, and densities decreased with depth as Fe[III] concentrations decreased. In the same core, the density of sulfate-reducing bacteria increased with depth, which suggests that iron-reducing bacteria can outcompete sulfate-reducers for metabolic substrates in salt marsh sediments when Fe[III] minerals are available. The fact that sulfate-reducers were still present in the surficial sediments supports the hypothesis that microenvironments were present where

sulfate reduction occurred within the Fe[III]-rich sediments. The presence of sulfidic microenvironments within Gambinini Marsh could explain the relatively high concentrations of MeHg observed in the sediments despite the absence of sulfide in the porewater or sediment samples.

4.4.2 Methylmercury in the Gambinini Marsh

The concentrations of MeHg measured in the sediments of Gambinini Marsh during this study were comparable to those reported in tidal marshes from the Bay-Delta (Table 4-2), Chesapeake Bay (Mitchell & Gilmour 2008), and coastal Louisiana (Kongchum et al. 2006). In the studies referenced in Table 4-2, sediments in nearby open water habitats typically had lower MeHg concentrations, suggesting that tidal wetlands were sources of MeHg. An exception was Clarisse et al. (2011), which reported values up to 6 times higher in Petaluma River channel sediments than in salt marsh sediment from nearby China Camp State Park. While additional studies are necessary to evaluate the transfer of MeHg from salt marsh sediments to the estuary and into the food web, data from the Gambinini Marsh support the idea that salt marshes have the potential to serve as sources of MeHg.

Strong seasonal patterns in sediment MeHg were not observed, as have been reported in other studies in the Bay-Delta (Choe et al. 2004, Heim et al. 2007) which showed higher concentrations in spring and summer than during the winter. However, Plots A, D, and E each exhibited their highest sediment MeHg concentrations during March or May 2010 as observed in open water sediments (Bloom et al. 1999, Heim et al. 2007). The increase could have been due to increased methylation rates at higher sediment temperatures. It has also possible that net methylation decreased in summer because the activity of microbes that demethylate MeHg increased relative to those that methylated mercury, as reported elsewhere (Marvin-DiPasquale & Agee 2003, Weber et al. 1998), or because sulfate reduction rates were decreased due to the lower concentrations of sulfate in the porewater occurring during the spring.

Previous research suggests that the presence of plants can also stimulate MeHg production (Valega et al. 2008, Weber et al. 1998, Windham-Myers et al. 2009). While sediment MeHg concentrations did not exhibit a dramatic seasonal shift, the change in pickleweed status from active growth between April and July to flowering in late July and early August and senescence in October may have caused the increase in porewater MeHg concentrations seen in July and August. From April to October 2010, at least half of the porewater samples from each date had MeHg concentrations below the detection limit, with the exception of July 27 (Day 575) and August 11 (Day 588). On these two days, 23 of the 24 samples had quantifiable MeHg concentrations, and this corresponded to the observed start of pickleweed flowering in the test plots. Porewater iron (Figure 4-2) and DOC (Figure 4-4) concentrations also exhibited higher average concentrations on these dates.

The phenology of salt marsh plants can affect sediment biogeochemistry. For example, in a salt marsh dominated by *Spartina alterniflora*, sulfate reduction rates decreased when the plants changed from an active growth phase to reproductive flowering, with the sediments becoming more reducing as growth slowed (Hines et al. 1989). These changes were attributed to less organic carbon leakage into the sediments after the plants entered the flowering stage, which resulted in decreased availability of labile carbon and lower rates of sulfate reduction. Furthermore, evapotranspiration is a primary driver of sediment redox conditions in salt marsh

systems, due to oxygen entering the sediment surface to replace the lost water (Dacey & Howes 1984, Howes et al. 1986). A decrease in evapotranspiration rates during the flowering phase of the pickleweed life history likely would have resulted in less oxygenation of the sediments and higher rates of sulfate and iron reduction. The increase in porewater Fe[II] concentrations on the dates when plants were flowering suggests that the sediments became more reducing. It is possible that the higher concentrations of porewater DOC also were due to increased organic carbon inputs from pickleweed roots during flowering or from the release of organic matter from the surface of Fe[III] minerals as they were reduced.

Since sediment MeHg concentrations did not increase when the plants flowered, the elevated porewater MeHg concentrations may have been due to changes in MeHg distribution rather than production. For example, as porewater DOC concentrations increased during the flowering event, the increased availability of DOC could have resulted in the formation of MeHg-DOC complexes in the porewater (Liu et al. 2008, Ravichandran 2004). For the dates when sediments were analyzed in 2010, the lowest particle-water partitioning coefficient values (K_d, Figure 4-9), where K_d is an operationally defined ratio of the sediment MeHg concentration to the porewater MeHg concentration (L kg^{-1}), occurred in each plot on August 11 (Day 588), which was during the period of pickleweed flowering and increased porewater DOC and iron concentrations.

The K_d values observed throughout this study (average log $K_d = 2.9 \pm 0.6$) were similar to those previously reported for freshwater sites in the Bay-Delta, where Choe et al. (2004) found an average value across all sites of log $K_d = 3.3 \pm 0.7$. Additionally, they observed the highest seasonal variability of K_d in their tidal freshwater marsh site. A previous study of sediment cores at open water sites in Lavaca Bay indicated that the lowest K_d values occurred at depths of maximum porewater iron concentrations (Bloom et al. 1999). This suggests that the solubility and mobility of MeHg could be controlled by adsorption to Fe-hydroxides or Fe-sulfides in the sediments, and that the dissolved fraction of MeHg increases when these minerals undergo reductive dissolution.

Gagnon et al. (1997) suggested that the interaction of MeHg with iron and manganese (hydr)oxides slows the transport of MeHg from marine sediments, where net fluxes out of the sediments could be limited by adsorption of MeHg in a thin oxic layer at the sediment surface. A recent study using incubations of benthic flux chambers in the Gulf of Trieste in the Adriatic Sea (Emili et al. 2011) demonstrated that MeHg fluxes from the sediments to the surface waters increased as the sediments became more reducing. Upon re-opening the incubation chambers to oxic waters, MeHg fluxes and concentrations in the porewater decreased. This again suggests that MeHg may be mobilized from sediments under anoxic, reducing conditions and that MeHg may have limited mobility under oxidized conditions. This interaction between MeHg and oxidized sediment minerals could also explain why the porewater concentrations were lower during the summer months of 2010, even while sediment MeHg remained approximately constant.

Organic matter has been shown to be one of the most important predictors of MeHg concentrations in some estuarine sediments (Lambertsson & Nilsson 2006, Rothenberg et al. 2008). Complexation of inorganic Hg[II] by dissolved organic matter (DOM) can be important in sediment porewater when sulfide concentrations are low (~μM levels). The reduction in the activity of Hg^{2+} results in decreased concentrations of bioavailable low molecular weight Hg[II] complexes (Barkay et al. 1997, Miller et al. 2007, Ravichandran 2004). However, DOM can also stimulate microbial activity in the sediments by providing a source of labile carbon to the

bacterial community (Ravichandran 2004). At the Gambinini Marsh, porewater DOC concentrations were highest in July 2009, then decreased by approximately 70% during the winter months, and stayed approximately constant throughout the next year of observation. This pattern was similar to trends observed for porewater MeHg. As a result, porewater DOC concentrations explain 52% of the variation in porewater MeHg (Figure 4-10, $p < 0.001$). While this correlation could be attributable to enhanced MeHg production when excess DOC was present, it could also be related to decreased partitioning of MeHg to surfaces in the presence of DOC. It is also noteworthy that the organic matter content of the sediments was high throughout the observation period (typically around 30-40% Loss on Ignition, data not shown). High sediment organic content is characteristic of older marshes, and Gambinini Marsh was found to have higher organic content than the other marshes sampled around north San Francisco Bay in Chapter 3. However, loss on ignition is a bulk measurement of organic content, and includes both labile and refractory components. Previous research has demonstrated that sediments with lower C/N ratios have higher net methylation rates (Drott et al. 2007, Kim et al. 2011). This relationship has been attributed to the higher lability of N-rich organic matter (Lehmann et al. 2002). In other words, the high C/N ratio of organic matter typically observed in salt marshes indicates that it is likely to be more refractory, which would mean that fresh carbon inputs from pickleweed root exudates and decay of plants could be much more important to the activity of mercury-methylating organisms than the sediment DOC.

Porewater MeHg concentrations were very high in July 2009, exceeding reported values for sites just downstream of known Hg sources (Bloom et al. 1999, Merritt & Amirbahman 2008). Concentrations then decreased and stayed low from October 2009 until the end of the experiments. While it is possible that there is always a pulse of MeHg in the late summer or early fall and year-to-year variations explained the differences between the two years, it is also possible that the poresize of the membranes in the samplers (average of 0.1 μM) could have excluded certain MeHg complexes (e.g., MeHg complexes with large humic substances) from being measured in the dissolved porewater fraction. Another possible explanation is that the installation of the porewater samplers altered the production or distribution of MeHg in the porewater. For example, installation of the samplers required the creation of a cut in the sediments that could have resulted in the oxidation of reduced species near the porewater sampler. This disturbance could have altered the microbial community in the short term. Additionally, pickleweed roots may have died after being cut for the sampler insertion, which could have accounted for the increased DOC concentrations during the first month of the study. However, porewater samplers were occasionally replaced during the experiment, which included a new cut in the sediments for installation, due to damage to the above-ground portion (one on March 16 and two on May 27), and similar increases in DOC and MeHg were not observed after installation of the new samplers.

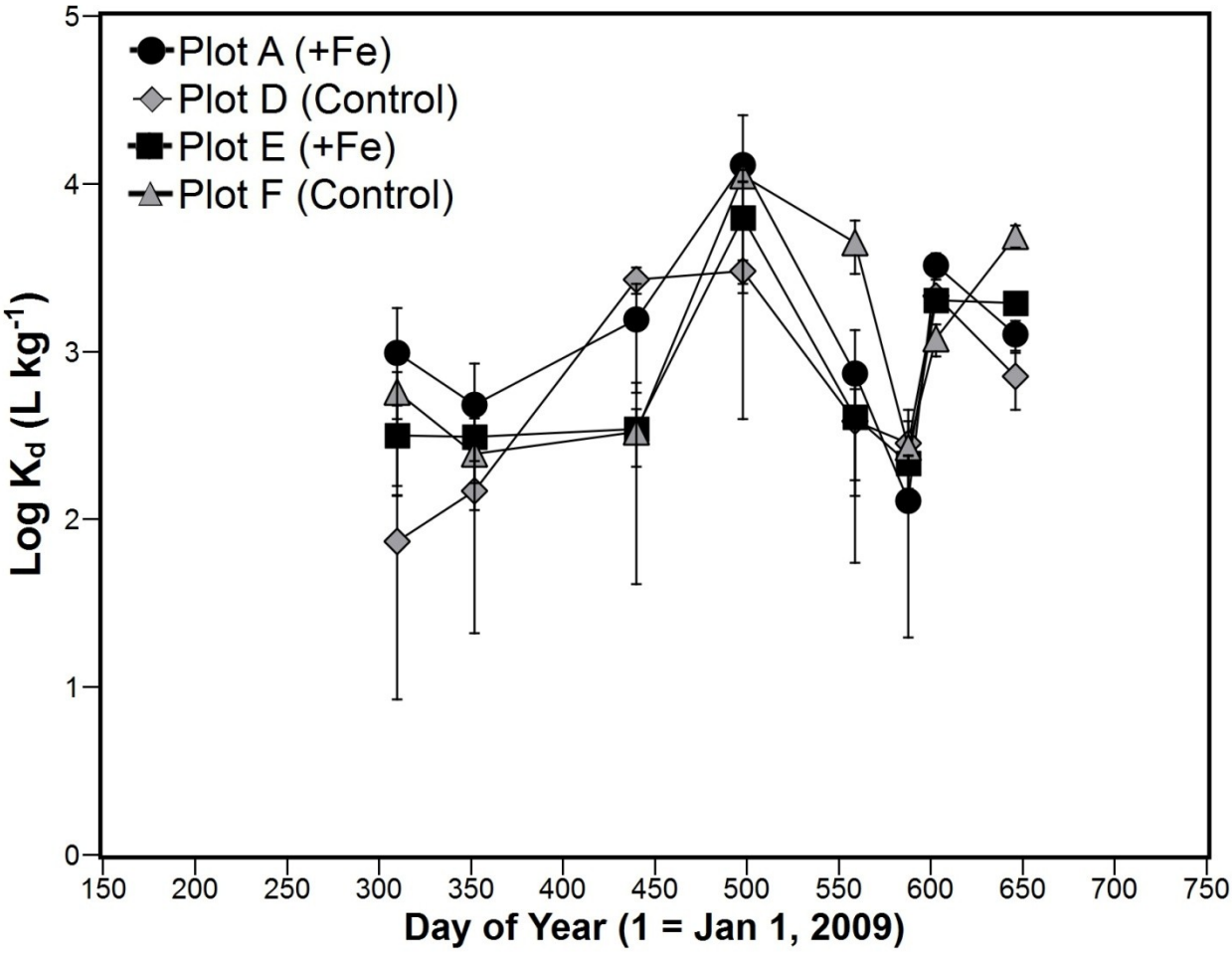

Figure 4-9. Log K_d values ($[MeHg]_{sed}/[MeHg]_{porewater}$) for the dates when both sediments and porewater concentrations were measured.

4.4.3 Interpretation of Iron Amendment Results

The iron addition was initiated in October (i.e., Day 303), which was after porewater MeHg concentrations had decreased to near or below detection. This seasonal or permanent decrease in porewater MeHg concentrations made it difficult to ascertain if there was any effect of the iron amendment. With the exception of porewater iron concentrations and pH immediately following the amendment, there did not appear to be any effect of the addition of iron on any of the other measured biogeochemical parameters. Ultimately, it appeared that the seasonal and interannual fluctuations in MeHg concentrations swamped any effect that the amendment could have caused. Our results demonstrate that during the winter months an iron amendment of this magnitude has no observable effect on MeHg concentrations in tidal salt marshes dominated by pickleweed. As was mentioned in the introduction, the absence of an effect of iron addition was not surprising given the biogeochemical conditions within the Gambinini Marsh. For example, the sediments did not have detectable concentrations of AVS or porewater sulfide. Additionally, in the microcosm experiments (Chapter 2), no decrease was observed in MeHg concentrations for the low-dose case (which was about 2.3 times the amended concentration of iron added to the field site). However, the low dose did result in a decrease in porewater sulfide concentrations.

Although the iron addition did not affect MeHg concentrations, some promising observations were made about the effect of adding iron to tidal marshes that could prove useful if this technique is found to be effective in other marsh systems. In addition, iron might be added for other purposes like phosphorus control (Sherwood & Qualls 2001) or as a coagulant for removal of metals associated with surface water DOM (Henneberry et al. 2011). The addition of the ferrous iron solution increased porewater iron concentrations by almost an order of magnitude, and increased concentrations were observed for at least six weeks. This is an important finding for the future consideration of iron amendment remediation strategies, because it suggests that iron is not quickly flushed from the sediments. Thus, the effect on porewater Fe[II] concentration could last for up to 6 weeks. Additionally, it was also noteworthy that a portion of the amendment stayed in the reduced form over that time period. This implies that oxygen diffusion into the sediments was limited or that Fe[III] reduction was relatively fast. The results of the *in-situ* core incubation experiments discussed in Chapter 3, however, suggest that the longevity of the Fe[II] could be seasonally influenced, because the cores were found to have much higher levels of reduced Fe[II] in November than in July. Thus, if the addition had occurred during the summer months, when the plants were active and the temperature was higher, the iron may have been oxidized more quickly.

While the sediment iron data did not demonstrate a long-term increase in iron concentrations in the amended plots, there was a 6-week period in July and August 2010 where porewater iron concentrations increased in all plots. In the iron-amended plots, the concentrations were up to 2.5 times higher relative to the control plots. Even though these concentrations did not reach the levels found immediately following the iron addition, this summer peak in porewater Fe[II] suggests that even 10 months following the amendment, the iron may still have an impact on sediment iron cycling.

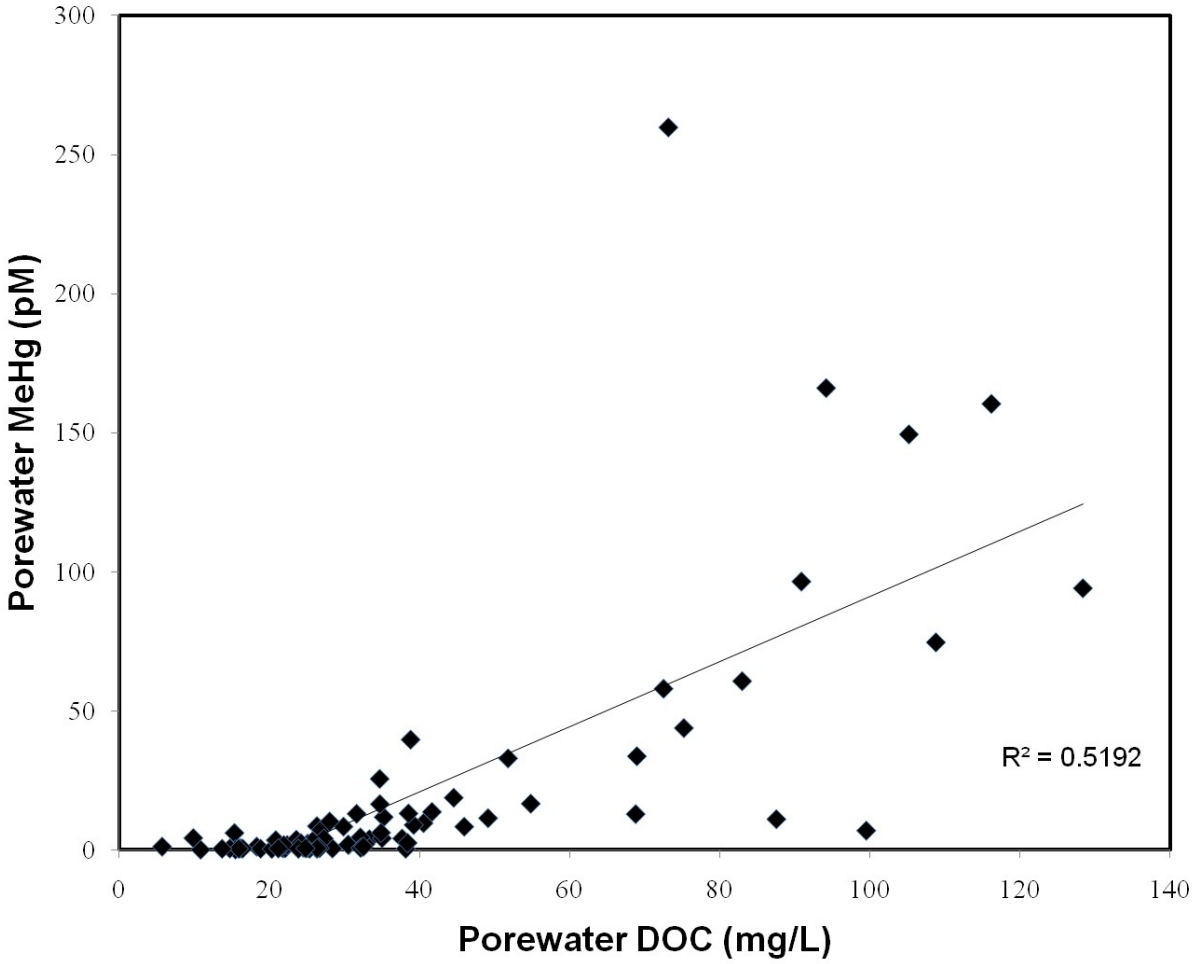

Figure 4-10. Correlation between porewater methylmercury and dissolved organic carbon (DOC) for each date that porewater was collected in the observation period. A statistically significant positive correlation (R^2= 0.5192, $p<0.001$) was found.

Chapter 5. Conclusions

The research described in this dissertation explored the efficacy of an iron sediment amendment for the control of methylmercury production in laboratory microcosms and field test plots. Additionally, long-term monitoring of a pickleweed-dominated marsh in the San Francisco Bay estuary provided new insight into the connection between iron and sulfur cycling and MeHg production.

5.1 Iron Amendment Strategies for MeHg Control

Previous research had demonstrated the potential for using of an iron amendment to control MeHg production in tidal wetland sediments by limiting the bioavailability of inorganic mercury to the methylating bacteria (Mehrotra et al. 2003, Mehrotra & Sedlak 2005). However, these studies were conducted for a short duration (i.e., 3 to 7 days) and inorganic mercury was added to the sediments prior to incubation. The experiments presented in Chapter 2 lasted for several months, did not employ addition of inorganic mercury, and included fluctuating tidal cycles, light, gas exchange, and native wetland plants.

The results of the devegetated experiment indicated that iron addition of 360 or 720 g-Fe/m^2 decreased the export of MeHg in the microcosm tidal surface water by over 80%. While a similar pattern was observed initially for the microcosms that contained live pickleweed plants, the export of MeHg was much more variable and it was not possible to confirm if the iron addition caused a significant decrease in MeHg export under these conditions. The iron addition experiment in the field study presented in Chapter 4 showed no observable effect on MeHg concentrations from the 77 g-Fe/m^2 amendment. These results suggest that an iron amendment strategy may not be effective in the low-sulfide environment of a high marsh plain dominated by pickleweed.

It was also evident that the tidal microcosm system used in this research altered the geochemistry of the Gambinini Marsh sediments relative to field conditions. While sediments in the field did not contain detectable concentrations of dissolved sulfide and concentrations of sulfur-containing minerals (i.e., acid-volatile sulfides and chromium reducible sulfur) were low, the microcosm sediments quickly became sulfidic, with milimolar concentrations of sulfide present after equilibration to laboratory conditions. The differences between the efficacy of the iron amendment in the microcosms and in the field suggest that an iron addition strategy has the potential to provide reduced MeHg export in tidal environments that have relatively high concentrations of sulfide. For example, low marsh areas dominated by *Spartina* typically have concentrations of sulfide comparable to those observed in the laboratory microcosms (Hyun et al. 2007, Koretsky et al. 2008) due to more frequent inundation. Tidal mudflat and open-water sediments also experience sulfidic conditions, and therefore could be amenable to an iron amendment.

Concern has been expressed over the use of an iron amendment to control MeHg production (Mitchell & Gilmour 2008) due to the ability of certain iron-reducing bacteria to methylate mercury (Fleming et al. 2006, Kerin et al. 2006). This is an important consideration in a wetland environment because additional iron could increase iron reduction rates. However, the results of the incubation experiments in Chapter 3 demonstrated that sulfate-reducing bacteria play a much greater role in MeHg production than iron-reducing bacteria under the conditions encountered in these sediments. The potential for the native microbial communities to produce

MeHg under iron-reducing or sulfate-reducing conditions should be determined on a specific basis if an iron amendment is being considered for application.

5.2 Redox Cycling and MeHg Production in Tidal Marsh Sediments

The concentrations of MeHg observed in the Gambinini Marsh sediments were comparable to those previously reported in tidal wetlands around San Francisco Bay (Table 4-2). Because wetland sediments contain higher concentrations of MeHg than most other areas, this research supports the concept that tidal wetlands can be significant sources of MeHg in the estuarine food web.

The research presented in this dissertation further illustrates the complex relationships between iron, sulfur, and mercury cycling under the dynamic conditions of tidal salt marsh sediments. The incubation experiments presented in Chapter 3 showed that when surficial sediments are incubated in a closed system, both Fe[III] reduction and sulfate reduction occur. This is in contrast with the traditional model of spatially segregated microbial communities that use different terminal electron acceptors (Mitsch & Gosselink 2007). The observed co-existence of these two types of bacteria agrees with recent observations from salt marsh sediments in other locations (Hyun et al. 2007, Koretsky et al. 2005, Kostka et al. 2002). This suggests that even when iron reduction is energetically favored due to the high availability of Fe[III] minerals, sulfate reduction can still occur within small microenvironments in the sediments (Jorgensen 1977, Sundby et al. 2003). Under these conditions, sulfide is likely to be quickly cycled to a different form (e.g., sulfide is readily oxidized by Fe[III]-containing minerals).

While long-term seasonal trends in concentrations of MeHg, iron, or dissolved organic carbon were not clearly observed during the 17-month field study, we did observe short-term increases in dissolved organic carbon and Fe[II] during the period of pickleweed flowering in late July and early August 2010. While the phenology of cordgrass (*Spartina spp.*) has been previously reported to affect sediment biogeochemistry (Hines et al. 1989), to our knowledge, this is the first study to show such an effect for pickleweed. Additionally, while we did not measure rates of oxygen release from the pickleweed roots directly, results from the *in situ* core experiment (Chapter 3) suggested that pickleweed may release oxygen into the sediments.

5.3 Future Research

This research provided new insight into MeHg production in pickleweed-dominated salt marshes, as well as the potential effectiveness of using an iron amendment to control MeHg production and export in tidal wetlands. However, further research is necessary to better understand the practicalities of utilizing an iron amendment for this purpose. The microcosm experiments demonstrated that an iron amendment has the potential to be effective in sulfide-rich environments, and test plot studies in the field would be necessary to determine the efficacy under field conditions. Experiments designed to evaluate the amendment over a spatial gradient at a single site that includes areas with elevated sulfide concentrations (i.e., covering the open water channel, mudflats, low marsh, and high marsh) would provide valuable information about the range of ecotones where an iron amendment could be an appropriate management strategy. Additionally, a detailed dosing analysis would be necessary within each ecotone to determine an

appropriate iron amendment level, since the microcosm experiment demonstrated that decreasing the dose by a factor of two (i.e., from 360 to 180 g-Fe/m^2 for the medium and low doses, respectively) substantially decreased the effectiveness of the amendment. Future studies should also address the potential for unintended consequences due to adding substantial amounts of iron to wetland systems, including toxicity to the wetland vegetation.

This research demonstrated that an iron amendment would not be effective in controlling MeHg production in the Gambinini Marsh. Due to the relatively high MeHg concentrations found pickleweed-dominated wetlands, alternative landscape-scale control strategies need to be developed. A better understanding of the factors contributing to the elevated MeHg concentrations in high marshes, as well as additional knowledge about the primary transfer pathways of MeHg into the salt marsh food web would be beneficial in developing new techniques. It would also be interesting to further explore the relationship between pickleweed phenology and MeHg production. If an increase in MeHg concentrations is found to be related to a certain life stage of pickleweed, this information could be used by managers to determine the most appropriate time to apply a control strategy to a restored wetland. Additionally, a study that quantitatively measured the capacity of pickleweed to transfer oxygen to the sediments would provide insight into the complex redox cycling observed in the marsh.

5.4 Concluding Remarks

Ultimately, balancing wetland restoration with increased MeHg production remains an unresolved problem. This is especially problematic in light of regulatory measures that have the potential to hinder the progress of wetland restoration projects. By demonstrating the effectiveness of an iron amendment in a laboratory microcosm system, and the persistence of added iron under field conditions, this research facilitates future applications of this control technique at larger scales in more suitable wetland environments. This research has also demonstrated that an iron amendment is not a remedy that will quickly fix the MeHg problem in the San Francisco Bay-Delta estuary. The complex biogeochemical cycling observed in the high marsh sediments of Gambinini Marsh illustrates that the control of MeHg production and export is an issue that will likely require innovative solutions and careful management to meet site-specific needs.

Cited References

Ackerman, J. T.; C. A. Eagles-Smith Agricultural Wetlands as Potential Hotspots for Mercury Bioaccumulation: Experimental Evidence Using Caged Fish. *Environmental Science & Technology* **2010**, *44*(4), 1451-1457.

Alvarez, M. D.; C. A. Murphy; K. A. Rose; I. D. McCarthy; L. A. Fuiman Maternal body burdens of methylmercury impair survival skills of offspring in Atlantic croaker (Micropogonias undulatus). *Aquatic Toxicology* **2006**, *80*(4), 329-337.

Ann, Y.; K. R. Reddy; J. J. Delfino Influence of chemical amendments on phosphorus immobilization in soils from a constructed wetland. *Ecological Engineering* **2000**, *14*(1-2), 157-167.

Avramescu, M. L.; E. Yumvihoze; H. Hintelmann; J. Ridal; D. Fortin; D. R. S. Lean Biogeochemical factors influencing net mercury methylation in contaminated freshwater sediments from the St. Lawrence River in Cornwall, Ontario, Canada. *Science of the Total Environment* **2011**, *409*(5), 968-978.

Babiarz, C. L.; J. P. Hurley; J. M. Benoit; M. M. Shafer; A. W. Andren; D. A. Webb Seasonal influences on partitioning and transport of total and methylmercury in rivers from contrasting watersheds. *Biogeochemistry* **1998**, *41*(3), 237-257.

Balls, P. W.; P. S. Liss Exchange of H2S between water and air. *Atmospheric Environment* **1983**, *17*(4), 735-742.

Barkay, T.; M. Gillman; R. R. Turner Effects of dissolved organic carbon and salinity on bioavailability of mercury. *Applied and Environmental Microbiology* **1997**, *63*(11), 4267-4271.

Benoit, J. M.; C. C. Gilmour; R. P. Mason; A. Heyes Sulfide controls on mercury speciation and bioavailability to methylating bacteria in sediment pore waters. *Environmental Science & Technology* **1999a**, *33*(6), 951-957.

Benoit, J. M.; C. C. Gilmour; R. P. Mason; G. S. Riedel; G. F. Riedel Behavior of mercury in the Patuxent River estuary. *Biogeochemistry* **1998**, *40*(2-3), 249-265.

Benoit, J. M.; R. P. Mason; C. C. Gilmour Estimation of mercury-sulfide speciation in sediment pore waters using octanol-water partitioning and implications for availability to methylating bacteria. *Environmental Toxicology and Chemistry* **1999b**, *18*(10), 2138-2141.

Benoit, J. M.; D. H. Shull; P. Robinson; L. R. Ucran Infaunal burrow densities and sediment monomethyl mercury distributions in Boston Harbor, Massachusetts. *Marine Chemistry* **2006**, *102*(1-2), 124-133.

Bertics, V. J.; W. Ziebis Bioturbation and the role of microniches for sulfate reduction in coastal marine sediments. *Environmental Microbiology* **2010**, *12*(11), 3022-3034.

Best, E. P. H.; H. Hintelmann; B. Dimock; A. J. Bednar Natural Cycles and Transfer of Mercury Through Pacific Coastal Marsh Vegetation Dominated by Spartina foliosa and Salicornia virginica. *Estuaries and Coasts* **2008**, *31*(6), 1072-1088.

Black, F. J.; K. W. Bruland; A. R. Flegal Competing ligand exchange-solid phase extraction method for the determination of the complexation of dissolved inorganic mercury(II) in natural waters. *Analytica Chimica Acta* **2007**, *598*(2), 318-333.

Bloom, N. Determination of picogram levels of methylmercury by aqueous phase ethylation, followed by cryogenic gas-chromatography with cold vapor atmoic fluorescence detection. *Canadian Journal of Fisheries and Aquatic Sciences* **1989**, *46*(7), 1131-1140.

Bloom, N.; W. F. Fitzgerald Determination of Volatile Mercury Species at the Picogram Level by Low-Temperature Gas-Chromatography with Cold-Vapor Atomic Fluorescence Detection. *Analytica Chimica Acta* **1988**, *208*(1-2), 151-161.

Bloom, N. S.; G. A. Gill; S. Cappellino; C. Dobbs; L. McShea; C. Driscoll; R. Mason; J. Rudd Speciation and cycling of mercury in Lavaca Bay, Texas, sediments. *Environmental Science & Technology* **1999**, *33*(1), 7-13.

Bouton, S. N.; P. C. Frederick; M. G. Spalding; H. McGill Effects of chronic, low concentrations of dietary methylmercury on the behavior of juvenile great egrets. *Environmental Toxicology and Chemistry* **1999**, *18*(9), 1934-1939.

Bower, J.; K. S. Savage; B. Weinman; M. O. Barnett; W. P. Hamilton; W. F. Harper Immobilization of mercury by pyrite (FeS2). *Environmental Pollution* **2008**, *156*(2), 504-514.

Brendel, P. J.; G. W. Luther Development of a gold amalgam voltammetric microelectrode fort he determination of dissolved Fe, Mn, O2, and S(-II) in porewaters of marine and fresh-water sediments. *Environmental Science & Technology* **1995**, *29*(3), 751-761.

Canario, J.; M. Caetano; C. Vale; R. Cesario Evidence for elevated production of methylmercury in salt marshes. *Environmental Science & Technology* **2007**, *41*(21), 7376-7382.

Canfield, D. E. Reactive iron in marine sediments. *Geochimica et Cosmochimica Acta* **1989**, *53*(3), 619-632.

Canfield, D. E.; R. Raiswell; S. Bottrell The reactivity of sedimentary iron minerals toward sulfide. *American Journal of Science* **1992**, *292*(9), 659-683.

CDC *CDC's Fourth National Report on Human Exposure to Environmental Chemicals*; Department of Health and Human Services, Centers for Disease Control and Prevention: 2009.

Celo, V.; D. R. S. Lean; S. L. Scott Abiotic methylation of mercury in the aquatic environment. *Science of the Total Environment* **2006**, *368*(1), 126-137.

Choe, K. Y.; G. A. Gill; R. D. Lehman; S. Han; W. A. Heim; K. H. Coale Sediment-water exchange of total mercury and monomethyl mercury in the San Francisco Bay-Delta. *Limnology and Oceanography* **2004**, *49*(5), 1512-1527.

Choi, S. C.; R. Bartha Environmental factors affecting mercury methylation in estuarine sediments. *Bulletin of Environmental Contamination and Toxicology* **1994**, *53*(6), 805-812.

Choi, S. C.; T. Chase; R. Bartha Enzymatic catalysis of mercury methylation by Desulfovibrio desulfuricans LS. *Applied and Environmental Microbiology* **1994a**, *60*(4), 1342-1346.

Choi, S. C.; T. Chase; R. Bartha Metabolic pathways leading to mercury methylation in Desulfovibrio desulfuricans LS. *Applied and Environmental Microbiology* **1994b**, *60*(11), 4072-4077.

Clarisse, O.; B. Dimock; H. Hintelmann; E. P. H. Best Predicting net mercury methylation in sediments using diffusive gradient in thin films measurements. *Environmental Science & Technology* **2011**, *45*(4), 1506-1512.

Cline, J. D. Spectrophotometric Determination of Hydrogen Sulfide in Natural Waters. *Limnology and Oceanography* **1969**, *14*(3), 454-458.

Compeau, G. C.; R. Bartha Sulfate-reducing bacteria - principle methylators of mercury in anoxic estuarine sediment. *Applied and Environmental Microbiology* **1985**, *50*(2), 498-502.

Conaway, C. H.; J. R. M. Ross; R. Looker; R. P. Mason; A. R. Flegal Decadal mercury trends in San Francisco estuary sediments. *Environmental Research* **2007**, *105*(1), 53-66.

Conaway, C. H.; S. Squire; R. P. Mason; A. R. Flegal Mercury speciation in the San Francisco Bay estuary. *Marine Chemistry* **2003**, *80*(2-3), 199-225.

Conaway, C. H.; E. B. Watson; J. R. Flanders; A. R. Flegal Mercury deposition in a tidal marsh of south San Francisco Bay downstream of the historic New Almaden mining district, California. *Marine Chemistry* **2004**, *90*(1-4), 175-184.

Costanza, R.; R. dArge; R. deGroot; S. Farber; M. Grasso; B. Hannon; K. Limburg; S. Naeem; R. V. Oneill; J. Paruelo; R. G. Raskin; P. Sutton; M. vandenBelt The value of the world's ecosystem services and natural capital. *Nature* **1997**, *387*(6630), 253-260.

CSWRCB *San Francisco Bay Basin Water Quality Control Plan: Adopted Basin Plan Amendment*; California State Water Resources Control Board; 2006. http://www.waterboards.ca.gov/sanfranciscobay/water_issues/programs/TMDLs/sfbaymercury/Adopted_BPA_080906.pdf

Dacey, J. W. H.; B. L. Howes Water uptake by roots controls water table movement and sediment oxidation in short Spartina marsh. *Science* **1984**, *224*(4648), 487-489.

Dahl, T. E. *Wetlands losses in the United States 1780's to 1980's*; U.S. Department of the Interior, Fish and Wildlife Service: Washington, D.C., 1990.

Dahl, T. E. *Status and Trends of Wetlands in the Conterminous United States, 1986 to 1997*; US Fish and Wildlife Service: Washington, DC, 2000.

Dingler, J. R. *USGS Fact Sheet: Coastal Wetlands and Sediments of the San Francisco Bay System* United States Geological Survey, Marine and Coastal Geology Program: 1996.

Dong, W. M.; Y. R. Bian; L. Y. Liang; B. H. Gu Binding Constants of Mercury and Dissolved Organic Matter Determined by a Modified Ion Exchange Technique. *Environmental Science & Technology* **2011**, *45*(8), 3576-3583.

Drott, A.; L. Lambertsson; E. Bjorn; U. Skyllberg Effects of oxic and anoxic filtration on determined methyl mercury concentrations in sediment pore waters. *Marine Chemistry* **2007a**, *103*(1-2), 76-83.

Drott, A.; L. Lambertsson; E. Bjorn; U. Skyllberg Importance of Dissolved Neutral Mercury Sulfides for Methyl Mercury Production in Contaminated Sediments. *Environmental Science & Technology* **2007b**, *41*(7), 2270-2276.

Durnford, D.; A. Dastoor; D. Figueras-Nieto; A. Ryjkov Long range transport of mercury to the Arctic and across Canada. *Atmospheric Chemistry and Physics* **2010**, *10*(13), 6063-6086.

Eagles-Smith, C. A.; J. T. Ackerman; S. E. W. De La Cruz; J. Y. Takekawa Mercury bioaccumulation and risk to three waterbird foraging guilds is influenced by foraging ecology and breeding stage. *Environmental Pollution* **2009**, *157*(7), 1993-2002.

Emili, A.; N. Koron; S. Covelli; J. Faganeli; A. Acquavita; S. Predonzani; C. De Vittor Does anoxia affect mercury cycling at the sediment-water interface in the Gulf of Trieste (northern Adriatic Sea)? Incubation experiments using benthic flux chambers. *Applied Geochemistry* **2011**, *26*(2), 194-204.

EPA *2008 Biennial National Listing of Fish Advisories (EPA-823-F-09-007)*; United States Environmental Protection Agency, Office of Water: Washington, D.C., September 2009, 2009.

Fitzgerald, W. F.; C. H. Lamborg; C. R. Hammerschmidt Marine biogeochemical cycling of mercury. *Chemical Reviews* **2007**, *107*(2), 641-662.

Fitzgerald, W. F.; R. P. Mason, Biogeochemical cycling of mercury in the marine environment. In *Metal Ions in Biological Systems, Vol 34*, Marcel Dekker: New York, 1997; Vol. 34, pp 53-111.

Fleming, E. J.; E. E. Mack; P. G. Green; D. C. Nelson Mercury methylation from unexpected sources: Molybdate-inhibited freshwater sediments and an iron-reducing bacterium. *Applied and Environmental Microbiology* **2006**, *72*(1), 457-464.

Gagnon, C.; E. Pelletier; A. Mucci Behaviour of anthropogenic mercury in coastal marine sediments. *Marine Chemistry* **1997**, *59*(1-2), 159-176.

Gardner, L. R. A modeling study of the dynamics of pore water seepage from intertidal marsh sediments. *Estuarine, Coastal and Shelf Science* **2005**, *62*(4), 691-698.

Gardner, L. R.; T. G. Wolaver; M. Mitchell Spatial variations in the sulfur chemistry of salt marsh sediments at North Inlet, South Carolina. *Journal of Marine Research* **1988**, *46*(4), 815-836.

Gilmour, C. C.; E. A. Henry Mercury methylation in aquatic systems affected by acid deposition. *Environmental Pollution* **1991**, *71*(2-4), 131-169.

Gilmour, C. C.; E. A. Henry; R. Mitchell Sulfate Stimulation of Mercury Methylation in Freshwater Sediments. *Environmental Science & Technology* **1992**, *26*(11), 2281-2287.

Gilmour, C. C.; G. S. Riedel; M. C. Ederington; J. T. Bell; J. M. Benoit; G. A. Gill; M. C. Stordal Methylmercury concentrations and production rates across a trophic gradient in the northern Everglades. *Biogeochemistry* **1998**, *40*(2-3), 327-345.

Gobeil, C.; R. W. Macdonald; J. N. Smith Mercury profiles in sediments of the Arctic Ocean basins. *Environmental Science & Technology* **1999**, *33*(23), 4194-4198.

Greenfield, B. K.; A. Jahn Mercury in San Francisco Bay forage fish. *Environmental Pollution* **2010**, *158*(8), 2716-2724.

Gribsholt, B.; J. E. Kostka; E. Kristensen Impact of fiddler crabs and plant roots on sediment biogeochemistry in a Georgia saltmarsh. *Marine Ecology-Progress Series* **2003**, *259*, 237-251.

Guentzel, J. L. Wetland influences on mercury transport and bioaccumulation in South Carolina. *Science of the Total Environment* **2009**, *407*(4), 1344-1353.

Hall, B. D.; G. R. Aiken; D. P. Krabbenhoft; M. Marvin-DiPasquale; C. M. Swarzenski Wetlands as principal zones of methylmercury production in southern Louisiana and the Gulf of Mexico region. *Environmental Pollution* **2008**, *154*(1), 124-134.

Hammerschmidt, C. R.; W. F. Fitzgerald Geochemical controls on the production and distribution of methylmercury in near-shore marine sediments. *Environmental Science & Technology* **2004**, *38*(5), 1487-1495.

Hammerschmidt, C. R.; W. F. Fitzgerald Photodecomposition of methylmercury in an arctic Alaskan lake. *Environmental Science & Technology* **2006**, *40*(4), 1212-1216.

Hammerschmidt, C. R.; W. F. Fitzgerald Sediment-water exchange of methylmercury determined from shipboard benthic flux chambers. *Marine Chemistry* **2008**, *109*(1-2), 86-97.

Hammerschmidt, C. R.; W. F. Fitzgerald; P. H. Balcom; P. T. Visscher Organic matter and sulfide inhibit methylmercury production in sediments of New York/New Jersey Harbor. *Marine Chemistry* **2008**, *109*(1-2), 165-182.

Hammerschmidt, C. R.; W. F. Fitzgerald; C. H. Lamborg; P. H. Balcom; P. T. Visscher Biogeochemistry of methylmercury in sediments of Long Island Sound. *Marine Chemistry* **2004**, *90*(1-4), 31-52.

Han, S.; A. Obraztsova; P. Pretto; D. D. Deheyn; J. Gieskes; B. M. Tebo Sulfide and iron control on mercury speciation in anoxic estuarine sediment slurries. *Marine Chemistry* **2008**, *111*(3-4), 214-220.

Harmon, S. M.; J. K. King; J. B. Gladden; G. T. Chandler; L. A. Newman Methylmercury formation in a wetland mesocosm amended with sulfate. *Environmental Science & Technology* **2004**, *38*(2), 650-656.

Heim, W.; M. Stephenson; A. Bonnema; A. Byington; A. Newman; D. Feliz; L. Sousa; K. Coale, Best management practices to reduce methylmercury concentrations and exports from seasonal wetlands in the Yolo Wildlife Area, California. In *6th Biennial Bay-Delta Science Conference*, Sacramento, California, 2010.

Heim, W. A.; K. H. Coale; M. Stephenson; K. Y. Choe; G. A. Gill; C. Foe Spatial and habitat-based variations in total and methyl mercury concentrations in surficial sediments in the San Francisco Bay-Delta. *Environmental Science & Technology* **2007**, *41*(10), 3501-3507.

Henneberry, Y. K.; T. E. C. Kraus; J. A. Fleck; D. P. Krabbenhoft; P. M. Bachand; W. R. Horwath Removal of inorganic mercury and methylmercury from surface waters following coagulation of dissolved organic matter with metal-based salts. *Science of the Total Environment* **2011**, *409*(3), 631-637.

Heyes, A.; R. P. Mason; E. H. Kim; E. Sunderland Mercury methylation in estuaries: Insights from using measuring rates using stable mercury isotopes. *Marine Chemistry* **2006**, *102*(1-2), 134-147.

Hines, M. E.; S. L. Knollmeyer; J. B. Tugel Sulfate reduction and other sedimentary biogeochemistry in a northern New England salt marsh. *Limnology and Oceanography* **1989**, *34*(3), 578-590.

Holmer, M.; B. Gribsholt; E. Kristensen Effects of sea level rise on growth of Spartina anglica and oxygen dynamics in rhizosphere and salt marsh sediments. *Marine Ecology-Progress Series* **2002**, *225*, 197-204.

Horvat, M.; L. Liang; N. S. Bloom Comparison of Distillation with Other Current Isolation Methods for the Determination of Methyl Mercury-Compounds in Low-Level Environmental-Samples .2. Water. *Analytica Chimica Acta* **1993**, *282*(1), 153-168.

Howarth, R. W. Pyrite: Its rapid formation in a salt marsh and its importance in ecosystem metabolism. *Science* **1979**, *203*(4375), 49-51.

Howarth, R. W. The ecological significance of sulfur in the energy dynamics of salt marsh and coastal marine sediments. *Biogeochemistry* **1984**, *1*(1), 5-27.

Howarth, R. W.; A. Giblin Sulfate reduction in the salt marshes at Sapelo Island, Georgia. *Limnology and Oceanography* **1983**, *28*(1), 70-82.

Howes, B. L.; J. W. H. Dacey; D. D. Goehringer Factors controlling the growth form of Spartina alterniflora: Feedbacks between above-ground production, sediment oxidation, nitrogen, and salinity. *Journal of Ecology* **1986**, *74*(3), 881-898.

Howes, B. L.; R. W. Howarth; J. M. Teal; I. Valiela Oxidation-reduction potentials in a salt marsh: Spatial patterns and interactions with primary production. *Limnology and Oceanography* **1981**, *26*(2), 350-360.

Hsieh, Y. P.; S. W. Chung; Y. J. Tsau; C. T. Sue Analysis of sulfides in the presence of ferric minerals by diffusion methods. *Chemical Geology* **2002**, *182*(2-4), 195-201.

Hsieh, Y. P.; Y. N. Shieh Analysis of reduced inorganic sulfur by diffusion methods: Improved apparatus and evaluation for sulfur isotopic studies. *Chemical Geology* **1997**, *137*(3-4), 255-261.

Hsu-Kim, H.; D. L. Sedlak Similarities between inorganic sulfide and the strong Hg(II) - Complexing ligands in municipal wastewater effluent. *Environmental Science & Technology* **2005**, *39*(11), 4035-4041.

Huerta-Diaz, M. A.; J. W. Morse Pyritization of trace metals in anoxic marine sediments. *Geochimica Et Cosmochimica Acta* **1992**, *56*(7), 2681-2702.

Hurley, J. P.; J. M. Benoit; C. L. Babiarz; M. M. Shafer; A. W. Andren; J. R. Sullivan; R. Hammond; D. A. Webb Influences of Watershed Characteristics on Mercury Levels in Wisconsin Rivers. *Environmental Science & Technology* **1995**, *29*(7), 1867-1875.

Hyun, J. H.; J. S. Mok; H. Y. Cho; S. H. Kim; K. S. Lee; J. E. Kostka Rapid organic matter mineralization coupled to iron cycling in intertidal mud flats of the Han River estuary, Yellow Sea. *Biogeochemistry* **2009**, *92*(3), 231-245.

Hyun, J. H.; A. C. Smith; J. E. Kostka Relative contributions of sulfate- and iron(III) reduction to organic matter mineralization and process controls in contrasting habitats of the Georgia saltmarsh. *Applied Geochemistry* **2007**, *22*(12), 2637-2651.

Jackel, U.; S. Russo; S. Schnell Enhanced iron reduction by iron supplement: A strategy to reduce methane emission from paddies. *Soil Biology & Biochemistry* **2005**, *37*(11), 2150-2154.

Jaeger, I.; H. Hop; G. W. Gabrielsen Biomagnification of mercury in selected species from an Arctic marine food web in Svalbard. *Science of the Total Environment* **2009**, *407*(16), 4744-4751.

Jay, J. A.; F. M. M. Morel; H. F. Hemond Mercury speciation in the presence of polysulfides. *Environmental Science & Technology* **2000**, *34*(11), 2196-2200.

Jeong, H. Y.; B. Klaue; J. D. Blum; K. F. Hayes Sorption of mercuric ion by synthetic nanocrystalline mackinawite (FeS). *Environmental Science & Technology* **2007**, *41*(22), 7699-7705.

Jorgensen, B. B. Bacterial sulfate reduction within reduced microniches of oxidized marine sediments. *Marine Biology* **1977**, *41*(1), 7-17.

Kehrig, H. A.; T. G. Seixas; A. P. Baeta; O. Malm; I. Moreira Inorganic and methylmercury: Do they transfer along a tropical coastal food web? *Marine Pollution Bulletin* **2010**, *60*(12), 2350-2356.

Kerin, E. J.; C. C. Gilmour; E. Roden; M. T. Suzuki; J. D. Coates; R. P. Mason Mercury methylation by dissimilatory iron-reducing bacteria. *Applied and Environmental Microbiology* **2006**, *72*(12), 7919-7921.

Kim, M.; S. Han; J. Gieskes; D. D. Deheyn Importance of organic matter lability for monomethylmercury production in sulfate-rich marine sediments. *Science of the Total Environment* **2011**, *409*(4), 778-784.

King, G. M. Sulfate reduction in Georgia salt marsh soils: An evaluation of pyrite formation by use of 35S and 55Fe tracers. *Limnology and Oceanography* **1983**, *28*(5), 987-995.

King, G. M.; B. L. Howes; J. W. H. Dacey Short-term endproducts of sulfate reduction in a salt marsh: Formation of acid volatile sulfides, elemental sulfur, and pyrite. *Geochimica et Cosmochimica Acta* **1985**, *49*(7), 1561-1566.

King, G. M.; M. J. Klug; R. G. Wiegert; A. G. Chalmers Relation of soil-water movement and sulfide concentration to Spartina alterniflor production in a Georgia salt marsh. *Science* **1982**, *218*(4567), 61-63.

King, J. K.; S. M. Harmon; T. T. Fu; J. B. Gladden Mercury removal, methylmercury formation, and sulfate-reducing bacteria profiles in wetland mesocosms. *Chemosphere* **2002**, *46*(6), 859-870.

King, J. K.; F. M. Saunders; R. F. Lee; R. A. Jahnke Coupling mercury methylation rates to sulfate reduction rates in marine sediments. *Environmental Toxicology and Chemistry* **1999**, *18*(7), 1362-1369.

Kongchum, M.; I. Devai; R. D. DeLaune; A. Jugsujinda Total mercury and methylmercury in freshwater and salt marsh soils of the Mississippi river deltaic plain. *Chemosphere* **2006**, *63*(8), 1300-1303.

Koretsky, C. M.; M. Haveman; A. Cuellar; L. Beuving; T. Shattuck; M. Wagner Influence of Spartina and Juncus on Saltmarsh Sediments. I. Pore Water Geochemistry. *Chemical Geology* **2008**, *255*(1-2), 87-99.

Koretsky, C. M.; D. Miller Seasonal influence of the needle rush Juncus roemarianus on saltmarsh pore water geochemistry. *Estuaries and Coasts* **2008**, *31*(1), 70-84.

Koretsky, C. M.; C. M. Moore; K. L. Lowe; C. Meile; T. J. Dichristina; P. Van Cappellen Seasonal oscillation of microbial iron and sulfate reduction in saltmarsh sediments (Sapelo Island, GA, USA). *Biogeochemistry* **2003**, *64*(2), 179-203.

Koretsky, C. M.; P. Van Cappellen; T. J. DiChristina; J. E. Kostka; K. L. Lowe; C. M. Moore; A. N. Roychoudhury; E. Viollier Salt marsh pore water geochemistry does not correlate with microbial community structure. *Estuarine, Coastal and Shelf Science* **2005**, *62*(1-2), 233-251.

Kostka, J. E.; B. Gribsholt; E. Petrie; D. Dalton; H. Skelton; E. Kristensen The rates and pathways of carbon oxidation in bioturbated saltmarsh sediments. *Limnology and Oceanography* **2002a**, *47*(1), 230-240.

Kostka, J. E.; G. W. Luther Seasonal cycling of Fe in salt-marsh sediments. *Biogeochemistry* **1995**, *29*(2), 159-181.

Kostka, J. E.; A. Roychoudhury; P. Van Cappellen Rates and controls of anaerobic microbial respiration across spatial and temporal gradients in saltmarsh sediments. *Biogeochemistry* **2002b**, *60*(1), 49-76.

Lambertsson, L.; M. Nilsson Organic material: The primary control on mercury methylation and ambient methyl mercury concentrations in estuarine sediments. *Environmental Science & Technology* **2006**, *40*(6), 1822-1829.

Lamborg, C. H.; C. M. Tseng; W. F. Fitzgerald; P. H. Balcom; C. R. Hammerschmidt Determination of the mercury complexation characteristics of dissolved organic matter in natural waters with "reducible Hg" titrations. *Environmental Science & Technology* **2003**, *37*(15), 3316-3322.

Langer, C. S.; W. F. Fitzgerald; P. T. Visscher; G. M. Vandal Biogeochemical cycling of methylmercury at Barn Island Salt Marsh, Stonington, CT, USA. *Wetlands Ecology and Management* **2001**, *9*(4), 295-310.

Lee, R. W. Oxidation of sulfide by Spartina alterniflora roots. *Limnology and Oceanography* **1999**, *44*(4), 1155-1159.

Lee, R. W. Physiological adaptations of the invasive cordgrass Spartina anglica to reducing sediments: rhizome metabolic gas fluxes and enhanced O-2 and H2S transport. *Marine Biology* **2003**, *143*(1), 9-15.

Lehmann, M. F.; S. M. Bernasconi; A. Barbieri; J. A. McKenzie Preservation of organic matter and alteration of its carbon and nitrogen isotope composition during simulated and in situ early sedimentary diagenesis. *Geochimica et Cosmochimica Acta* **2002**, *66*(20), 3573-3584.

Li, H. L.; L. Li; D. Lockington Aeration for plant root respiration in a tidal marsh. *Water Resources Research* **2005**, *41*(6).

Liu, G. L.; Y. Cai; T. Philippi; P. Kalla; D. Scheidt; J. Richards; L. Scinto; C. Appleby Distribution of total and methylmercury in different ecosystem compartments in the Everglades: Implications for mercury bioaccumulation. *Environmental Pollution* **2008**, *153*(2), 257-265.

Liu, J. R.; K. T. Valsaraj; R. D. Delaune Inhibition of Mercury Methylation by Iron Sulfides in an Anoxic Sediment. *Environmental Engineering Science* **2009**, *26*(4), 833-840.

Lovley, D. R.; E. J. P. Phillips Rapid assay for microbially reducible ferric iron in aquatic sediments. *Applied and Environmental Microbiology* **1987**, *53*(7), 1536-1540.

Lowe, K. L.; T. J. Dichristina; A. N. Roychoudhury; P. Van Cappellen Microbiological and geochemical characterization of microbial Fe(III) reduction in salt marsh sediments. *Geomicrobiology Journal* **2000**, *17*(2), 163-176.

Macleod, M.; T. E. McKone; D. Mackay Mass balance for mercury in the San Francisco Bay Area. *Environmental Science & Technology* **2005**, *39*(17), 6721-6729.

Marba, N.; C. M. Duarte; M. Holmer; M. L. Calleja; E. Alvarez; E. Diaz-Almela; N. Garcias-Bonet Sedimentary iron inputs stimulate seagrass (Posidonia oceanica) population growth in carbonate sediments. *Estuarine Coastal and Shelf Science* **2008**, *76*(3), 710-713.

Maricle, B. R.; R. W. Lee Root respiration and oxygen flux in salt marsh grasses from different elevational zones. *Marine Biology* **2007**, *151*(2), 413-423.

Marvin-DiPasquale, M.; J. Agee; C. McGowan; R. S. Oremland; M. Thomas; D. Krabbenhoft; C. C. Gilmour Methyl-mercury degradation pathways: A comparison among three mercury-impacted ecosystems. *Environmental Science & Technology* **2000**, *34*(23), 4908-4916.

Marvin-DiPasquale, M.; J. L. Agee Microbial mercury cycling in sediments of the San Francisco Bay-Delta. *Estuaries* **2003**, *26*(6), 1517-1528.

Marvin-DiPasquale, M. C.; J. L. Agee; R. M. Bouse; B. E. Jaffe Microbial cycling of mercury in contaminated pelagic and wetland sediments of San Pablo Bay, California. *Environmental Geology* **2003**, *43*(3), 260-267.

Mason, R. P.; W. F. Fitzgerald; F. M. M. Morel The biogeochemical cycling of elemental mercury: Anthropogenic influences. *Geochimica Et Cosmochimica Acta* **1994**, *58*(15), 3191-3198.

Mason, R. P.; D. Heyes; A. Sveinsdottir Methylmercury concentrations in fish from tidal waters of the Chesapeake Bay. *Archives of Environmental Contamination and Toxicology* **2006**, *51*(3), 425-437.

Mason, R. P.; J. R. Reinfelder; F. M. M. Morel Bioaccumulation of mercury and methylmercury. *Water Air and Soil Pollution* **1995**, *80*(1-4), 915-921.

Mehrotra, A. S.; A. J. Horne; D. L. Sedlak Reduction of net mercury methylation by iron in Desulfobulbus propionicus (1pr3) cultures: Implications for engineered wetlands. *Environmental Science & Technology* **2003**, *37*(13), 3018-3023.

Mehrotra, A. S.; D. L. Sedlak Decrease in net mercury methylation rates following iron amendment to anoxic wetland sediment slurries. *Environmental Science & Technology* **2005**, *39*(8), 2564-2570.

Merritt, K. A.; A. Amirbahman Mercury dynamics in sulfide-rich sediments: Geochemical influence on contaminant mobilization within the Penobscot River estuary, Maine, USA. *Geochimica Et Cosmochimica Acta* **2007**, *71*(4), 929-941.

Merritt, K. A.; A. Amirbahman Methylmercury cycling in estuarine sediment pore waters (Penobscot River estuary, Maine, USA). *Limnology and Oceanography* **2008**, *53*(3), 1064-1075.

Miles, A. K.; M. A. Ricca Temporal and spatial distributions of sediment mercury at salt pond wetland restoration sites, San Francisco Bay, CA, USA. *Science of the Total Environment* **2010**, *408*(5), 1154-1165.

Miller, C. L.; R. P. Mason; C. C. Gilmour; A. Heyes Influence of dissolved organic matter on the complexation of mercury under sulfidic conditions. *Environmental Toxicology and Chemistry* **2007**, *26*(4), 624-633.

Miller, R. L.; R. Fujii Plant community, primary productivity, and environmental conditions following wetland re-establishment in the Sacramento-San Joaquin Delta, California. *Wetlands Ecology and Management* **2010**, *18*(1), 1-16.

Millero, F. J. The oxidation of H2S in the Chesapeake Bay. *Estuarine Coastal and Shelf Science* **1991**, *33*(5), 521-527.

Millero, F. J.; S. Hubinger; M. Fernandez; S. Garnett Oxidation of H2S in seawater as a function of temperature, pH, and ionic strength. *Environmental Science & Technology* **1987a**, *21*(5), 439-443.

Millero, F. J.; S. Sotolongo; M. Izaguirre The oxidation kinetics of Fe(II) in seawater. *Geochimica et Cosmochimica Acta* **1987b**, *51*(4), 793-801.

Mitchell, C. P. J.; C. C. Gilmour Methylmercury production in a Chesapeake Bay salt marsh. *Journal of Geophysical Research-Biogeosciences* **2008**, *113*, 14.

Mitsch, W. J.; J. G. Gosselink, *Wetlands: Fourth Edition*. Fourth Edition ed.; John Wiley & Sons, Inc: Hoboken, New Jersey, 2007.

Morel, F. M. M.; A. M. L. Kraepiel; M. Amyot The chemical cycle and bioaccumulation of mercury. *Annual Review of Ecology and Systematics* **1998**, *29*, 543-566.

Mucha, A. P.; C. M. R. Almeida; A. A. Bordalo; M. Vasconcelos Exudation of organic acids by a marsh plant and implications on trace metal availability in the rhizosphere of estuarine sediments. *Estuarine Coastal and Shelf Science* **2005**, *65*(1-2), 191-198.

Neubauer, S. C.; K. Givler; S. K. Valentine; J. P. Megonigal Seasonal patterns and plant-mediated controls of subsurface wetland biogeochemistry. *Ecology* **2005**, *86*(12), 3334-3344.

Olson, M. L.; L. B. Cleckner; J. P. Hurley; D. P. Krabbenhoft; T. W. Heelan Resolution of matrix effects on analysis of total and methyl mercury in aqueous samples from the Florida Everglades. *Fresenius Journal of Analytical Chemistry* **1997**, *358*(3), 392-396.

Oremland, R. S.; D. G. Capone Use of specific inhibitors in biogeochemistry and microbial ecology. *Advances in Microbial Ecology* **1988**, *10*, 285-383.

Oremland, R. S.; C. W. Culbertson; M. R. Winfrey Methylmercury decomposition in sediments and bacerial cultures: Involvement of methanogens and sulfate reducers in oxidative demethylation. *Applied and Environmental Microbiology* **1991**, *57*(1), 130-137.

Oremland, R. S.; B. F. Taylor Sulfate reduction and methanogenesis in marine sediments. *Geochimica Et Cosmochimica Acta* **1978**, *42*(2), 209-214.

Otero, X. L.; F. Macias Variation with depth and season in metal sulfides in salt marsh soils. *Biogeochemistry* **2002**, *61*(3), 247-268.

Page, G. W.; L. E. Stenzel; J. E. Kjelmyr Overview of shorebird abundance and distribution in wetlands of the Pacific Coast of the contiguous United States. *Condor* **1999**, *101*(3), 461-471.

Pickhardt, P. C.; N. S. Fisher Accumulation of inorganic and methylmercury by freshwater phytoplankton in two contrasting water bodies. *Environmental Science & Technology* **2007**, *41*(1), 125-131.

Poulton, S. W.; M. D. Krom; R. Raiswell A revised scheme for the reactivity of iron (oxyhydr)oxide minerals towards dissolved sulfide. *Geochimica et Cosmochimica Acta* **2004**, *68*(18), 3703-3715.

Ravichandran, M. Interactions between mercury and dissolved organic matter - a review. *Chemosphere* **2004**, *55*(3), 319-331.

Ravichandran, M.; G. R. Aiken; J. N. Ryan; M. M. Reddy Inhibition of precipitation and aggregation of metacinnabar (mercuric sulfide) by dissolved organic matter isolated from the Florida Everglades. *Environmental Science & Technology* **1999**, *33*(9), 1418-1423.

Reese, B. K.; M. A. Andersorr; C. Amrhein Hydrogen sulfide production and volatilization in a polymictic eutrophic saline lake, Salton Sea, California. *Science of the Total Environment* **2008**, *406*(1-2), 205-218.

Rickard, D.; J. W. Morse Acid volatile sulfide (AVS). *Marine Chemistry* **2005**, *97*(3-4), 141-197.

Robinson, E.; R. C. Robbins Gaseous sulfur pollutants from urban and natural sources. *Journal of the Air Pollution Control Association* **1970**, *20*(4), 233-235.

Roden, E. E.; R. G. Wetzel Organic carbon oxidation and suppression of methane production by microbial Fe(III) oxide reduction in vegetated and unvegetated freshwater wetland sediments. *Limnology and Oceanography* **1996**, *41*(8), 1733-1748.

Rothenberg, S. E.; R. F. Ambrose; J. A. Jay Mercury cycling in surface water, pore water and sediments of Mugu Lagoon, CA, USA. *Environmental Pollution* **2008**, *154*(1), 32-45.

Ruiz-Halpern, S.; S. A. Macko; J. W. Fourqurean The effects of manipulation of sedimentary iron and organic matter on sediment biogeochemistry and seagrasses in a subtropical carbonate environment. *Biogeochemistry* **2008**, *87*(2), 113-126.

Schluter, M.; E. Sauter; H. P. Hansen; E. Suess Seasonal variations of bioirrigation in coastal sediments: Modelling of field data. *Geochimica et Cosmochimica Acta* **2000**, *64*(5), 821-834.

Schwarzbach, S. E.; J. D. Albertson; C. M. Thomas Effects of predation, flooding, and contamination on reproductive success of California Clapper Rails (Rallus longirostris obsoletus) in San Francisco Bay. *Auk* **2006**, *123*(1), 45-60.

Sellers, P.; C. A. Kelly; J. W. M. Rudd; A. R. MacHutchon Photodegradation of methylmercury in lakes. *Nature* **1996**, *380*(6576), 694-697.

Sherwood, L. J.; R. G. Qualls Stability of phosphorus within a wetland soil following ferric chloride treatment to control eutrophication. *Environmental Science & Technology* **2001**, *35*(20), 4126-4131.

Simpson, S. L.; S. C. Apte; G. E. Batley Effect of short-term resuspension events on the oxidation of cadmium, lead, and zinc sulfide phases in anoxic estuarine sediments. *Environmental Science & Technology* **2000**, *34*(21), 4533-4537.

Skyllberg, U. Competition among thiols and inorganic sulfides and polysulfides for Hg and MeHg in wetland soils and sediments under suboxic conditions: Illumination of controversies and implications for MeHg net production. *Journal of Geophysical Research-Biogeosciences* **2008**, *113*.

Skyllberg, U.; A. Drott Competition between Disordered Iron Sulfide and Natural Organic Matter Associated Thiols for Mercury(II)-An EXAFS Study. *Environmental Science & Technology* **2010**, *44*(4), 1254-1259.

Slowey, A. J.; G. E. Brown Transformations of mercury, iron, and sulfur during the reductive dissolution of iron oxyhydroxide by sulfide. *Geochimica Et Cosmochimica Acta* **2007**, *71*(4), 877-894.

Smolders, A. J. P.; R. C. Nijboer; J. G. M. Roelofs Prevention of sulphide accumulation and phosphate mobilization by the addition of iron(II) chloride to a reduced sediment: An enclosure experiment. *Freshwater Biology* **1995**, *34*(3), 559-567.

St Louis, V. L.; J. W. M. Rudd; C. A. Kelly; K. G. Beaty; N. S. Bloom; R. J. Flett Importance of Wetlands as Sources of Methyl Mercury to Boreal Forest Ecosystems. *Canadian Journal of Fisheries and Aquatic Sciences* **1994**, *51*(5), 1065-1076.

St Louis, V. L.; J. W. M. Rudd; C. A. Kelly; R. A. Bodaly; M. J. Paterson; K. G. Beaty; R. H. Hesslein; A. Heyes; A. R. Majewski The rise and fall of mercury methylation in an experimental reservoir. *Environmental Science & Technology* **2004**, *38*(5), 1348-1358.

Stockdale, A.; W. Davison; H. Zhang Micro-scale biogeochemical heterogeneity in sediments: A review of available technology and observed evidence. *Earth-Science Reviews* **2009**, *92*(1-2), 81-97.

Stockdale, A.; W. Davison; H. Zhang Formation of iron sulfide at faecal pellets and other microniches within suboxic surface sediment. *Geochimica et Cosmochimica Acta* **2010**, *74*(9), 2665-2676.

Stookey, L. L. Ferrozine - A new spectrophotometric reagent for iron. *Analytical Chemistry* **1970**, *42*(7), 779-781.

Sundby, B.; C. Vale; M. Caetano; G. W. Luther Redox chemistry in the root zone of a salt marsh sediment in the Tagus Estuary, Portugal. *Aquatic Geochemistry* **2003**, *9*(3), 257-271.

Sunderland, E. M.; F. A. P. C. Gobas; B. A. Branfireun; A. Heyes Environmental controls on the speciation and distribution of mercury in coastal sediments. *Marine Chemistry* **2006**, *102*(1-2), 111-123.

Sveinsdottir, A. Y.; R. P. Mason Factors controlling mercury and methylmercury concentrations in largemouth bass (Micropterus salmoides) and other fish from Maryland reservoirs. *Archives of Environmental Contamination and Toxicology* **2005**, *49*(4), 528-545.

Takekawa, J. Y.; A. K. Miles; D. H. Schoellhamer; N. D. Athearn; M. K. Saiki; W. D. Duffy; S. Kleinschmidt; G. G. Shellenbarger; C. A. Jannusch Trophic structure and avian communities across a salinity gradient in evaporation ponds of the San Francisco Bay estuary. *Hydrobiologia* **2006**, *567*, 307-327.

Takekawa, J. Y.; N. Warnock; G. M. Martinelli; A. K. Miles; D. C. Tsao Waterbird use of Bayland Wetlands in the San Francisco Bay estuary: Movements of long-billed Dowitchers during the winter. *Waterbirds* **2002**, *25*, 93-105.

Tsao, D. C.; A. K. Miles; J. Y. Takekawa; I. Woo Potential Effects of Mercury on Threatened California Black Rails. *Archives of Environmental Contamination and Toxicology* **2009**, *56*(2), 292-301.

Ullrich, S. M.; T. W. Tanton; S. A. Abdrashitova Mercury in the aquatic environment: A review of factors affecting methylation. *Critical Reviews in Environmental Science and Technology* **2001**, *31*(3), 241-293.

Ursino, N.; S. Silvestri; M. Marani Subsurface flow and vegetation patterns in tidal environments. *Water Resources Research* **2004**, *40*(5).

USEPA *Method 1630: Methyl Mercury in Water by Distillation, Aqueous Ethylation, Purge and Trap, and CVAFS*; United States Environmental Protection Agency, Office of Water: Washington, D.C., 2001.

Valega, M.; A. I. Lillebo; M. E. Pereira; W. T. Corns; P. B. Stockwell; A. C. Duarte; M. A. Pardal Assessment of methylmercury production in a temperate salt marsh (Ria de Aveiro Lagoon, Portugal). *Marine Pollution Bulletin* **2008**, *56*(1), 153-158.

Van der Welle, M. E. W.; K. Niggebrugge; L. P. M. Lamers; J. G. M. Roelofs Differential responses of the freshwater wetland species Juncus effusus L. and Caltha palustris L. to iron supply in sulfidic environments. *Environmental Pollution* **2007**, *147*(1), 222-230.

Vazquez, F.; J. Z. Zhang; F. J. Millero Effect of metals on the rate of the oxidation of H2S in seawater. *Geophysical Research Letters* **1989**, *16*(12), 1363-1366.

Viollier, E.; P. W. Inglett; K. Hunter; A. N. Roychoudhury; P. Van Cappellen The ferrozine method revisited: Fe(II)/Fe(III) determination in natural waters. *Applied Geochemistry* **2000**, *15*(6), 785-790.

Watson, E. B.; R. Byrne Abundance and diversity of tidal marsh plants along the salinity gradient of the San Francisco Estuary: implications for global change ecology. *Plant Ecology* **2009**, *205*(1), 113-128.

Weber, J. H.; R. Evans; S. H. Jones; M. E. Hines Conversion of mercury(II) into mercury(0), monomethylmercury cation, and dimethylmercury in saltmarsh sediment slurries. *Chemosphere* **1998**, *36*(7), 1669-1687.

Weiss, J. V.; D. Emerson; J. P. Megonigal Geochemical control of microbial Fe(III) reduction potential in wetlands: comparison of the rhizosphere to non-rhizosphere soil. *FEMS Microbiology Ecology* **2004**, *48*(1), 89-100.

Wiener, J. G.; B. C. Knights; M. B. Sandheinrich; J. D. Jeremiason; M. E. Brigham; D. R. Engstrom; L. G. Woodruff; W. F. Cannon; S. J. Balogh Mercury in soils, lakes, and fish in Voyageurs National Park (Minnesota): Importance of atmospheric deposition and ecosystem factors. *Environmental Science & Technology* **2006**, *40*(20), 6261-6268.

Windham-Myers, L.; M. Marvin-Dipasquale; D. P. Krabbenhoft; J. L. Agee; M. H. Cox; P. Heredia-Middleton; C. Coates; E. Kakouros Experimental removal of wetland emergent vegetation leads to decreased methylmercury production in surface sediment. *Journal of Geophysical Research-Biogeosciences* **2009**, *114*, 14.

Wolfe, M. F.; S. Schwarzbach; R. A. Sulaiman Effects of mercury on wildlife: A comprehensive review. *Environmental Toxicology and Chemistry* **1998**, *17*(2), 146-160.

Wood, M. L.; C. Foe; J. Cooke Sacramento – San Joaquin Delta Estuary TMDL for Methylmercury: Staff Report. **2006**.

Yee, D.; L. J. McKee; J. J. Oram A regional mass balance of methylmercury in San Francisco Bay, California, USA. *Environmental Toxicology and Chemistry* **2011**, *30*(1), 88-96.

Zelewski, L. M.; G. Benoit; D. E. Armstrong Mercury dynamics in Tivoli South Bay, a freshwater tidal mudflat wetland in the Hudson River. *Biogeochemistry* **2001**, *52*(1), 93-112.

Zhang, L. M.; L. P. Wright; P. Blanchard A review of current knowledge concerning dry deposition of atmospheric mercury. *Atmospheric Environment* **2009**, *43*(37), 5853-5864.